Chapter 5

Chemical characterisation and source apportionment of PM10 and PM2.5

Atmospheric PM is a multi-component system constituted by a large number of natural and anthropogenic species of different grain size distribution. Although this variety of PM sources is recognised, PM is regarded as a single pollutant in most national air quality standards, and limit values are only defined for bulk particulate concentrations in TSP, PM10 or PM2.5.

This diversity of PM sources may induce significant variations in PM levels and composition in the rural, urban to industrial environments. Moreover, variations in PM levels and composition from Northern to Southern Europe may be induced by variations in the main types of anthropogenic PM source emissions, natural load, prevailing meteorology and factors influencing the gas to particle conversion. The Mediterranean basin is affected by two major PM sources: a) Europe as a major source of anthropogenic pollutants; b) North Africa as a principal source of natural mineral dust (e.g. Dulac et al., 1992, Kubilay et al., 2000). Although considerable literature is available on the mineral and chemical composition of African dust and on the influence on deposition chemistry, there is still a lack of information on the actual contribution of African dust to PM10 and PM2.5 levels in Southern Europe. Furthermore, the Mediterranean is characterised by a complex meteorology which favours the ageing of polluted air masses in the basin (Millán et al., 1997), inducing high levels of photo-oxidants and airborne particles. In fact, high levels of anthropogenic aerosols in air masses transported from the Western Mediterranean to the remote North Atlantic have been reported (McGovern et al., 1999).

This study is focused on the chemical characterisation and source apportionment of PM10 in three types of environment in Eastern Spain: a rural, an urban and an industrial area affected by primary PM emissions. A similar simultaneous PM2.5 study was conducted at the urban station. The sampling stations were the MONAGREGA rural site, the L'HOSPITALET traffic/urban station (Barcelona Metropolitan Area) and the ONDA industrial site affected by primary PM emissions from ceramic manufacture. At these sites, a simultaneous PM10 sampling (PM10 and PM2.5 at L'HOSPITALET) was performed following the methodology described in chapter 3. The location of these sites is indicated in Figure 5-1, and their main characteristics are highlighted in chapter 3.

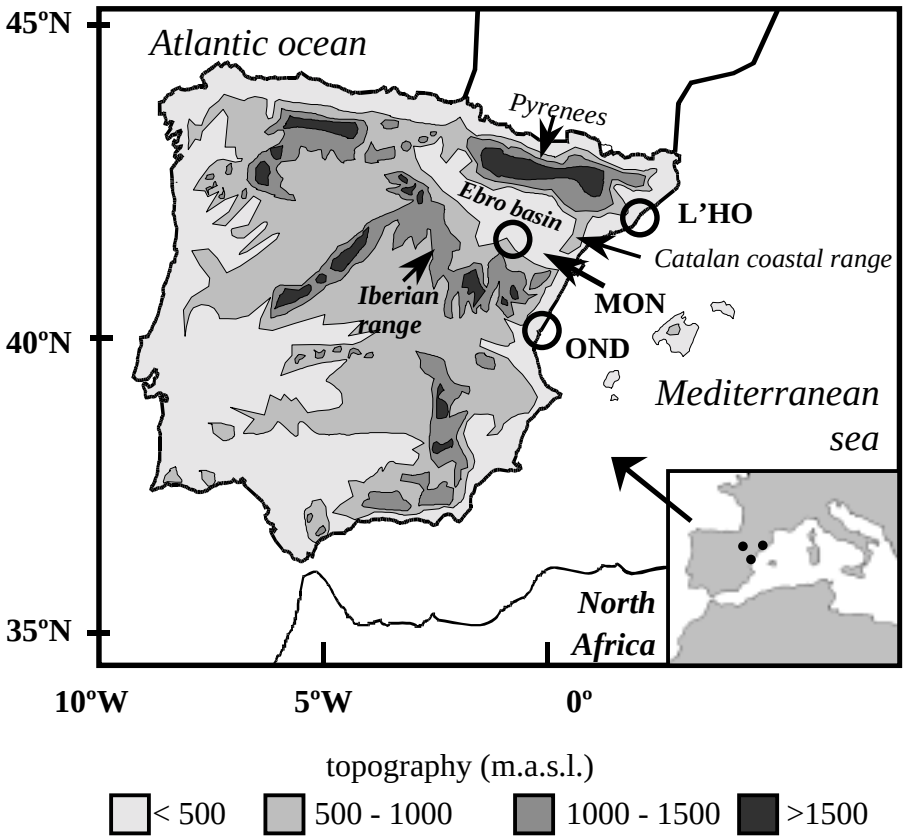

Figure 5-1. Location of the MONAGREGA (MON) rural, the L'HOSPITALET (L'HO) urban and the OND (ONDA) industrial (of primary PM emissions) stations for PM sampling in Eastern Spain.

The study is focused on the identification of sources and atmospheric processes inducing high PM10 levels, and special emphasis is laid on African dust. In order to characterise the extent of the regional air pollution and the impact of African dust, the results obtained at the three sites were compared.

5.1 Mean chemical composition

A statistical analysis of the levels of the PM components is presented in Table 5-1.

At the MONAGREGA rural site, the annual PM10 level reached 22.0µg/m^3 in the period June 1999 – June 2000. The components with the highest mean contributions (>4% of bulk PM10) were nss-$SO_4^=$ (17.3%), OC+EC (10.5%), NO_3^-(9.9%), SiO_2(8.6%), $CO_3^=$(7.7%), NH_4^+(5.8%) and Ca(4.5%). On average, the sum of the elements determined reached 74% of the bulk PM10 mass.

At the L´HOSPITALET urban site, the annual PM10 level reached 49.5µg/m^3 during the period June 1999 – June 2000. The components with the highest mean contributions (>4% of bulk PM10) were OC+EC (22.0%), nss-$SO_4^=$(13.4%), NO_3^-(11.7%), $CO_3^=$ (8.2%), SiO_2(6.0%), NH_4^+(5.4%) and Ca(4.6%). On average, the sum of the elements determined attained 83% of the bulk PM10 mass.

At the L´HOSPITALET urban site, the annual PM2.5 level reached 33.9µg/m^3 in the period June 1999 – June 2000. The components with the highest mean contributions (>4% of bulk

Table 5-1 (A, B). Statistic of PM10 component levels (in ng/m^3) at the MONAGREGA rural (112 samples taken from June 1999 to June 2000) and at the ONDA industrial sites (48 daily samples taken from June to October 1999).

	A) Rural (Ebro basin)					
	Mean	Max.	75thP	50thP	25thP	Min.
PM10	22020	45438	28709	21640	15000	5431
Ca	930	5802	1196	726	399	111
Al_2O_3	757	3610	929	516	324	25
SiO_2	1893	9024	2323	1289	810	62
Fe	222	966	269	170	116	8
Mg	117	496	154	89	52	20
K	203	769	260	167	105	16
C	2643	7678	3439	2191	1500	410
OC+EC	2306	5689	3003	1929	1354	367
$CO_3^=$	1688	9943	2179	1312	729	217
Na	294	1710	359	217	133	17
Cl	349	2316	355	266	207	100
$SO_4^=$	3877	10558	5236	3634	2169	579
nss-$SO_4^=$	3803	10131	5146	3580	2136	575
ss-$SO_4^=$	74	427	90	54	33	4
NO_3^-	2177	13251	2536	1227	733	391
NH_4^+	1284	4269	1777	1125	528	196
Zn	30	130	43	27	14	2
Ti	20	96	25	14	8	<1
P	22	58	27	20	14	5
Pb	10	54	13	8	4	<1
Ba	8	28	13	5	2	<1
Sr	5	33	6	3	2	<1
Mn	5	18	6	4	3	1
Ni	5	41	5	3	1	<1
Cu	3	7	3	2	2	<1
V	2	11	3	2	8	<1
Cr	<1	9	<1	<1	<1	<1
N samples	112					
Determined	16206					
% of PM	74					

	B) Industrial (Castelló)					
	Mean	Max.	75thP	50thP	25thP	Min.
PM10	33261	64000	38656	33121	28750	16000
Ca	1082	2366	1309	1072	857	389
Al_2O_3	1591	4867	1782	1407	1113	166
SiO_2	3977	12168	4455	3517	2784	414
Fe	432	1453	465	376	298	53
Mg	254	577	302	238	170	101
K	583	1143	710	575	449	34
C	4520	8590	5710	4211	3274	1749
CO+CE	4193	8264	5329	3877	3028	1633
$CO_3^=$	2258	4993	2717	2204	1710	835
Na	913	2291	1234	875	521	226
Cl	445	1555	471	341	266	167
$SO_4^=$	6887	13418	8570	7253	5080	1511
nss-$SO_4^=$	6658	12844	8261	7034	4950	1454
ss-$SO_4^=$	229	574	309	219	130	57
NO_3^-	1903	6911	2574	1588	1140	467
NH_4^+	1682	5215	2298	1622	853	124
Zn	203	776	280	142	67	18
Ti	43	152	48	37	29	9
P	41	81	48	39	33	21
Pb	164	682	210	130	89	11
Ba	9	27	12	8	5	<1
Sr	4	11	5	4	3	<1
Mn	7	21	8	6	5	2
Ni	4	29	5	4	2	<1
Cu	5	11	6	5	4	<1
V	6	19	7	6	4	<1
Cr	3	6	4	3	3	<1
N samples	48					
Determined	26688					
% of PM	80					

Table 5-1 (C, D). Statistic of PM10 and PM2.5 component levels (in ng/m^3) at the L'HOSPITALET urban site based on 115 and 63 samples (taken from June 1999 to June 2000), respectively.

	C) Urban (Barcelona)					
	Mean	Max.	75thP	50thP	25thP	Min.
PM10	49508	119092	57889	45548	33656	12770
Ca	2258	6317	2728	2205	1641	431
Al_2O_3	1184	3451	1346	1018	752	304
SiO_2	2961	8627	3365	2546	1880	761
Fe	891	2973	1053	766	559	207
Mg	278	992	327	239	193	86
K	416	1390	513	352	260	96
C	11711	38629	14188	9301	6741	2927
OC+EC	10895	36482	13223	8508	6162	2705
$CO_3^=$	4082	10736	4826	3967	2897	1108
Na	939	3237	1132	815	476	170
Cl	1045	4216	1419	772	412	54
$SO_4^=$	6891	14626	9721	6701	4373	1481
nss-$SO_4^=$	6656	13817	9438	6497	4254	1438
ss-$SO_4^=$	235	809	283	204	119	43
NO_3^-	5779	26529	7598	4033	2500	1007
NH_4^+	2669	13677	3210	1959	1349	299
Zn	319	3794	400	238	112	8
Ti	54	157	66	48	36	12
P	44	114	55	41	30	12
Pb	144	470	180	109	71	22
Ba	31	103	39	25	17	2
Sr	6	20	7	5	4	2
Mn	24	82	30	20	15	<1
Ni	7	39	9	6	4	1
Cu	72	266	88	62	42	14
V	13	46	16	12	8	3
Cr	6	18	7	5	4	1
N samples	115					
Determined	41008					
% of PM	83					

	D) Urban (Barcelona)					
	Mean	Max.	75thP	50thP	25thP	Min.
PM2.5	33918	82595	44084	30169	22993	8845
Ca	516	2805	537	400	268	109
Al_2O_3	422	1895	608	306	165	54
SiO_2	1056	4737	1521	765	413	134
Fe	258	810	301	234	155	41
Mg	68	287	80	55	41	22
K	229	731	306	192	136	19
C	11140	38820	13279	9181	5889	2430
OC+EC	10952	37835	13084	9028	5780	2379
$CO_3^=$	944	4926	975	766	543	252
Na	228	475	267	208	161	4
Cl	486	2504	640	372	171	15
$SO_4^=$	5631	10534	7356	5434	3989	1132
nss-$SO_4^=$	5574	10415	7289	5382	3949	1131
ss-$SO_4^=$	57	119	67	52	40	1
NO_3^-	4001	18119	4649	2364	1019	223
NH_4^+	3200	13349	4019	2476	1759	525
Zn	162	683	204	157	69	7
Ti	16	75	18	13	9	4
P	25	68	30	23	16	7
Pb	120	392	137	93	57	24
Ba	14	42	19	12	5	<1
Sr	2	20	2	1	<1	<1
Mn	14	54	17	11	8	1
Ni	6	34	7	5	3	<1
Cu	49	254	51	40	30	14
V	9	37	11	8	5	2
Cr	6	63	4	2	2	<1
N samples	63					
Determined	28417					
% of PM	84					

PM2.5) were OC+EC (32.3%), nss-$SO_4^=$(16.4%), NO_3^-(11.8%) and NH_4^+(9.4%). On average, the sum of the elements determined reached 84% of the bulk PM2.5 mass.

At the ONDA industrial site, the mean PM10 level in the studied period (June – October 1999) was 33.0µg/m^3, and the components with the highest mean contributions were nss-$SO_4^=$(20.0%), SiO_2(12.0%), OC+EC(12.6%), $CO_3^=$(4.9%), NO_3^-(5.7%), NH_4^+(5.1%) and Al_2O_3(4.8%). On average, the sum of the elements determined attained 81% of bulk PM10 mass.

As expected, the concentrations of all PM10 components at the urban site exceeded those at the rural site. The highest urban/rural concentration (U/R) ratios were attained by Cu (28.2), Pb(14.4) and Zn(10.6). U/Rs in the range of 2-7 were attained by V(6.5), Mn(4.8), OC+EC(4.4), Cr(4.7), Fe(4.0), Ba(4.0), Ti(2.7), NO_3^-(2.6), Ca(2.4), Mg(2.4), NH_4^+(2.1), K(2.0) and P(2.0). U/R for Na and Cl reached 3.1 as expected owing to the higher marine influence at the coastal urban site. The lowest U/Rs were obtained for nss-$SO_4^=$(1.8), Al(1.6), Ni(1.6) and Sr(1.2).

The concentrations of all PM10 components at the industrial site also exceeded those at the rural site in the period of simultaneous PM10 sampling (June – October 1999). The highest industrial/rural concentration ratio (I/R) was attained by Pb(14.1). I/Rs in the range of 2-7 were attained by Zn(6.6), Cr(3.4), Na(3.4), K(3.2), V(2.3), Cu(2.2), Al (2.2), Mg(2.1) and Ti(2.1). I/Rs in the range of 1-2 were attained by Fe(1.9), OC+EC(1.9), P(1.8), Ba(1.8), NO_3^-(1.4), nss-$SO_4^=$(1.4), Mn(1.3), Ca(1.2), Cl(1.1) and NH_4^+(1.0). The lowest U/R (<1) was obtained for Sr(0.9).

Most of the PM10 components presented higher concentrations at the urban than at the industrial site during the simultaneous PM10 sampling period (June – October 1999). The highest urban/industrial concentration ratio (U/I) was attained by Cu(13.7). U/Is in the range of 2-7 were attained by Mn(3.0), Ba(2.8), OC+EC(2.3), V(2.1), Cl(2.0) and NO_3^-(2.0). U/Is in the range of 1-2 were obtained for Ca(1.9), Fe(1.6), Cr(1.7), Ni(1.6), Sr(1.4), Zn(1.4), Ti(1.3), NH_4^+(1.2), Mg(1.2), Na(1.2), nss-$SO_4^=$(1.2) and P(1.1). The lowest U/Is (<1) were obtained for Al(0.8), Pb(0.8) and K(0.7). These U/I ratios are not as low as a priori expected, bearing in mind the high emission rates of clay and other pollutants in the area of ceramic manufacture. However, it should be taken into account that ONDA is located southward of the ceramic production area, and can be regarded as an industrial background monitoring station. Note that PM10 levels are relatively low when compared with those at the L'HOSPITALET urban site in Barcelona Metropolitan Area.

5.2 Identification of sources and processes affecting PM composition

The chemical profiles of PM sources were determined by Principal Component Analysis (PCA). This treatment was applied by using only the direct analytical determinations. PM components at very low concentrations were not introduced in the PCA given that the magnitude of the analytical errors may be close to the magnitude of the variations in the concentrations of these components in ambient air, which could be a source of noise (Castro, 1997). In the PCA at some sites, ozone and/or meteorological variables were introduced in order to assess the relationship of aerosol composition with the ambient conditions and levels of oxidant gases.

Table 5-2. Factor loading matrix for the MONAGREGA rural PM10 chemical composition obtained after applying a varimax normalised rotation.

	Factor1	Factor2	Factor3	Factor4
PM10	0,46	0,76		
Ca	0,81			
Al	0,96			
Fe	0,94			
Mg	0,87		0,26	
Ti	0,96			
Sr	0,82			
K	0,86			
Mn	0,81			
Pb	0,27	0,50		0,45
Zn		0,70		
V	0,63	0,57		
C		0,63		0,25
Na			0,92	
Cl			0,95	
nss-$SO_4^=$		0,89		
NO_3^-				0,93
NH_4^+		0,86		
%var	42	20	11	8
	Crustal	Industrial	Marine	Vehicular

Note: Factor loadings smaller than /± 0.25/ are not shown.

5.2.1 PM10 at the MONAGREGA rural site

Table 5-2 shows the results of the PCA applied to the whole chemical PM10 data set. The PCA was also performed on a seasonal basis introducing data of temperature and ozone concentration in order to study the previously identified (chapter 4) summer Regional episodes. The PCA obtained on a seasonal basis is discussed below and shown in appendix 5. Four main chemical profiles (or sources) were identified as contributing to PM10 levels at the MONAGREGA rural site (Table 5-2). These sources accounted for 81% of the variance in the PCA. The first factor (source 1) represents the crustal contribution to ambient PM10 levels given that this is defined by typical soil elements, such as Ca, Sr, Mn and a fraction of Mg occurring as carbonates, or Al, Ti, Fe, K, V and a fraction of Mg occurring as clay minerals. The main components defining the second factor (source 2) are nss-$SO_4^=$ and NH_4^+, which derive from gas to particle conversion processes of products of the SO_2 oxidation and NH_3. This factor also presents a high factor loading for V and Pb, which may derive from combustion emissions. Carbon also presents a high factor loading. Given the high association with nss-$SO_4^=$ a considerable influence of industrial sources, such as emitting SO_2 power plants, is expected in factor 2. This factor showed a higher summer/winter factor loading for ammonium, carbon, ozone and temperature (appendix 5), which suggests that the photochemical processes play a significant role in the formation of particulate pollutants. The third factor (source 3) represents the marine aerosol, as deduced from the high factor loading of Na and Cl. Mg is also a typical sea spray component (magnesium-sulphate; Warneck, 1988), and is also

present in the chemical profile of factor 3. Finally, the chemical profile of the fourth factor (source 4) is mainly defined by NO_3^-, which also derives from gas to particle conversion processes of products of the NOx oxidation. In addition to NO_3^-, this factor presents higher factor loading with ammonium and carbon in winter than in summer. Given the high factor loading of Pb and NO_3^-, a significant influence of NOx emission sources such as vehicle exhaust is expected.

The evolution time of the main components defining each PM chemical profile is discussed below.

Mineral dust

Most of the soil elements showed slightly increased background levels in spring and summer (Figure 5-2), probably due to the re-suspension of mineral particles from the semi-arid soil of the Ebro basin. However, sharp peak concentrations were recorded during African dust outbreaks (from Sahara/Sahel regions) over the Iberian peninsula. Arrows in Figure 5-2 highlight the occurrence of African dust outbreaks, as deduced from the previous meteorological and satellite image analysis. African dust is the most important source of Al, Mg, Fe and Ti at the rural site since these elements showed sharp peak concentrations (up to 5 times above background concentrations) only during African dust events. The concentrations of other mineral elements, such as Ca, K, Mn or Sr also showed significant increases during the African events, but additional peaks were recorded during non-African events because of their natural regional sources in the Ebro basin (e.g. high Ca and Sr soils). The North African mineral dust is mainly made up of clay minerals and quartz (Glaccum and Prospero, 1980; Goudie and Middleton, 2001), whereas the content of calcium-carbonate varies depending on the North African source region (Chiapello et al., 1997). The fact that the concentrations of Al, Fe and Ti undergo much higher increases than Ca concentrations during African dust events supports the clay rather than the carbonate composition of the African dust. Moreover, it should be pointed out that Mg is not present as a Ca-Mg carbonate (dolomite) but as a Mg-bearing clay mineral, given the high Mg/Al group element correlation ($r>0.9$). Smectite (a Mg-bearing clay) is a major component of African dust (Avila et al., 1997).

Sea salt

At the MONAGREGA rural site, the concentrations of Na and Cl presented low variability in summer (Figure 5-3 A). From mid-autumn to spring the concentrations of Na and Cl episodically underwent abrupt increases (up to 5 times the background levels). The back-trajectories and synoptic chart analyses showed that these sharp increases in Na and Cl concentrations occurred during abrupt entries of WNW Atlantic air into the Mediterranean basin in the cold season (examples in Figure 5-3 C and D). The concentrations of Na and Cl recorded on the Mediterranean side of the Iberian peninsula (at the MONAGREGA rural, the L'HOSPITALET urban and the ONDA industrial sites, Table 5-1) are significantly lower than those reported in clean and polluted environments at coastal and inland sites on the Atlantic side of the Peninsula (4-7 times lower than at the coastal sites of Portugal; Harrison et al., 1997a; Pio et al., 1991, 1996). Model simulations

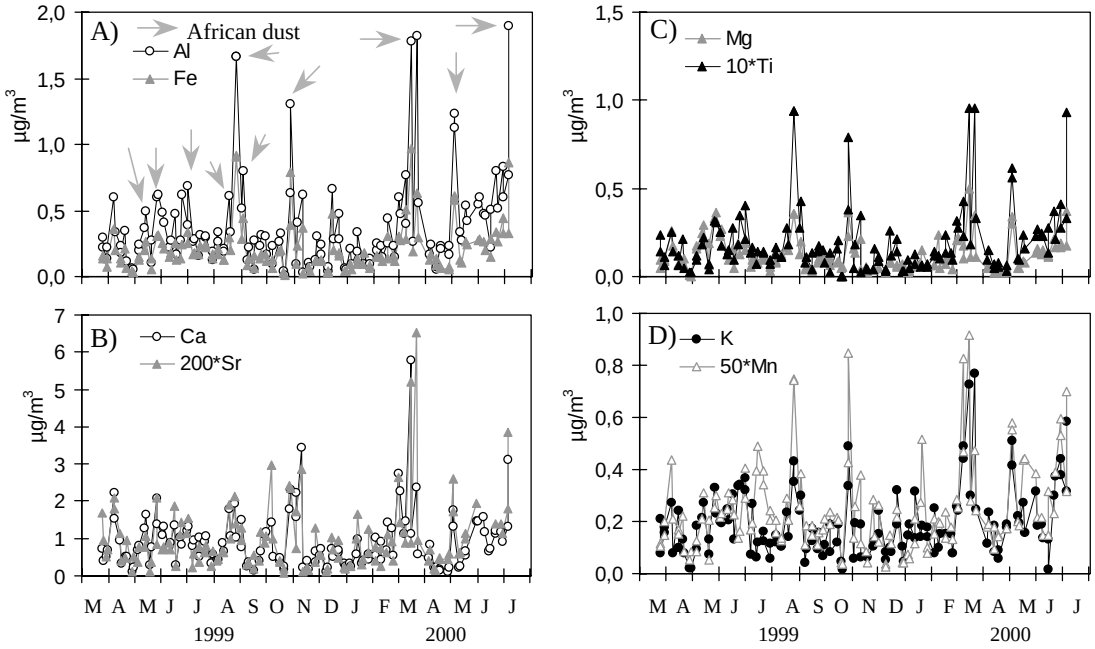

Figure 5-2. Daily concentrations of crustal components in PM10 at the MONAGREGA rural site. Grey arrows indicate the occurrence of African dust outbreaks.

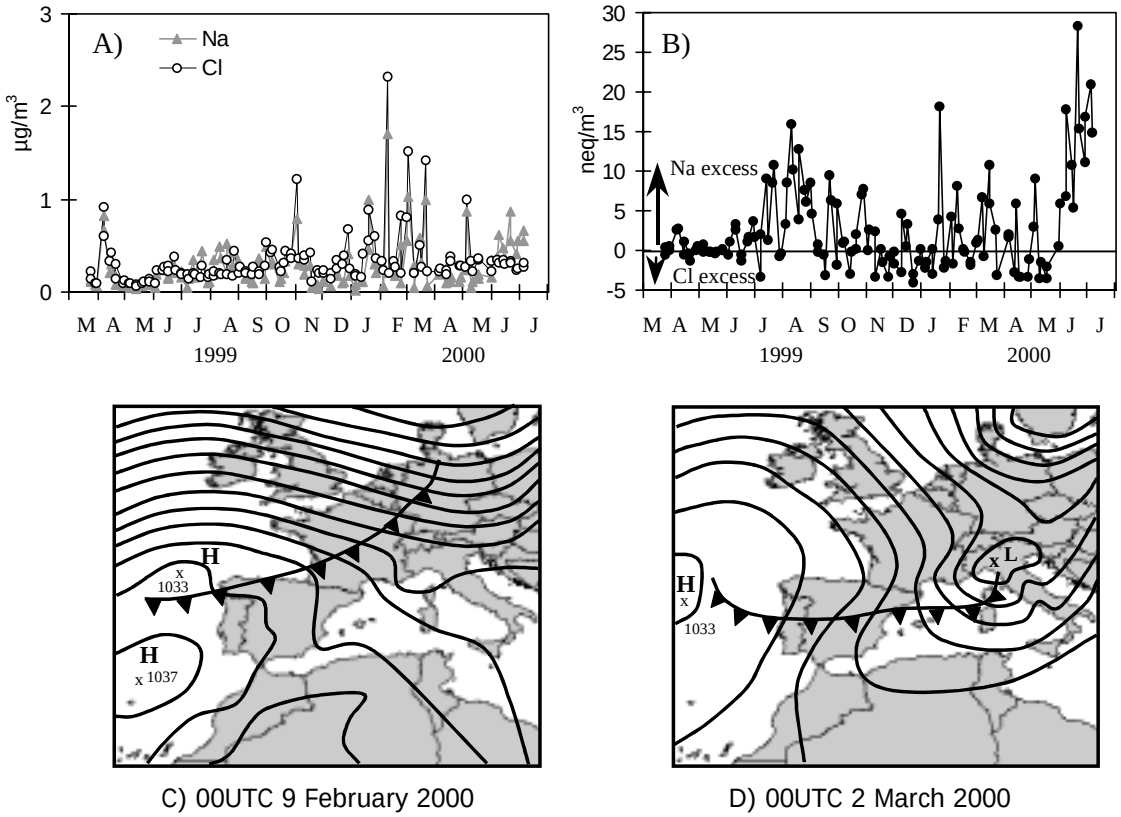

C) 00UTC 9 February 2000 D) 00UTC 2 March 2000

Figure 5-3. A) Daily concentrations of Na and Cl in PM10 at the MONAGREGA rural site. B) Na/Cl excess with respect to the marine Na/Cl ratio. C, D) Synoptic chart of pressure at the sea level for selected days of high Na and Cl concentrations.

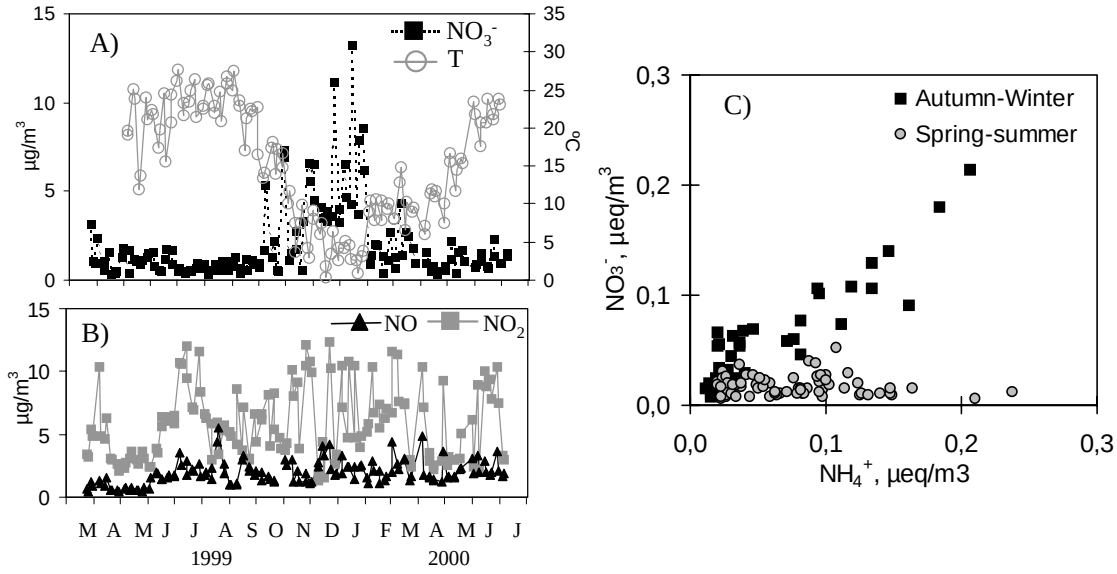

Figure 5-4. A) Daily mean values of nitrate concentrations in PM10 and temperature at the MONAGREGA rural site. B) Daily mean concentrations of NO and NO_2 during the periods for which NO_3^- concentrations were determined. C) Nitrate versus ammonium concentrations.

have shown that sea salt concentrations over the Atlantic ocean are significantly higher than over the Mediterranean sea because of the higher wind speed and surf activity over the Atlantic (Grini et al., 2001). This view is supported by the peak levels of Na and Cl recorded in the rural Ebro basin during abrupt entries of Atlantic air masses.

Nitrate

Nitrate, which is the main component of the fourth factor, exhibited the highest concentrations in autumn and winter (Figure 5-4 A). During the cold months, NO_3^- and NH_4^+ levels exhibited a strong association which was not observed in spring and summer (Figure 5-4 C). The anti-correlated seasonal evolution of NO_3^- levels and temperature (Figure 5-4 A) strongly suggests that thermodynamic properties of nitric acid play a key role in the formation of ammonium-nitrate by means of the reaction $NH_3(g)+HNO_3(g) \leftrightarrow NH_4NO_4(s \text{ or } aq)$. Nitric acid is mainly found in the gas phase in the low troposphere and in non Polar latitudes because of its relatively high vapour pressure. Experimental and theoretical data have shown that the formation of ammonium-nitrate is thermodynamically favoured at low temperatures, whereas in warmer environments the occurrence of gaseous nitric acid is favoured (Warneck, 1988 and Mészáros, 1999, and references therein; Adams et al., 1999). Thus, in our study area the enhanced formation (thermal stability) of ammonium-nitrate in the cold season accounts for the seasonal evolution of NO_3^-. In the warm season, minor amounts of ammonium-nitrate are expected, and the occurrence of NO_3^- is mainly attributed to the reaction of gaseous HNO_3^- with mineral species such as calcium-carbonate to form $Ca(NO_3)_2$ and/or with sea-salt to form $NaNO_3$ (Harrison and Kito, 1990; Wakamatsu et al., 1996). The latter is supported by the slight Na/Cl excess observed in spring and summer in 1999 and

2000 (Figure 5-2 B) given that the reactions leading to $NaNO_3$ formation induce the Cl volatilisation (Pio and Lopes, 1998) by mean of the reaction $NaCl(s) + HNO_3(g) \rightarrow NaNO_3(s)+HCl(g)$.

It should be noted that levels of NOx did not show a seasonal trend (Figure 5-4 B). Consequently the seasonal evolution of NO_3^- cannot be attributed to an increase in the NOx (NO_3^- gaseous precursors) concentrations in the rural atmosphere.

At the rural site in the Ebro basin the nitrate load reaches <10% and 30-40% of bulk PM10 in summer and winter, respectively.

Nss-sulphate

At the MONAGREGA rural site the highest concentrations of nss-$SO_4^=$ were reached in the warm season (Figure 5-5A). Nss-$SO_4^=$ and NH_4^+ showed a strong association during the study period (Figure 5-5C), which indicates that nss-$SO_4^=$ is mainly present as ammonium-sulphate ($(NH_4)_2SO_4$ and/or NH_4HSO_4). The seasonal evolution of nss-$SO_4^=$ characterised by a summer maximum is favoured by two factors: 1. higher SO_2 concentrations at a low altitude in the boundary layer in summer than in winter, and 2. enhanced photochemical activity, favouring the rapid conversion of SO_2 to sulphate.

At the rural site, SO_2 concentrations experienced a seasonal evolution characterised by a summer maximum. These higher summer SO_2 concentrations at a low altitude (near the ground level) are caused by the higher frequency of impacts on the ground of the SO_2 plumes emitted in tall stacks, induced by the strong convective activity caused by the heating of the land during the noon and afternoon periods (Querol et al., 1998b, 1999b). In the particular case of the MONAGREGA monitoring station, the SO_2 plume proceeds from the Teruel power plant.

The highest nss-$SO_4^=$ concentrations recorded in June and July were associated with high ozone concentrations and temperature increases, which suggests that enhanced photochemical activity is involved in the formation of ammonium-sulphate in summer (Figure 5-6 A). It is not easy to determine the chemical reactions that account for the simultaneous nss-$SO_4^=$ and ozone peak events in summer in the rural environment. This suggests that SO_2 is oxidised by O_3 on the aqueous surface of particles or in the gas phase by OH radicals given that ozone photolysis is the main source of OH (Warneck, 1988 and references therein). A similar nss-$SO_4^=$ summer maximum due to enhanced photochemical activity has also been reported in California (Meagher et al., 1983; Switzer et al., 1996).

It should be pointed out that although SO_2 and nss-$SO_4^=$ concentrations maximise in summer, there is no correlation between the day-to-day variations in the SO_2 and the nss-$SO_4^=$ concentrations (Figure 5-6 B). Most of the high nss-$SO_4^=$ events were recorded under relatively low SO_2 concentrations. This indicates that nss-$SO_4^=$ is not provided by fresh SO_2 emissions, i.e. direct impact of the Teruel power plant SO_2 plume on the MONAGREGA station. Thus, nss-$SO_4^=$ is associated with aged polluted air rather than with fresh SO_2 emissions. This association of nss-$SO_4^=$ with aged polluted air is probably caused by the relatively low oxidation rate of SO_2, maximum rates of 6%/h in summer (Hidy, 1994; Querol et al., 1999b).

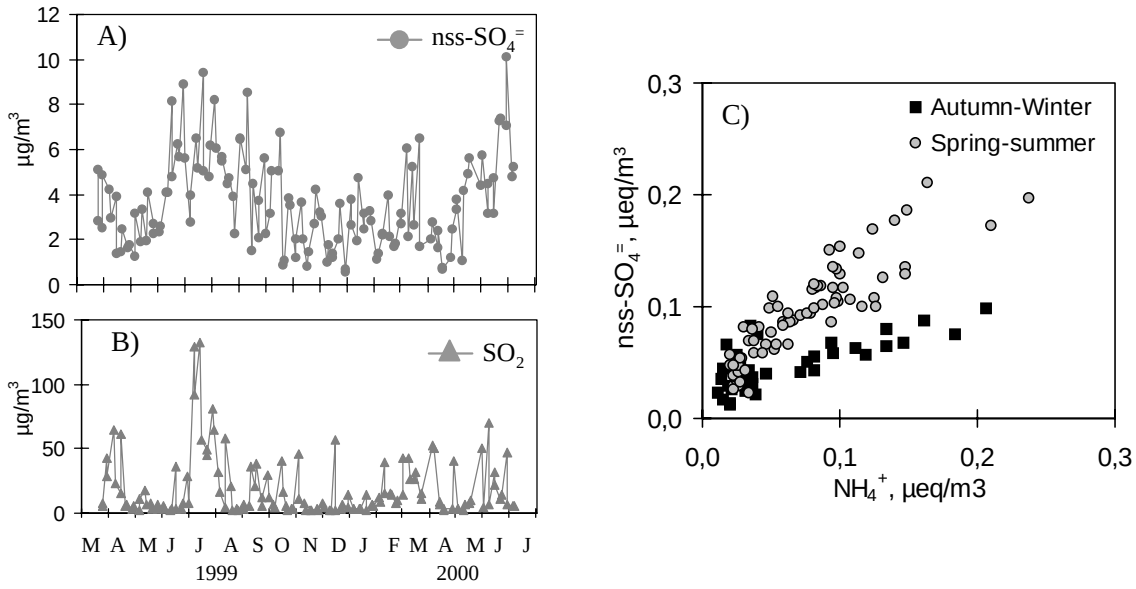

Figure 5-5. A) Daily mean values of nss-sulphate concentrations in PM10 at the MONAGREGA rural site in the Ebro basin. B) Daily mean concentrations of SO_2 during the periods for which nss-sulphate concentrations were determined. C) Nss-sulphate versus ammonium concentrations.

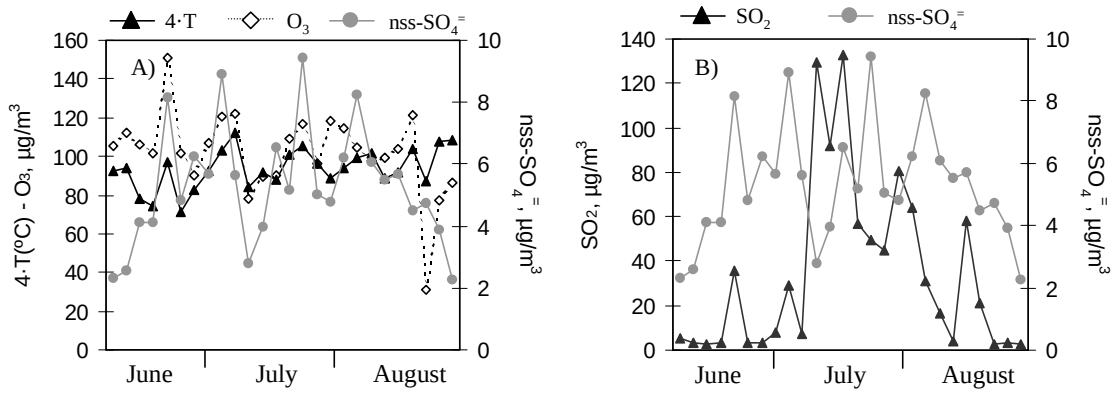

Figure 5-6. A) Daily mean values of nss-$SO_4^=$ in PM10 and O_3 concentrations and temperature at the rural site in the Ebro basin in summer months 1999. B) Daily mean values of nss-SO_4= and SO_2 concentrations.

At the rural site, the nss-$SO_4^=$ load accounted for 15-35% and 5-20% of bulk PM10 in summer and winter, respectively.

Carbonaceous aerosols

At the MONAGREGA rural site the concentrations of total carbon exhibited a large variability, but 3 periods of high carbon levels may be differentiated (Figure 5-7 A): from mid–spring to early summer (May to July both 1999 and 2000) and winter (December 1999 to January 2000). The average content of organic, elemental and mineral carbon fractions accounted for 83%, 8% and 10% of total carbon in PM10, respectively (Figure 5-7 B). Thus, average annual concentrations were estimated at 2.19µgOCm^{-3}, 0.20µgECm^{-3} and 0.27µgMCm^{-3} for the organic, elemental and mineral fractions in the PM10, respectively.

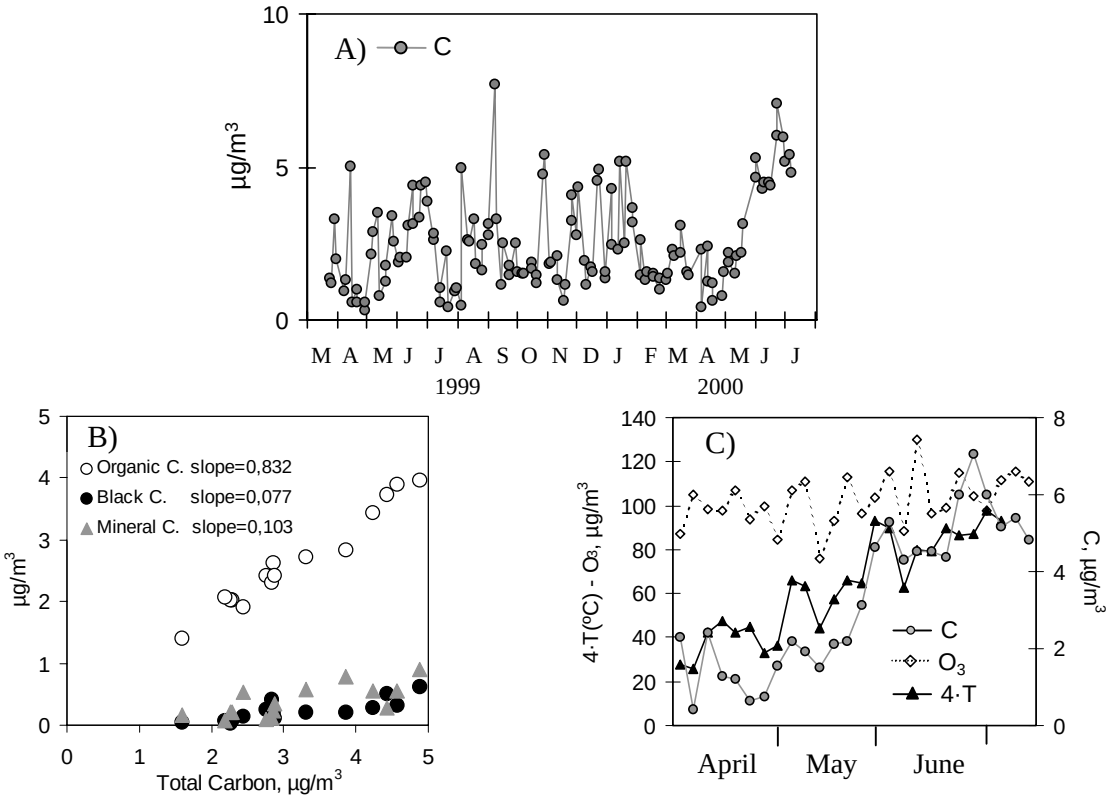

Figure 5-7. A) Daily mean concentrations of carbon in PM10 at the MONAGREGA rural site in the Ebro basin. B). Organic, black and mineral carbon contents versus concentrations of total carbon. C) Daily mean concentrations of carbon, O_3 and temperature from mid-spring to early-summer 2000.

Organic carbon, which accounts for the largest fraction of total carbon in PM10 at the rural site in the Ebro basin, is emitted into the atmosphere by natural biogenic and diverse anthropogenic sources. A significant fraction of the organic aerosol is formed by oxidation of organic gaseous precursors. Owing to the thermodynamic properties, some of these oxidation products tend to be distributed among the gas and aerosol phases, depending on ambient conditions (e.g. T and RH; Raes et al., 2000; Hoffmann, 2001 and references therein). At the MONAGREGA rural site, total carbon, temperature and ozone were associated with factor2 in the PCA (Table 5-2 and appendix 5) in spring and summer, suggesting that a significant fraction of organic carbon could occur in secondary organic aerosols. Moreover, from early to late spring (the transition from the cold to the warm season) temperature and carbon concentrations showed a parallel increasing trend (Figure 5-7 C). This suggests that during this period an important fraction of secondary organic aerosols could arise from biogenic emissions given their increase in the warm season due to enhanced plant transpiration. In winter, carbon was associated with ammonium and nitrate in factor4 (appendix 5), suggesting an increase in the fraction of carbon from vehicle exhausts during this period.

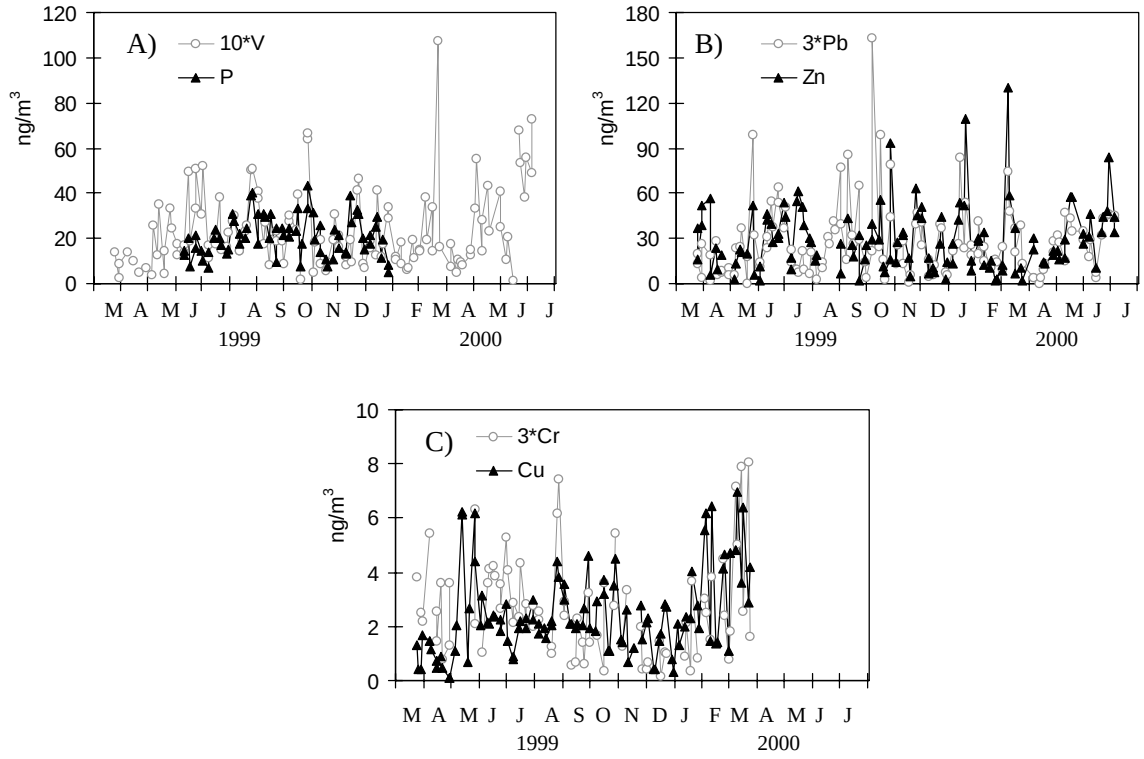

Figure 5-8. Daily mean concentrations of trace elements in PM10 at the MONAGREGA rural site.

It should be noted that although a significant fraction of carbon has been associated with the Industrial factor (mainly in summer; Table 5-2 and appendix 5), it is probable that nss-$SO_4^=$ (the main component representing the Industrial factor) and C do not proceed from the same source. Vehicle exhaust emissions are expected to contribute to C levels also in summer. The association of carbon, nss-$SO_4^=$ and ozone in the same factor in summer (appendix 5) is probably due to the fact that secondary carbonaceous and sulphate particles are formed under the same ambient conditions, such as those associated with the Regional events described in chapter 4.

The total carbon load accounted for 5-20% of bulk PM10 at the rural site.

Minor components

Sources of some trace metals (Cu, Cr, and Ni) at MONAGREGA could not be identified by PCA. Some chemical species of PM10 such as V and Pb are linked to several factors (Table 5-2). Vanadium is associated with the Industrial and Crustal factors (Table 5-2) owing to the typical association with natural clay mineral and coal combustion emissions. The influence of both sources is noted at MONAGREGA. Vanadium undergoes a slight seasonal evolution with a summer maximum (similar to nss-$SO_4^=$, Figure 5-5 B), suggesting that the emissions from the Teruel power plant are a possible V source. Overlapping this trend, V presented peak concentrations during African dust events (e.g. late August and late October). Cr, which may be released by coal combustion emissions (Singh et al., 2002) and mineral dust re-suspension, showed a summer

maximum. Copper showed a significant number of correlated peaks with Cr, suggesting a common source for these particulates. Phosphorus is a typical soil component, and its concentrations reached a maximum in summer, suggesting that soil re-suspension is the main source. Moreover, note that peak P levels were reached during the African dust events occurred in late August and late October. Lead is associated with three factors: Crustal, Industrial and Vehicles (Table 5-2). The significant number of Pb peak concentrations not associated with African dust events, but associated with NO_3^- and nss-$SO_4^=$ indicate a major anthropogenic origin, from vehicles and probably from the Teruel power plant, respectively. Zn showed significant correlated variations with Pb for long periods, which suggests a common source. This is reasonable since both coal combustion emissions and vehicle pollution have been identified as significant Zn and Pb sources (Pacyna, 1998; SLB, 2001).

5.2.2 PM10 at the L'HOSPITALET urban site

Table 5-3 shows the results of the PCA applied for the whole chemical PM10 data set. Four main chemical profiles (or sources) were also identified as contributing to PM10 levels at the L'HOSPITALET urban site. These four factors accounted for 85% of the variance in the PCA. The first factor (source 1) represents the crustal contribution to ambient PM10 levels given that this factor is defined by typical soil elements, such as Ca, Al, Fe, Sr, K, Ti and Mg. The chemical profile of this factor is very close to that obtained in the factor representing the mineral dust at the rural site (Table 5-2 discussed above). The main components defining the second factor (source 2) are nss-$SO_4^=$, NO_3^- and NH_4^+, which are derived from gas to particle conversion processes. This factor also shows a high factor loading for V and Ni, typically associated with fuel-oil combustion. As at the rural site, the high factor loading of nss-$SO_4^=$ indicates a significant influence of industrial sources in this factor. The third factor (source 3) constitutes the marine aerosol contribution to ambient PM10 levels, as evidenced by the high Na, Cl and Mg factor loadings. Finally, the fourth factor presents a high factor loading for road traffic pollutants such as vehicle exhaust products (C, Pb, Zn, Cu, Cl, Mn, NO_3^- and NH_4^+) and, in a minor proportion, road dust components (Ti, Fe, Ca).

The evolution time of the main components defining the PM sources is discussed below.

Mineral dust

Natural and anthropogenic sources contribute to ambient levels of crustal components at L'HOSPITALET in the Barcelona Metropolitan Area. During African dust outbreaks over Eastern Spain sharp peak concentrations of Al and Sr were recorded (Figure 5-9), indicating that African dust is the most important source of these crustal components in the Barcelona Metropolitan Area. During most of the African events similar Al concentrations tend to be simultaneously recorded at the rural Ebro basin site (MONAGREGA, Figure 5-2) and at the Barcelona area (L'HOSPITALET, Figures 5-9). Moreover, these peak Al concentrations in NE Spain are similar to those frequently recorded in Corsica (Bergametti et al., 1989; Dulac et al., 1992) and Sardinia (Molinaroli et al., 1993; Guerzoni et al., 1997). Owing to the lack of important sources of Al and Sr in the Barcelona

Table 5-3. Factor loading matrix for the L'HOSPITALET urban PM10 chemical composition obtained after applying a varimax normalised rotation.

	Factor1	Factor2	Factor3	Factor4
PM10	0,50	0,47		0,68
Ca	0,80			0,42
Al	0,93			
Fe	0,70			0,65
Mg	0,69		0,58	
Ti	0,86			0,38
Sr	0,88			
K	0,79			0,29
Mn	0,60			0,63
Pb	0,39			0,85
Zn			-0,57	0,52
Cu	0,29			0,75
Cr	0,44			0,73
Ni		0,66		
P	0,76			0,33
V		0,73		0,37
C	0,33			0,80
Na			0,89	-0,31
Cl			0,81	0,52
nss-$SO_4^=$		0,90		
NO_3^-		0,57		0,64
NH_4^+		0,78		0,48
%var	33	16	11	25
	Crustal	Industrial	Marine	Vehicles

Note: Factor loadings smaller than /± 0.25/ are not shown.

Metropolitan Area, these elements presented the lowest urban/rural concentration ratio (1.6 for Al and 1.2 for Sr) from the PM10 components determined. The concentrations of other typical mineral elements such as Ca, Fe, Ti, V or K also showed significant increases during the African events, but additional non-African peaks were recorded owing to the contribution of local urban sources of dust, such as road traffic and demolition dust. In fact, components such as Ca and Fe tend to show raised concentrations during winter as do traffic derived gaseous pollutants such as NO and CO. Owing to the influence of local urban sources of mineral dust, the levels of some crustal components in Barcelona are significantly higher than those recorded at the rural site in the Ebro basin (representative of the regional natural levels). As stated above, urban/rural concentration ratios were 2.4 for Ca, 2.7 for Ti and 4.0 for Fe, respectively.

The fact that mineral components are supplied by several sources in Barcelona is also supported by the chemical profiles of PM sources obtained in the PCA (Table 5-3). Thus, factor 1 (Table 5-3) accounts for the variations in the crustal component elements caused by the African dust events since it is the only factor including Al and Sr. However, the influence of the natural regional contribution derived from the re-suspension of the semi-arid soils, and the influence of

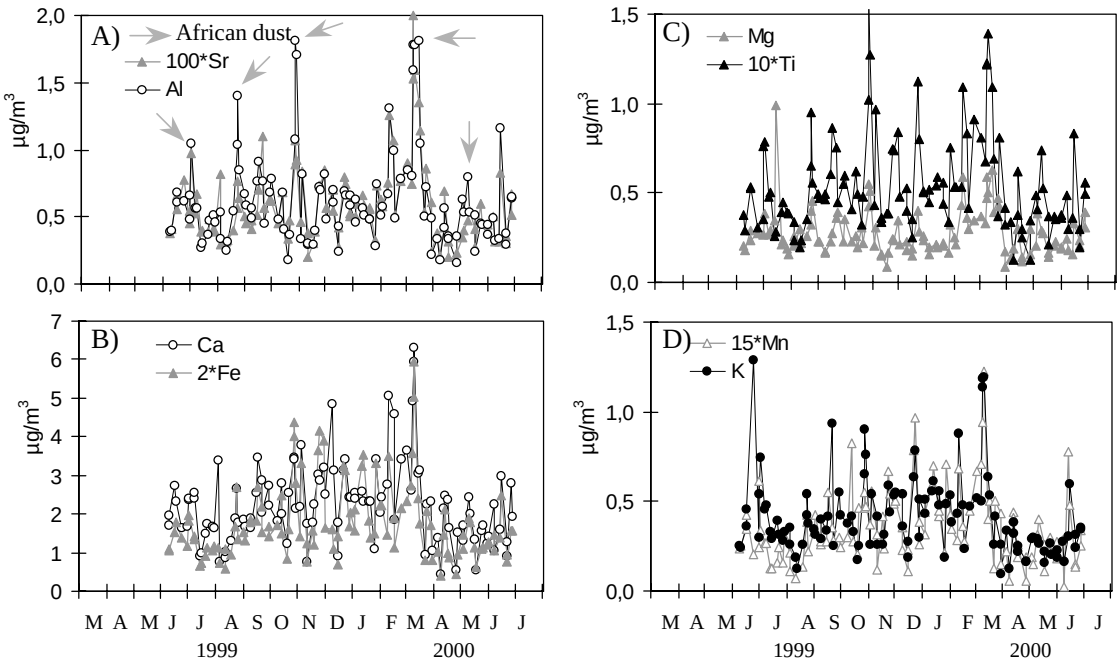

Figure 5-9. Daily concentrations of crustal components in PM10 at the L'HOSPITALET urban site. Grey arrow highlights the occurrence of African dust outbreak.

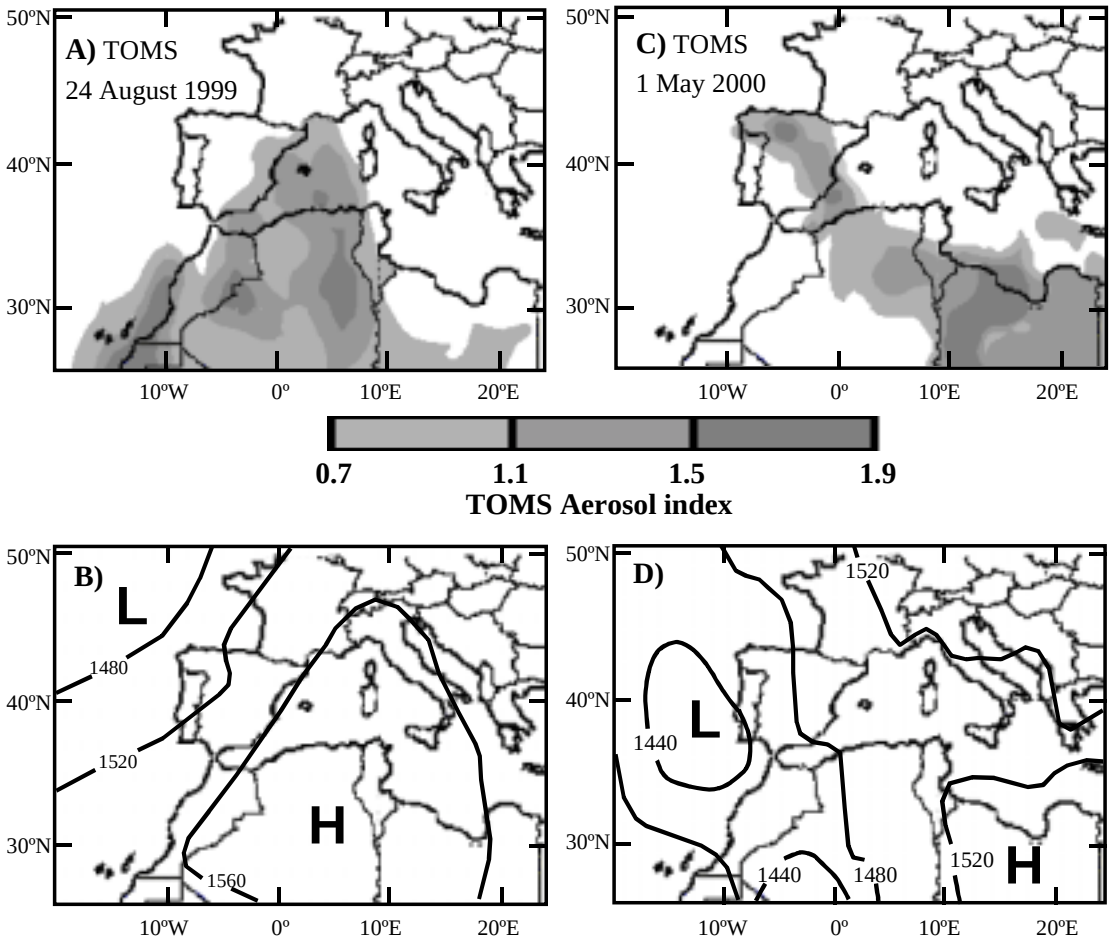

Figure 5-10. TOMS Absorbing aerosol index maps for 1 May 2000 (A) and 24 August 1999 (C). Altitude of the 850hPa pressure surface for 1 May 2000 (B) and (D) 24 August 1999.

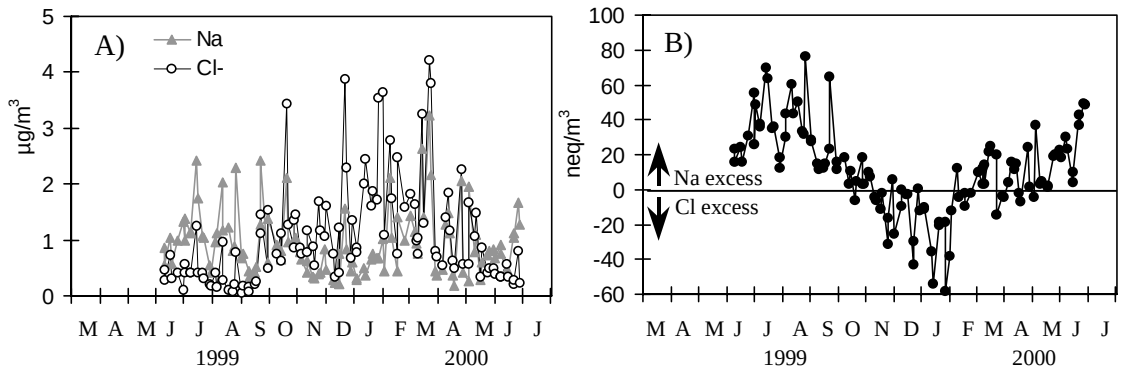

Figure 5-11. A) Daily concentrations of Na and Cl in PM10 at the L'HOSPITALET urban site. B) Na/Cl excess with respect to the marine Na/Cl ratio.

urban sources of crustal components, are also included here. Factor 4, associated with road traffic (road traffic + vehicles exhaust products), also included mineral dust components such as Ca, Fe, P, Ti, Mn, Pb and V.

Examples of African events are shown in Figure 5-10. In early May 2000 a depression located off Portugal originated a plume of dust which rapidly expanded from the Southeast of Spain to the North of Portugal. The event is evidenced in the time series of Al and other soil components at the MONAGREGA rural site (Ebro basin, Figure 5-2), but not at the L'HOSPITALET urban site in Barcelona since the Northeast of Spain was beyond the influence of the dust plume (Figure 5-9). A typical summer African dust episode occurred in late August 1999. Peak concentrations of Al were simultaneously reported in the Ebro basin and in Barcelona (Figures 5-2 and 5-9).

Sea salt

The time series of Cl and Na levels (Figure 5-11 A) exhibited reverse patterns with maximum Cl and minimum Na winter concentrations. However, frequent simultaneous concentration peaks of Cl and Na are superimposed on this seasonal trend because of the influence of marine emissions. The Na/Cl excess and deficit recorded in spring-summer and autumn-winter (Figure 5-11 B), respectively, is attributed to: 1. the presence of an anthropogenic source of Cl, and 2. the volatilisation of Cl in ambient air by the reaction of NaCl with acidic chemical species, such as HNO_3 and H_2SO_4 (Pio and Lopes, 1998). The anthropogenic origin of a significant fraction of Cl is supported by the source identification performed by means of the PCA (Table 5-3) since Cl is also included in the factor associated with traffic emissions. Moreover, the source identification in the PM2.5 (further presented) will also support the anthropogenic contribution to Cl ambient levels. The influence of the acid species in the volatilisation of Cl in summer is discussed below together with nitrate.

Nitrate

Concentrations of nitrate at L'HOSPITALET exhibited a seasonal evolution characterised by an autumn-winter maximum (Figure 5-12 A). Moreover, during the cold season NO_3^- and NH_4^+

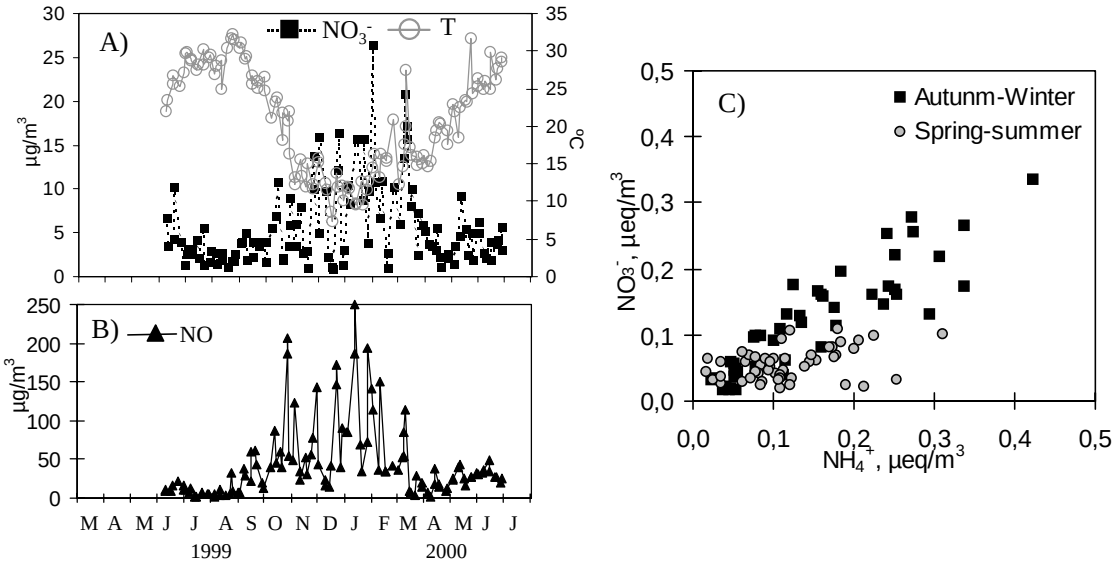

Figure 5-12. A) Daily mean values of nitrate concentrations in PM10 and temperature at the L'HOSPITALET urban site. B) Daily mean concentrations of NO during the periods for which NO_3^- concentrations were determined. C) Nitrate versus ammonium concentrations.

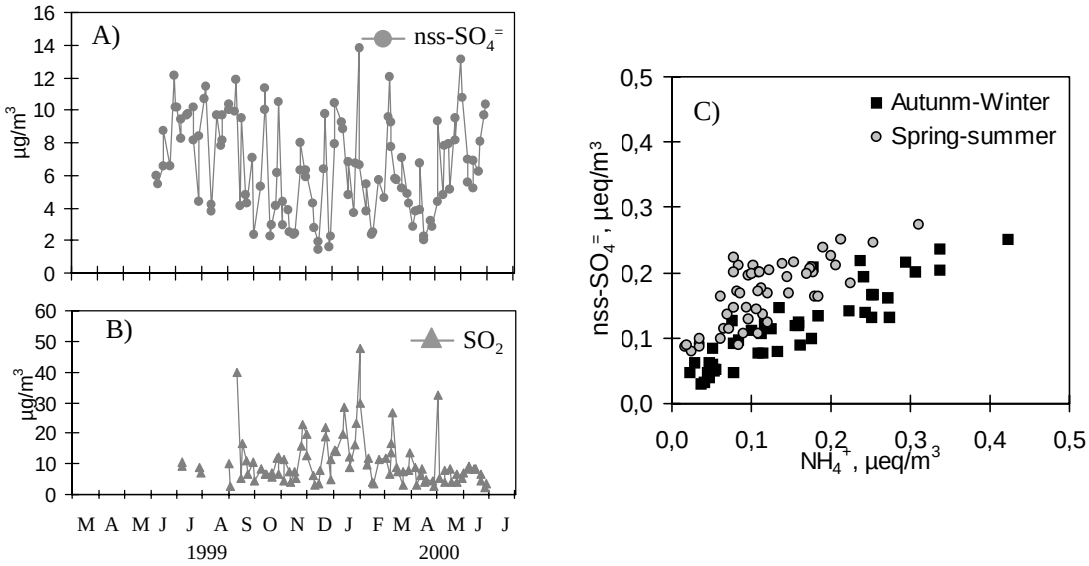

Figure 5-13. A) Daily mean values of nss-sulphate concentrations in PM10 at the L'HOSPITALET urban site in the Barcelona Metropolitan Area. B) Daily mean concentrations of SO_2 during the periods for which nss-sulphate concentrations were determined. C) Nss-sulphate versus ammonium concentrations.

levels exhibited a strong association that was not observed in spring and summer (Figure 5-12 C). Thus, as described for the rural site, the seasonal evolution of nitrate in Barcelona is due to the enhanced thermal stability of ammonium-nitrate in the cold season. In the warm season, minor concentrations of ammonium-nitrate are expected, and the occurrence of NO_3^- is mainly attributed to the reaction of gaseous HNO_3 with mineral species such as calcium-carbonate and/or with sea-salt to form $Ca(NO_3)_2$ and $NaNO_3$, respectively (Harrison and Kito, 1990, Wakamatsu et al., 1996). The latter is strongly supported by the Na/Cl excess observed in spring and summer in 1999 and 2000 at L'HOSPITALET (Figure 5-11 B), given that the reactions leading to $NaNO_3$ formation induce the Cl volatilisation (Pio and Lopes, 1998) by means of the reaction $NaCl(s) + HNO_3(g) \rightarrow NaNO_3(s)+HCl(g)$.

In the urban environment of Barcelona the seasonal evolution of nitrate is parallel to the seasonal evolution of NO, which is characterised by an autumn-winter maximum. This behaviour is different to that previously described at the rural site, where NOx did not show a seasonal trend.

In the urban environment of Barcelona the nitrate load reaches <15% and 15-30% of bulk PM10 in summer and winter, respectively.

Nss-sulphate

At the L'HOSPITALET urban site, the concentrations of nss-$SO_4^=$ exhibited a high background and a low variability during the summer, and a high variability in the cold season (Figure 5-13 A). As at the rural site, nss-$SO_4^=$ and NH_4^+ showed a strong association during the study period (Figure 5-13 C), which indicates that nss-$SO_4^=$ is mainly present as ammonium-sulphate ($(NH_4)_2SO_4$ and/or NH_4HSO_4). The high summer background concentrations are favoured by: 1. an enhanced photochemical activity which increases the SO_2 to sulphate conversion rates, and 2. the summer meteorology in the Western Mediterranean basin which favours the re-circulation of polluted air masses and the ageing of secondary pollutants in the study area (chapter 4). The latter contrasts with the autumn-winter situation, when the successive occurrence of urban pollution episodes and advections of Atlantic air masses (usually associated with cold fronts and rain) induce a wide variability in the concentrations of nss-$SO_4^=$ and other particulates (e.g. C, NO_3^-, NH_4^+ or Pb) and gaseous (NOx, CO or SO_2) pollutants (Figure 5-11, 5-12, 5-13, 5-14 and 5-15).

In the Barcelona area levels of SO_2 present a seasonal trend characterised by an autumn-winter maximum. This seasonal trend of SO_2 is similar to that observed in other gaseous pollutants (NOx or CO), and is highly influenced by the reduced capacity of dilution and dispersion of pollutants in autumn-winter (chapter 4). Emissions of SO_2 into the urban environment of Barcelona accounts for the occurrence of high nss-$SO_4^=$ events along the year. Given the high relative humidity in Barcelona (70-75% throughout the year), the formation of nss-$SO_4^=$ in the aqueous phase is expected to be important, especially during the cold season.

At the urban site in Barcelona, the nss-$SO_4^=$ load accounted for 15-35% and 5-20% of bulk PM10 in summer and winter, respectively.

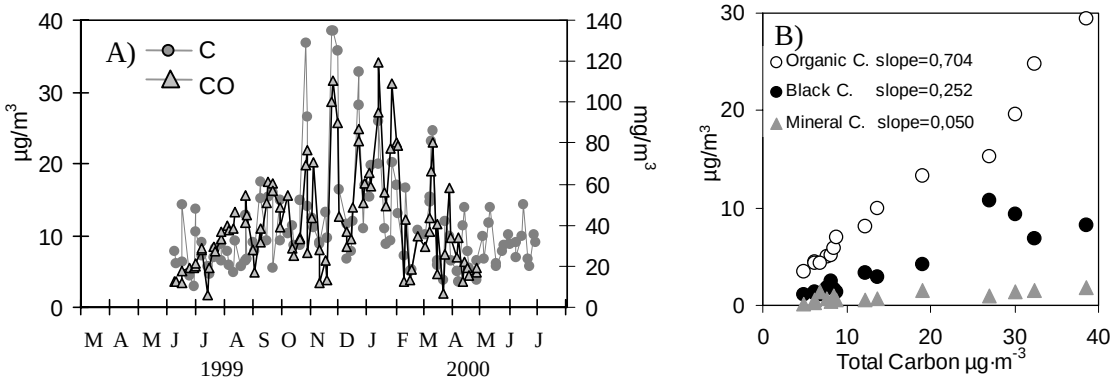

Figure 5-14. A) Daily mean concentrations of carbon in PM10 at the L'HOSPITALET urban site in Barcelona Metropolitan Area. B). Organic, black and mineral carbon contents versus concentrations of total carbon.

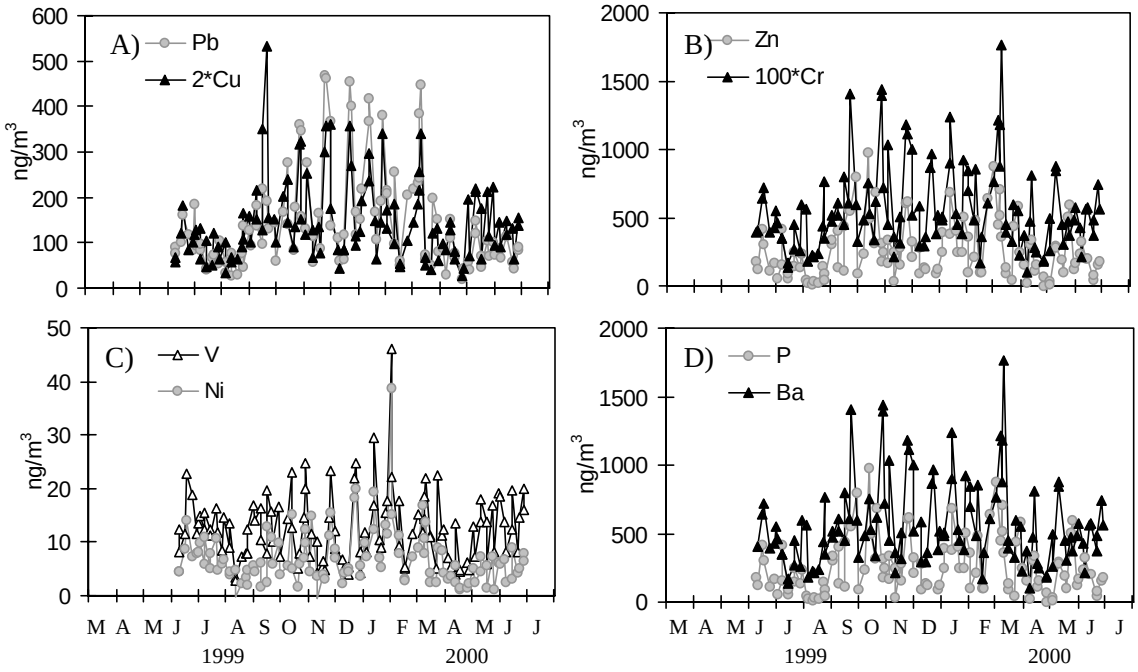

Figure 5-15. Daily mean concentrations of trace elements in PM10 at the L'HOSPITALET urban site

Carbonaceous aerosol

At the L'HOSPITALET urban site, the seasonal trend of carbon levels is characterised by an autumn-winter maximum (October to February). The mean organic (OC), elemental (EC) and mineral (MC) carbon fractions accounted for 70%, 26% and 5% of total carbon in PM10, respectively (Figure 5-14 B). Thus, the average annual concentrations for the carbonaceous species were estimated at 8µgOCm^{-3}, 3µgECm^{-3} and 0.6µgMCm^{-3}.

Although a contribution to ambient levels of organic carbon from biogenic emissions (e.g. from the coniferous forest located at the Collserola coastal range just behind Barcelona Metropolitan Area; Toll and Baldasano, 2000) cannot be ruled out, the winter maximum of carbon concentrations provides evidence of a major local anthropogenic origin. Poor dispersion conditions in the boundary layer together with an enhanced condensation due to the low temperatures account for the seasonal evolution (characterised by a autumn-winter maximum, Figure 4-14A) of carbon in the urban environment of Barcelona.

The total carbon load accounted for 15-30% and for 20-40% of bulk PM10 in spring-summer and autumn-winter, respectively.

Minor components

The levels of some trace elements in PM10 exhibited different seasonal patterns according to the different source origin and/or thermodynamic properties. Levels of Pb, Cu, Zn, Ni, Cr and Ba experienced a seasonal evolution characterised by an autumn-winter maximum (Figure 5-15). Although contributions from industrial emissions (e.g. Zn emissions from smelting) cannot be excluded, a major contribution from road traffic is expected, as deduced from the PCA (Table 5-3) and the similar trend observed in road traffic gaseous and particulate pollutants (e.g. CO, NO, carbon, NO_3^- in Figures 5-12 and 5-14). Zn, Cu, and Cr has been identified as particulate pollutants derived from road traffic. Cu and Zn are associated with vehicle emissions (Heinrichs and Brumsack, 1996). A significant fraction of Zn in urban air is associated with tyre remains. Moreover, Cu, Ba, Zn, Ni and minor amounts of Cr are associated with brake lining particles (SLB, 2001; Sternbeck et al., 2002).

Levels of Mn, K and Ti presented frequent high peak concentrations attributed to local urban sources (Figure 5-9) in autumn-winter. Overlapping this trend, these components present additional peak concentrations during African dust outbreaks, as in the case of the trend of Ca and Fe. This indicates that these components proceed from diverse sources. In addition to the African mineral dust inputs, these components may also be supplied by anthropogenic activities, such as demolition and traffic forced re-suspension of crustal material.

V and Ni show a significant number of correlated peak concentrations. Fuel-oil fired power plants in Barcelona (e.g. Besos power plant) may account for these elements in PM10, since V and Ni are typically associated with oil combustion (Heinrichs and Brumsack, 1996).

Finally, sources of phosphorus and barium have not been identified, although the PCA (Table 5-3) point to a possible combined crustal and road traffic contributions.

5.2.3 PM2.5 at the L'HOSPITALET urban site

The proportion of PM10 components distributed between the PM2.5 (fine fraction) and PM2.5-10 (coarse fraction) fractions provides information in addition to that provided by PCA for identifying PM sources (Table 5-4). Most of the soil components of PM10 (Ca, Mg Sr, Ti, Fe and Al) are present (>70% of its mass) in the coarse range (2.5-10µm). Sea spray PM10 components such as Na and a fraction of Mg also occurs in the coarse fraction. However, Cl is present in a smaller proportion than Na in the coarse fraction due to its partial anthropogenic origin (Table 5-3). A number of PM10 components (e.g. V, Ni, Zn, PK, Mn or Cu) have a significant fraction distributed between both fine and coarse fractions of PM (30-70%). This is due to the fact that these species are emitted by sources of different natures. For example, Mn, K and V are soil components (mainly coarse size), but are also supplied by combustion processes (mainly fine size). NO_3^- is present in the coarse and fine fractions because it occurs both as fine ammonium-nitrate and coarse sodium-nitrate and calcium-nitrate. The largest proportion of mass in the fine fraction was found for C, nss-$SO_4^=$ and Pb. The "anomalous" negative value for the percentage of NH_4^+-mass in the coarse fraction (which indicates a higher amount of NH_4^+ in PM2.5 that in PM10) is discussed below.

Table 5-4. Percentage of mass distribution between the fine and coarse fractions of PM10.

	Coarse	Fine
	% PM 2.5-10	% PM 2.5
Ca	81	19
Mg	77	23
Sr	75	25
Ti	74	26
Fe	73	27
Na	72	28
Al	71	29
Ba	63	37
Cr	60	40
Cl	53	47
Mn	48	52
K	48	52
P	48	52
NO_3^-	47	53
Cu	40	60
Zn	39	61
Ni	36	64
V	31	69
Pb	20	80
$SO_4^=$	20	80
C	18	82
NH_4^+	-35	135

Table 5-5. Factor loading matrix for the L'HOSPITALET urban PM2.5 chemical composition obtained after applying a varimax normalised rotation.

	Factor1	Factor2	Factor3	Factor4
PM2.5	0,74		0,52	
Ca		0,94		
Al		0,85		0,31
Fe	0,59	0,75		
Mg		0,94		
Ti		0,94		
Sr		0,93		
K	0,57	0,55	0,33	
Mn	0,65	0,37		
Pb	0,95			
Zn	0,81			
Cu	0,75			
Cr	0,85			
Ni	0,51		0,65	
P				0,53
V	0,32		0,68	
C	0,90			
Na				0,74
Cl	0,72			
$SO_4^=$			0,84	0,29
NO_3^-	0,67		0,54	-0,27
NH_4^+	0,48		0,82	
%var	26	26	15	7
	Vehicles	Soil	Industrial	Industrial ?

Note: Factor loadings smaller than /± 0.25/ are not shown.

A total of 64 PM2.5 samples were collected. Table 5-5 shows the results of the PCA applied to the whole chemical PM2.5 data set. After applying PCA to the PM2.5 chemical data set, four main chemical profiles (or sources) were identified as contributing to ambient PM2.5 levels at L'HOSPITALET in the Barcelona Metropolitan Area. These four factors accounted for 74% of the variance. The first factor represents the contribution of vehicle exhaust products to ambient PM2.5 levels, as indicated by a high factor loading of NO_3^-, C, Pb, Cl and Fe. The chemical profile of this vehicular factor in PM2.5 and that obtained in PM10 also at L'HOSPITALET only differ in the road dust components (Ca, P and Ti), which are not present in the PM2.5 vehicular factor. The second factor represents the contributions of crustal particulate matter since typical soil components present high factor loading (e.g. Ca, Al, Fe, Mg, Ti or Sr). The third factor includes secondary particles (nss-$SO_4^=$, NO_3^- and NH_4^+) and other potential products of combustion (Mn and V). Thus, an important contribution of industrial sources is expected in this factor. The fourth factor, which accounts for a minor fraction of variance (only 7%), presents a chemical profile mainly constituted by Na, P and Al, but it was not possible to identify a definitive emission source. This may be due to an unidentified industrial activity. This is the only factor (or source) that has no equivalent in the chemical profiles of PM10.

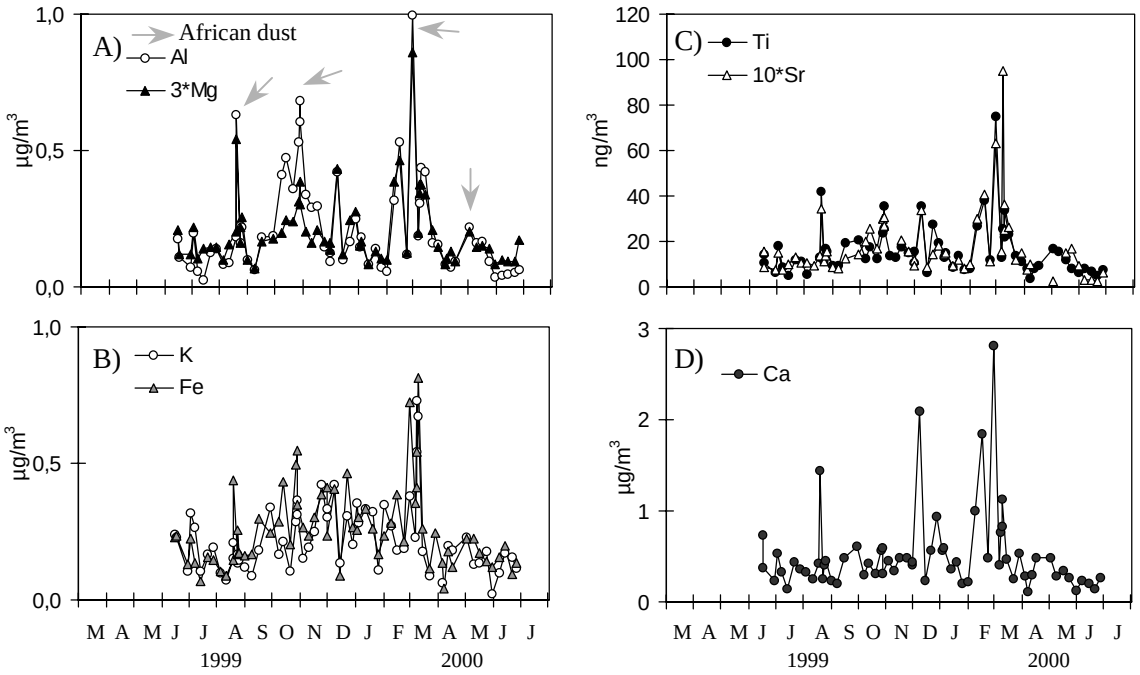

Figure 5-16. Daily concentrations of crustal components in PM2.5 at the L'HOSPITALET urban site. Grey arrows indicate the occurrence of African dust outbreaks.

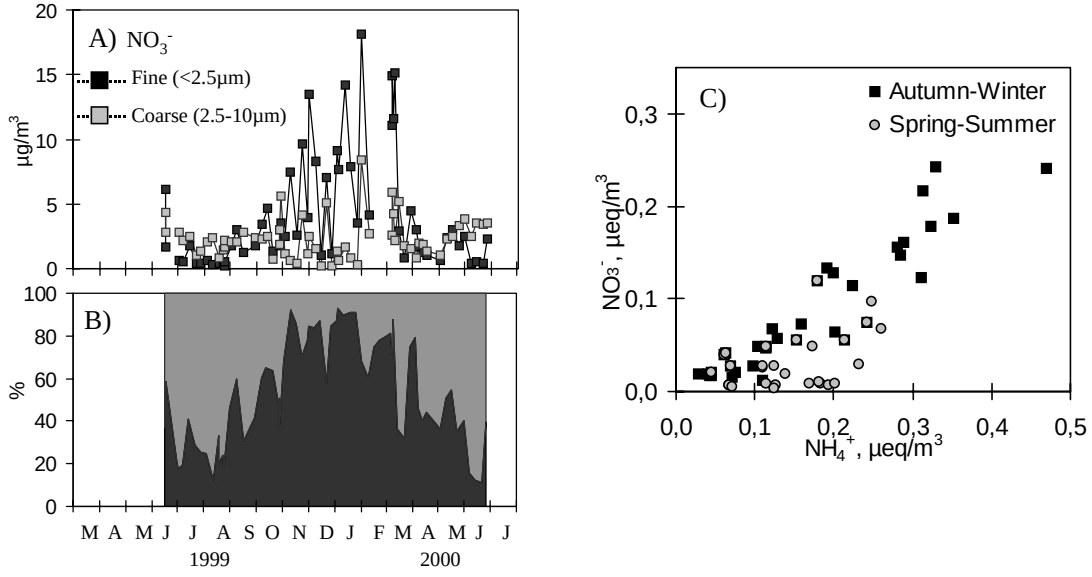

Figure 5-17. A) Daily mean values of nitrate concentrations in PM2.5 and in the PM2.5-10 at the L'HOSPITALET urban site in the Barcelona Metropolitan Area. B) Mass distribution of nitrate in PM2.5 (black area) and PM2.5-10 (grey area). C) Nitrate versus ammonium concentrations.

The evolution time of the main PM2.5 components defining the identified chemical profiles is discussed below.

Mineral dust

The influence of the African dust inputs is also evident in the time series of crustal component levels in PM2.5 in Barcelona (Figure 5-16). Levels of Al, Mg, Sr, Ti and Fe reached the highest concentrations during African dust events. Levels of K, Mn and Ca not only showed large increases during African dust events, but also presented additional non-African peaks due to the influence of the local urban "Vehicular" source (Table 5-5). It should be pointed out that Ca in PM2.5 is a better tracer of the African dust inputs than Ca in PM10. This indicates a dominant coarse mode (2.5-10µm) for Ca associated with urban sources (mainly road and demolition dust). This is also supported by the seasonal evolution of Ca, which was characterised by an autumn-winter maximum in PM10 and did not show a significant seasonal trend in PM2.5.

Nitrate

Levels of nitrate in PM2.5 exhibited a seasonal evolution characterised by an autumn-winter maximum (Figure 5-17 A). This trend resembles that described for nitrate in PM10 (Figure 5-12) because the seasonal evolution of nitrate is induced by the higher thermal stability ammonium-nitrate in the cold season and because ammonium-nitrate occurs in the fine fraction of PM (<2.5µm). Thus, levels of NO_3^- and NH_4^+ in the PM2.5 exhibited a strong association in autumn-winter. In spring-summer, a weaker correlation is observed with lower nitrate concentrations (Figure 5-17 C). Figure 5-17 A shows the time series of nitrate levels in the coarse (2.5-10µm) fraction. Nitrate levels in the coarse fraction show slightly higher background levels in summer. Moreover, the levels of nitrate in summer in the coarse fraction are significantly higher than those in the fine fraction. This is due to the fact that nitrate in the coarse fraction is present as sodium-nitrate and/or calcium-nitrate, and both (calcium and sodium) occur in the coarse fraction of PM. The previously discussed percentage of distribution of nitrate-mass between fine and coarse mode (Table 5-4) undergoes a marked seasonal evolution (Figure 5-17 B) as a consequence of this nitrate partitioning.

The previously highlighted "anomalous" negative value for the percentage of NH_4^+-mass in the coarse fraction is also related to the nitrate reactivity (Table 5-4). During the period June 1999 – June 2000, 62 simultaneous PM10 and PM2.5 samples were taken, and in 51 cases the levels of NH_4^+ in PM2.5 were higher than in PM10. The concentrations of NH_4^+ in PM2.5 exceeded those in PM10 by 14 % on average (Figure 5-18). This anomalous feature is due to the well known reaction between NH_4NO_3 and NaCl: $NH_4NO_3(a) + NaCl(a) \rightarrow NaNO_3(a) + NH_4Cl(g)$. This reaction results in the loss of gaseous NH_4Cl, which is volatilised from the PM10 filter. This reaction occurs in the PM10 filter, not in the PM2.5 one given that the NaCl marine aerosol does not reach the PM2.5 filter since it is retained in the PM2.5-inlet. Thus, an artificial loss of NH_4^+ and Cl takes place when sampling PM10 but not when sampling PM2.5.

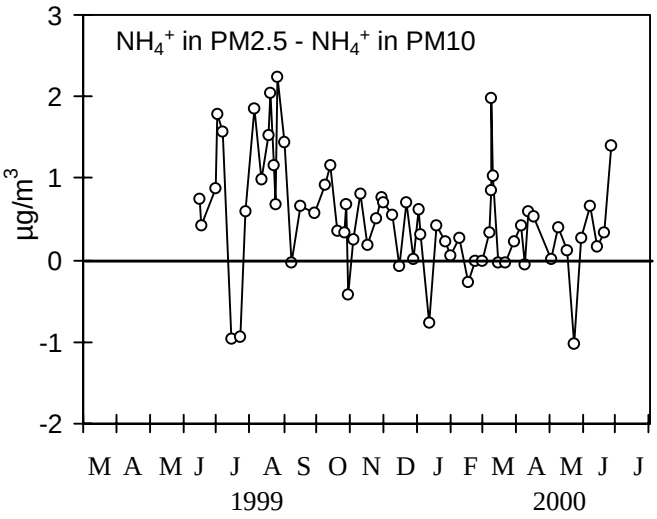

Figure 5-18. Difference between NH_4^+ concentrations in PM2.5 and PM10 at the L´HOSPITALET urban site.

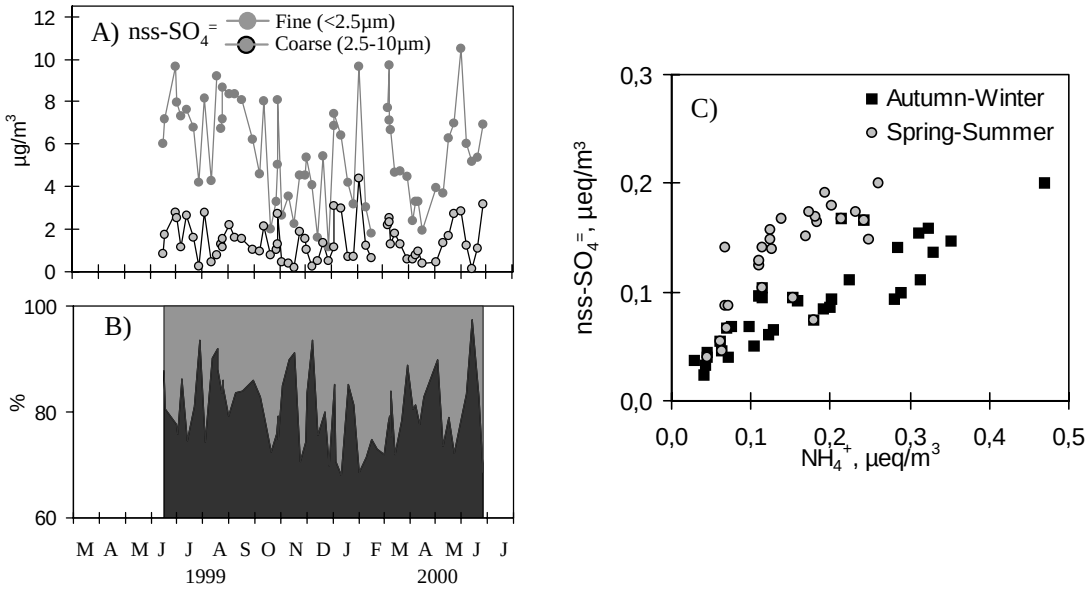

Figure 5-19. A) Daily mean values of nss-$SO_4^=$ concentrations in PM2.5 and in PM2.5-10 at the L'HOSPITALET urban site in the Barcelona Metropolitan Area. B) Mass distribution of nss-$SO_4^=$ in PM2.5 (black area) and PM2.5-10 (grey area). C) nss-$SO_4^=$ versus ammonium concentrations.

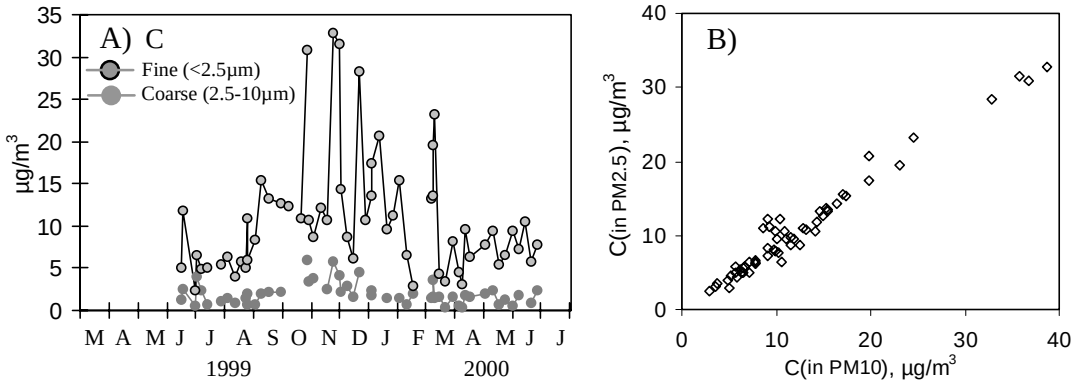

Figure 5-20. A) Daily mean concentration values of carbon in PM2.5 and PM2.5-10 fractions at the L'HOSPITALET urban site in the Barcelona Metropolitan Area. B) Concentrations of carbon in PM2.5 versus carbon concentrations in PM10.

At the L'HOSPITALET urban site in Barcelona the nitrate load represents <5% and 15-25% of bulk PM2.5 in summer and winter, respectively.

Nss-sulphate

Levels of nss-$SO_4^=$ in PM2.5 exhibited a high background and a low variability during the summer, and a high variability in the cold season (Figure 5-19 A). Levels of nss-$SO_4^=$ and NH_4^+ in the PM2.5 exhibited a strong association during the study period (Figure 5-19 C), which indicates that nss-$SO_4^=$ is mainly present as ammonium-sulphate ($(NH_4)_2SO_4$ and/or NH_4HSO_4). This behaviour is similar to that described for nss-$SO_4^=$ in PM10 owing to the fact that nss-$SO_4^=$ mainly occurs in PM2.5 (Figure 5-19 B). Thus, the discussion applied to nss-$SO_4^=$ in PM10 also applies to nss-$SO_4^=$ in PM2.5. Nss-$SO_4^=$ levels in the coarse fraction of PM did not show a significant seasonal trend (Figure 5-19 B).

At the urban site in Barcelona, the nss-$SO_4^=$ load accounted for 30-50% and 10-20% of bulk PM2.5 in summer and winter, respectively.

Carbonaceous aerosol

At the L'HOSPITALET urban site, levels of total carbon showed a seasonal trend characterised by an autumn-winter maximum (from October to February). This trend is similar to that described for C in PM10 given that most carbon-mass occurs in PM2.5 (Table 5-4). Thus, most of the discussion applied to C in PM10 also applies to C in PM2.5 with the only exception of the percentages of organic, elemental and mineral carbons in total carbon. This is due to the fact that calcium-carbonate mainly occurs in the coarse fraction of PM. Consequently, higher percentages of organic and elemental carbons in PM2.5 than in PM10 and a smaller fraction of mineral carbon in PM2.5 than in PM10 are expected.

The total carbon load accounted for 15-40% and for 30-60% of bulk PM2.5 in spring-summer and autumn-winter, respectively.

Minor components

Special attention is paid here to the evolution time of trace element concentrations (Figure 5-21) in the fine (<2.5µm) and coarse (2.5-10µm) modes.

As discussed above, Pb is mainly associated with traffic emissions and is mainly in the fine fraction mode (80% on average; Table 5-4). The high Pb Urban/Rural concentration ratio (14.4, Table 5-1) was due to leaded gasoline, which was still in use during the sampling period. The highest Pb levels were attained in autumn-winter. This seasonal evolution of lead is observed in the fine mode, whereas non significant variations occurs in the coarse mode. Zn and Cu, which are related to road traffic emissions (Table 5-3 and 5-5), are mainly present in the fine fraction (~60% on average). A significant correlation between the levels of each component in the fine and coarse fractions is observed, which suggests that the road traffic source (which involves exhaust emissions, tyre dust and brake lining particles) affects both size modes. As stated above, industrial contributions to these components cannot be ruled out owing to the high degree of industrialisation of the Barcelona Metropolitan Area.

V and Ni, which are both related to fuel-oil combustion (Table 5-3 and 5-5), are mainly in the fine mode range (70% of V and 64% of Ni). The levels of these components in the coarse mode do not show significant variations.

Phosphorus is distributed between the coarse and fine fractions in approximately equal proportions. Time series of phosphorus levels in the fine and coarse fractions do not show significant correlations, which suggests that P in the fine and coarse fractions are supplied by different sources. For example, P in the coarse fraction could be associated with soil re-suspension and in the fine fraction with a non-identified industrial source (as also suggested by the PCA; factor 4 in Table 5-5).

Ba and Cr are mostly present in the coarse fraction mode (63% of Ba and 60% of Cr). Ba emissions are associated with brake lining particles (Sternbeck et al., 2002). The coarse size of Cr points to road traffic (traffic forced re-suspension and/or brake lining particles) as a main source.

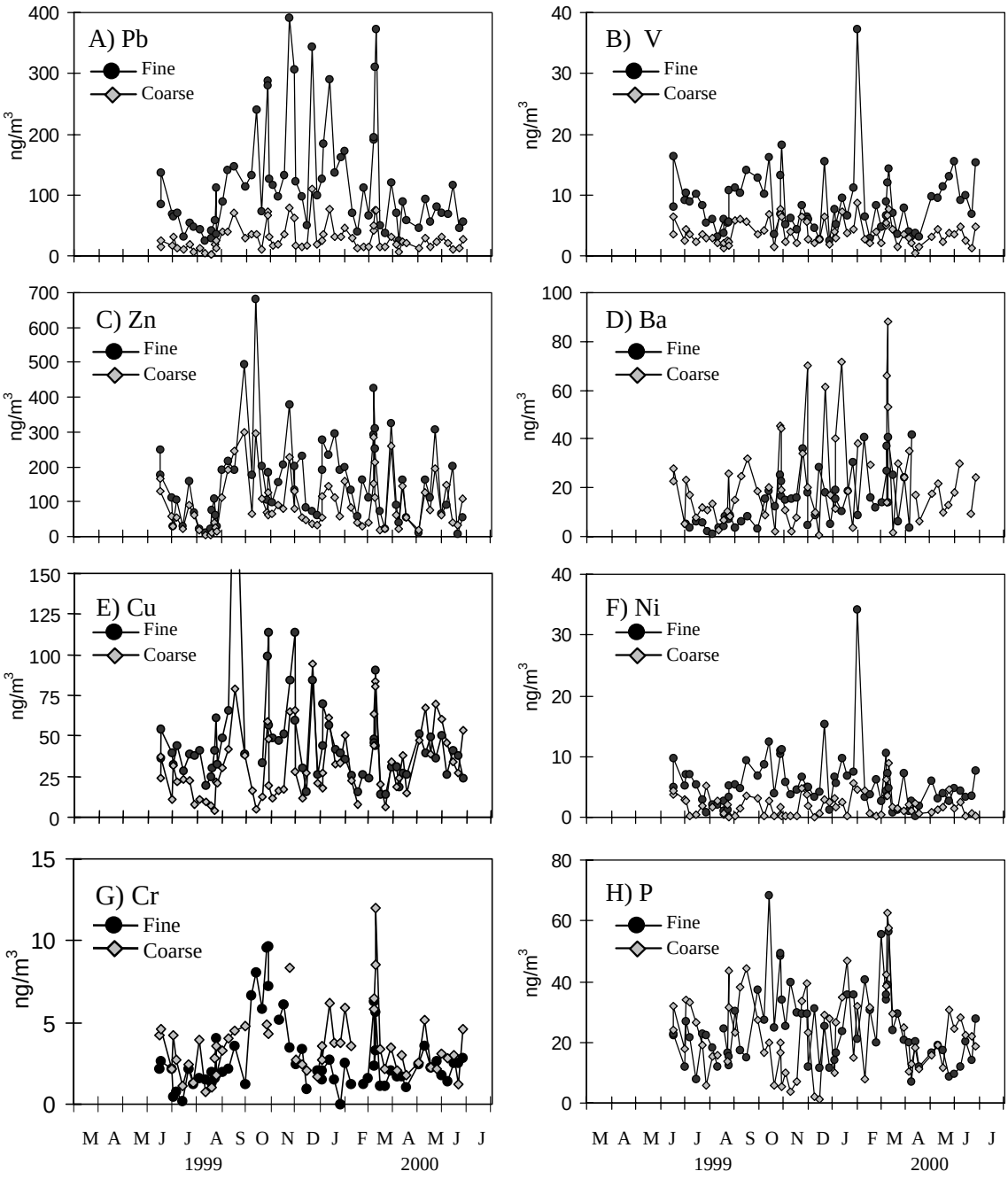

Figure 5-21. Daily mean values of trace elements in the fine (PM2.5) and coarse (2.5-10µm) fractions at the L'HOSPITALET urban site.

5.2.4 PM10 at the ONDA industrial site

At the ONDA industrial site (affected by the primary PM emissions from the ceramic factories), the sampling was performed from June – October 1999. A total of 48 samples were collected. Given the relatively low number of samples collected, the source identification by PCA at ONDA is less representative than at MONAGREGA and L'HOSPITALET, where 112 and 115 PM10 samples were collected, respectively. After applying PCA to the whole PM10 chemical data set, four main chemical profiles (or sources) were identified as contributing to PM10 levels, which accounted for 78% of the variance in the PCA (Table 5-6). The first factor (source 1) represents the crustal contribution to ambient PM10 levels given that Al, Ca, K, Mg, Fe, Sr or Ti present a high factor loading. The second factor (Industrial-1) is made up of secondary particles (nss-$SO_4^=$, NO_3^- and NH_4), V and Zn. The high factor loading of nss-$SO_4^=$, NO_3^- and V in the Industrial-1 factor suggests that this is related to the power generation at the Castelló power plant (which uses fuel-oil). Power co-generation units (using fuel-oil) from the ceramic factories may also contribute to this factor. The third factor presents a high factor loading for typical marine (Na, Cl and Mg) and anthropogenic (Ni, V and NO_3^-) components. The mixing of marine and anthropogenic species is attributed to a simultaneous inland transport of sea spray and particulate pollutants from urban/industrial coast sources during the inland sea-breeze period. The emissions from the petrochemical zone (located on the coast of Castelló) may account for the high factor loading of Ni, V and NO_3^- in the third factor. The fourth factor presents a high factor loading for K and trace elements such as Pb, Cu and Cr. A contribution from road traffic in this factor cannot be excluded (note that also NO_3^- and Ca present a high factor loading). However, a considerable industrial contribution is expected. Note that Pb levels at the ONDA industrial background site are slightly higher than at the L'HOSPITALET traffic site in Barcelona (Table 5-1), the road traffic density being much higher in Barcelona. Frit manufacture for tile covering in the ceramic production area may account for important emissions of Pb, Zn, Ni, Cu and Cr. Finally, the fifth factor is associated with C, P and O_3. This factor is considered to be associated with the bio-mass combustion in the burning of orange tree wastes, typical of the summer period in this area. Bio-mass burning has been widely reported to give rise to carbonaceous particles emissions and ozone formation (Crutzen and Andreae, 1990; Morales et al., 1990; Sanhueza et al., 1999). It should be pointed out that the introduction of ozone in the PCA did not alter the chemical profiles of theses factors since the same profiles were obtained when ozone was not introduced in the PCA.

Mineral dust

Anthropogenic and natural sources contribute to ambient levels of crustal components at ONDA. Levels of Al, Mg, Fe, and Ti at ONDA are twice those recorded at the MONAGREGA rural site, as discussed in section 4.1. These high background levels of crustal components are attributed to the emissions derived from the ceramic industry in the Millars valley, where the ONDA station is located. In contrast, mean levels of Ca and Sr at ONDA are very close to those recorded at the MONAGREGA rural site (Table 5-1). The fact that the load of Ca and Sr is lower than the load of Al, Mg, Fe and Ti is due to the use of clay in the ceramic industry. The natural input is

Table 5-6. Factor loading matrix for ONDA industrial PM10 chemical composition and O_3 levels obtained after applying a varimax normalised rotation.

	Factor 1	Factor 2	Factor 3	Factor 4	Factor 5
PM10	0,53	0,59		0,42	
Ca	0,82			0,36	
Al	0,96				
Fe	0,98				
Mg	0,72		0,66		
Ti	0,96				
Sr	0,93				
K	0,65		0,34	0,56	
Mn	0,96				
Pb		0,29		0,78	
Zn		0,61			0,31
Cu				0,74	
Cr	0,60	0,27			
Ni		0,41	0,67		
P	0,43				0,67
V	0,30	0,56	0,51		
C					0,88
Na			0,91		
Cl	0,34		0,63		
nss-$SO_4^=$		0,93			
NO_3^-		0,40	0,49	0,24	
NH_4^+		0,93			
O_3		0,28			0,83
%var	36	14	14	10	11
	Crustal	Industrial-1	Marine + Industrial-2	Industrial-3	Bio-mass burning

Note: Factor loadings smaller than /± 0.25/ are not shown.

evident since the highest concentrations of Al, Ti, Fe, Sr, Mg and Mn were recorded during the African dust outbreaks in late August and late October 1999 (Figure 5-22), and also at the MONAGREGA rural (Figure 5-2) and the L'HOSPITALET urban (Figure 5-9) sites. Other crustal components such as Ca, K, or V showed high levels during African events and additional non-African peaks due to the influence of local sources such as the ceramic industry and road traffic (vehicular factor for Ca and K in Table 5-6).

Sea salt

The time series of Cl and Na levels (Figure 5-23A) frequently exhibited simultaneous peak concentration events which indicate an influence of marine emissions, as evidenced by the results of the PCA. However, an excess of Na with respect to the marine Na/Cl ratio (Figure 5-23B) was recorded during the whole sampling period, which suggests: 1. volatilisation of Cl due to the reaction of NaCl with acid species, and/or 2.the occurrence of local Na sources. The former is supported by NO_3^- analysis (discussed below). However, Na is also associated with emissions from the frit production for tile covering.

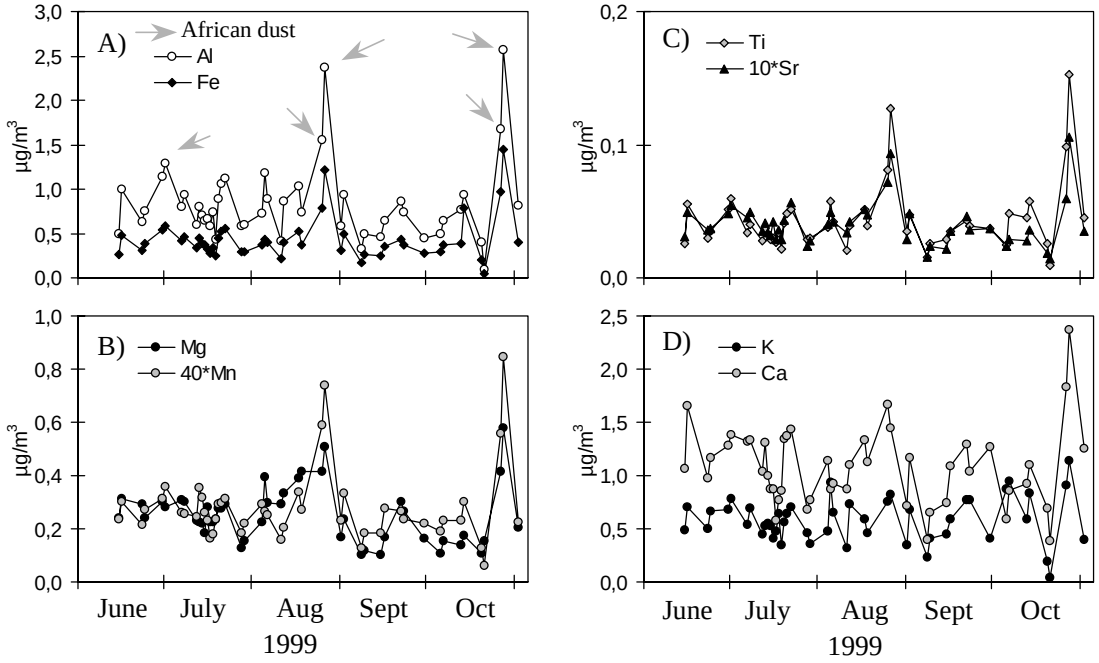

Figure 5-22. Daily concentrations of crustal components in PM10 at the ONDA industrial site. Grey arrows indicate the occurrence of African dust outbreaks.

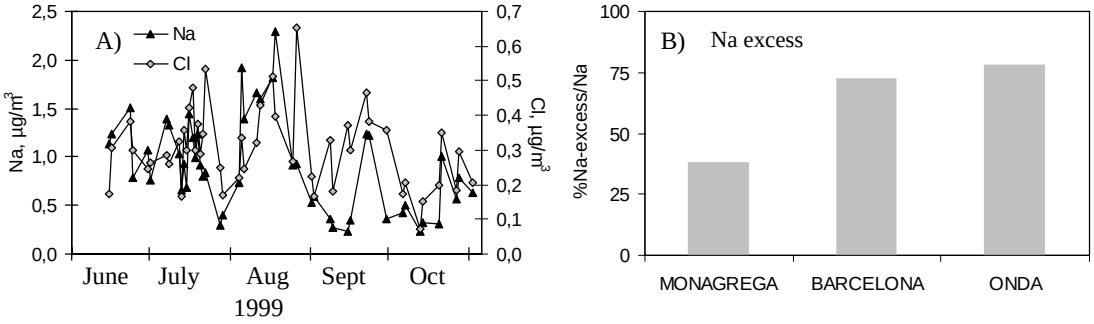

Figure 5-23. A) Daily concentrations of Na and Cl in PM10 at the ONDA industrial site. B) Mean percentage of Na excess (with respect to the marine Na/Cl ratio) at the MONAGREGA rural, the ONDA industrial and the L'HOSPITALET (BARCELONA) urban sites from June – October 1999.

Nitrate

At the ONDA industrial site, NO_3^- and NH_4^+ levels did not show a significant degree of correlation (Figure 5-24 C), which indicates that ammonium-nitrate is not the major form of nitrate occurrence. This is in agreement with nitrate behaviour previously described for the MONAGREGA rural and the L'HOSPITALET urban sites. The correlation between the levels of NO_3^- and the Na–excess (with respect to Na/Cl marine ratio) point to the occurrence of $NaNO_3$ (Figure 5-24B). The occurrence of $NaNO_3$ accounts for the above described Na/Cl excess by means of the reaction $HNO_3(g) + NaCl(a) \rightarrow NaNO_3(s) + HCl(g)$ in the ambient air.

At the ONDA industrial site the nitrate load accounted for 4-8% of bulk PM10 in summer.

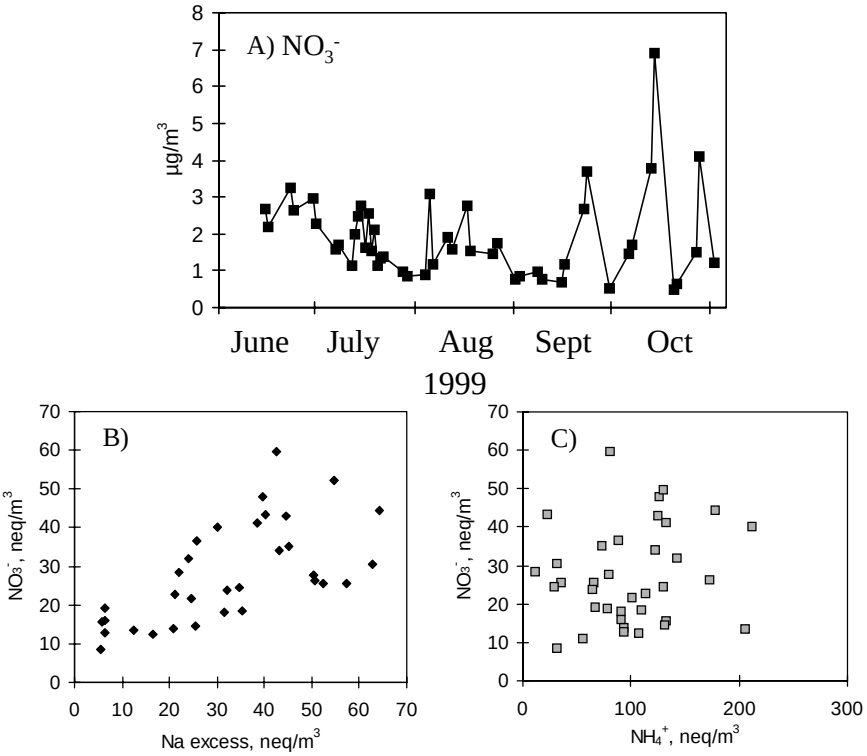

Figure 5-24. A) Daily mean values of nitrate concentrations in PM10 at the ONDA industrial site. B) Nitrate versus Na-excess (respect to the Na/Cl ratio) concentrations. C) Nitrate versus ammonium concentrations.

Nss-sulphate

At the ONDA industrial site nss-$SO_4^=$ and NH_4^+ exhibited a significant association, which indicates the occurrence of ammonium-sulphate ($(NH_4)_2SO_4$ and/or NH_4HSO_4). Levels of nss-$SO_4^=$ underwent a significant decrease from July-August to October – December, which suggests that nss-$SO_4^=$ undergoes a seasonal evolution characterised by a summer maximum. Moreover, peak concentrations of SO_2 are more frequently recorded in July-August, and SO_2 and nss-$SO_4^=$ show anti-correlated variations. This indicates that nss-$SO_4^=$ is not supplied by fresh SO_2 emissions, but that nss-$SO_4^=$ is associated with aged polluted air. Similar conclusions were obtained at the MONAGREGA rural site.

At the ONDA industrial site the nss-$SO_4^=$ load accounted for 20-35% of bulk PM10 in summer.

Carbonaceous aerosol

Carbon at ONDA reached the highest levels in the period mid-July to September, when carbon and ozone exhibited correlated variations. This is probably related to the emissions associated with the burning of orange tree wastes in this period. Note that P, which is a plant nutrient, is also associated with C and O_3. Bio-mass burning results in carbonaceous particles emissions and ozone production (Crutzen and Andreae, 1990; Sanhueza et al., 1999).

The carbon load accounted for 10-25% of bulk PM10 in summer.

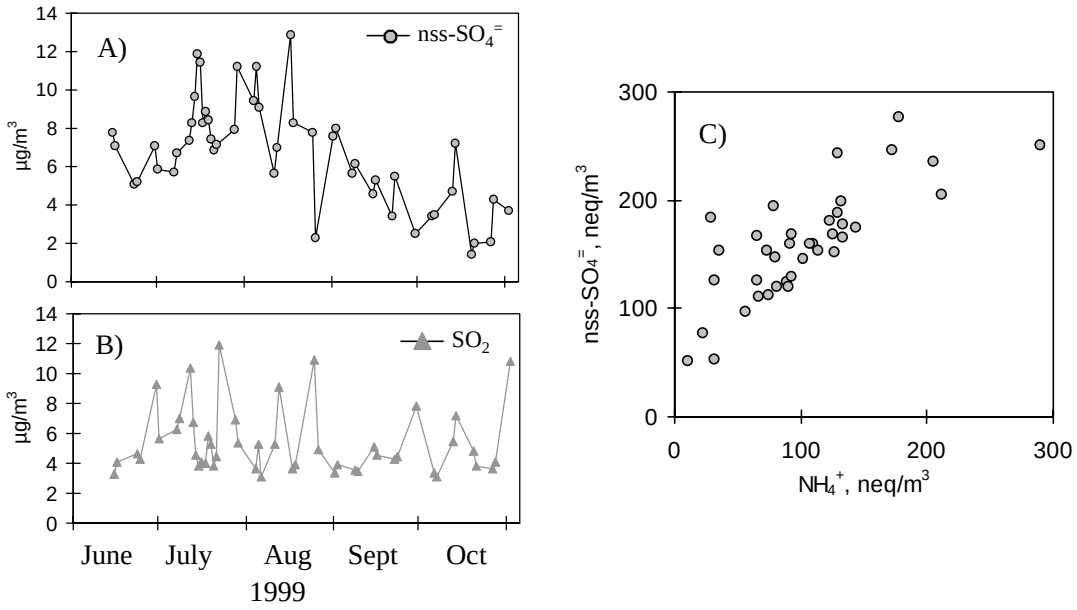

Figure 5-25. A) Daily mean values of nss-sulphate concentrations in PM10 at the ONDA industrial site. B) Daily mean concentrations of SO_2 in the periods for which nss-sulphate concentrations were determined. C) Nss-sulphate versus ammonium concentrations.

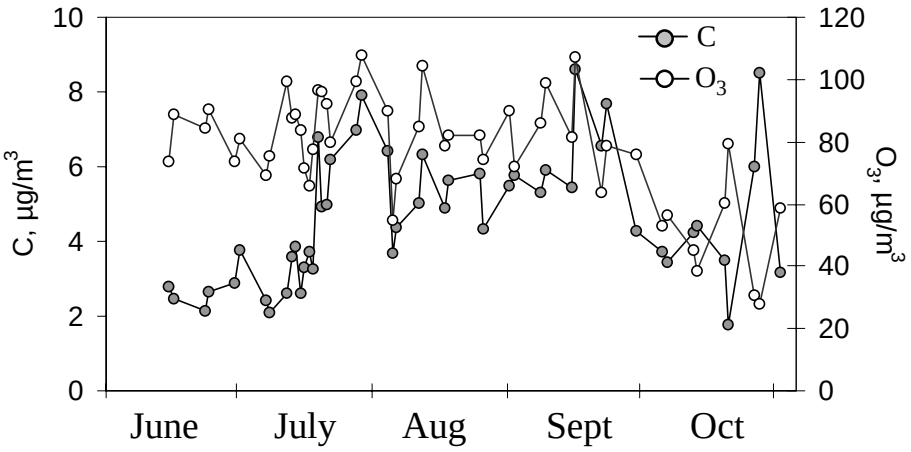

Figure 5-26. A) Daily mean concentrations of carbon in PM10 and O_3 at the ONDA industrial site from June – October 1999.

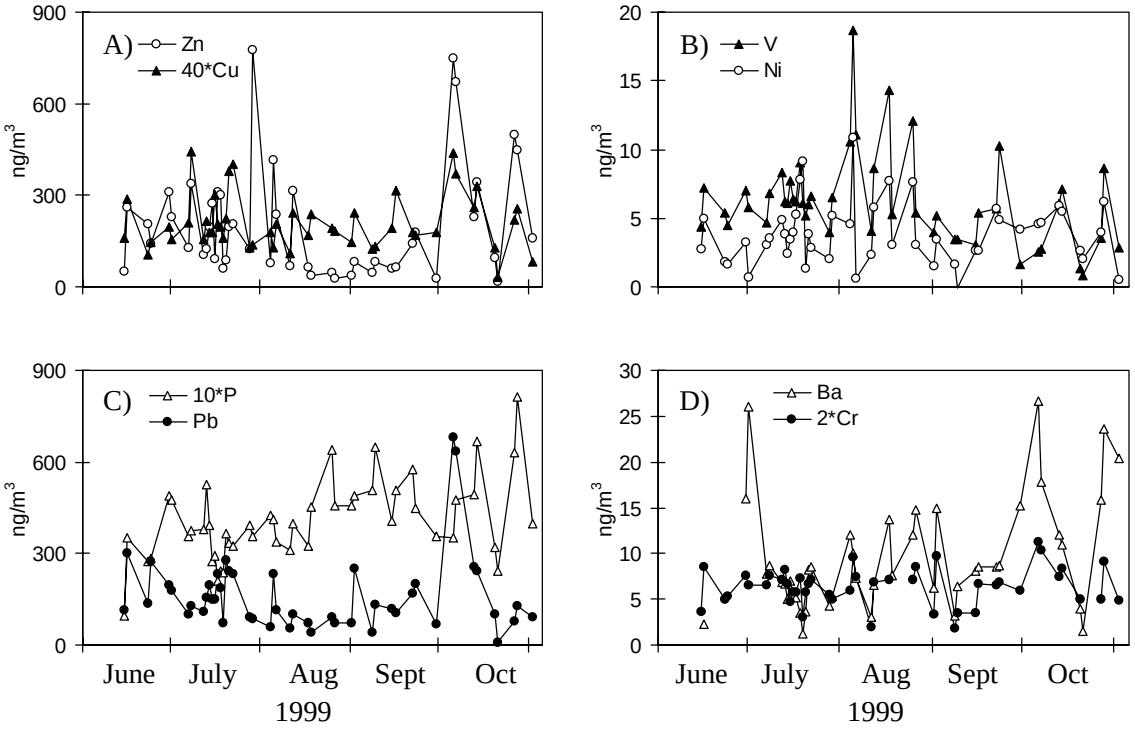

Figure 5-27. Daily mean concentrations of trace elements in PM10 at the ONDA industrial site.

Minor components

A detailed identification of source origin of trace elements at ONDA is not an easy task owing to the large number of industrial activities that are associated with the ceramic manufacture. The possible source origins of these trace elements (plotted in Figure 5-27) are discussed, taking into account the type of environment where the ONDA station is located.

The following activities are considered as potential sources of trace elements:

- Frit production for tile manufacture in the ceramic industry as a potential source of Pb, Zn, Ba, Ni, Cu, Fe, Cr and Na. These elements are frequently present in pigments, and are also used to reduce the melting point in frit production,
- Road traffic as a potential minor source of Pb, Cu, Zn and Cr (brake lining particles and vehicle exhaust products; SLB, 2001),
- Petrochemical activities (located in the coastal area) and/or power co-generation from fuel-oil as potential sources of Ni and V,

5.3 Source contribution

As stated in chapter 3, the source apportionment of PM10 and PM2.5 was performed using two methodologies: 1) Multi-linear Regression Analysis (MLRA), and 2) Mass Balance Analysis (MBA). In the MLRA, the contribution of each source (or chemical profile identified by PCA) was calculated by using the absolute score factors and the bulk PM levels as independent and dependent variables, respectively. In the MBA, the contribution of each source was determined as the sum of the PM components associated with each factor identified by PCA.

5.3.1 PM10 at the MONAGREGA rural site

5.3.1.1 Multi-linear regression analysis

Initially, the contribution of each identified source (Table 5-2) to PM10 levels at the MONAGREGA rural site was determined using the absolute score factors obtained after applying PCA to the whole PM10 data set (March 1999 – July 2000) as source tracers. However, the results showed an important underestimation of the Vehicular factor since the bulk Vehicular factor contribution (which in addition to nitrate also includes ammonium, lead, carbon, etc..) was lower than the nitrate concentrations. Since this underestimation of the Vehicular factor is believed to be caused by 1) the much higher variations in the nitrate concentrations in winter than in summer and 2) by the opposite seasonal trends of nitrate and sulphate, the source contribution to PM10 was performed on a seasonal basis. Thus, the absolute score factors, the multi-linear regression and the intersection constant were determined for different periods (March – September 1999, October 1999 – March 2000, and April – July 2000). This seasonal approach is also useful in assessing the impact of the emissions of the Teruel power plant on its surrounding area since the impact of the SO_2 plume on the ground level is more frequent in summer.

The mean PM10 source contributions were estimated at: 32% Industrial factor (source 2 = nss-$SO_4^=$ + others; Table 5-2), 24% Crustal factor (source 1 = mineral dust), 22% Vehicular factor (source 3 = NO_3^- + others), 11% Marine factor (source 3 = sea salt) and 11% attributed to other non-identified sources (determined by the intersection constant in the multi-linear regression). Figure 5-28 shows the daily contribution determined for each source. The Crustal factor (Figure 5-28 A) exhibited a slightly enhanced background contribution in summer and spring probably due to the semi-arid soil dust re-suspension in the Ebro basin. High mineral dust concentrations (20-25µg/m^3) were caused by African dust outbreaks. The contribution of this source accounts for the regional natural mineral dust. The contribution of the Industrial factor (Figure 5-28 B) is higher in summer because of the seasonal evolution of nss-sulphate and the enhanced association of ammonium and carbon with this factor in summer. As stated above, this source is associated with summer ozone episodes. The Marine factor (Figure 5-28 C) accounts for a low contribution in all seasons. The contribution of the Vehicular factor (Figure 5-28 D) was higher in the cold season because of the seasonal evolution of nitrate and the association of ammonium and carbon with this factor in autumn and winter. The contribution of this source to PM10 levels is strongly

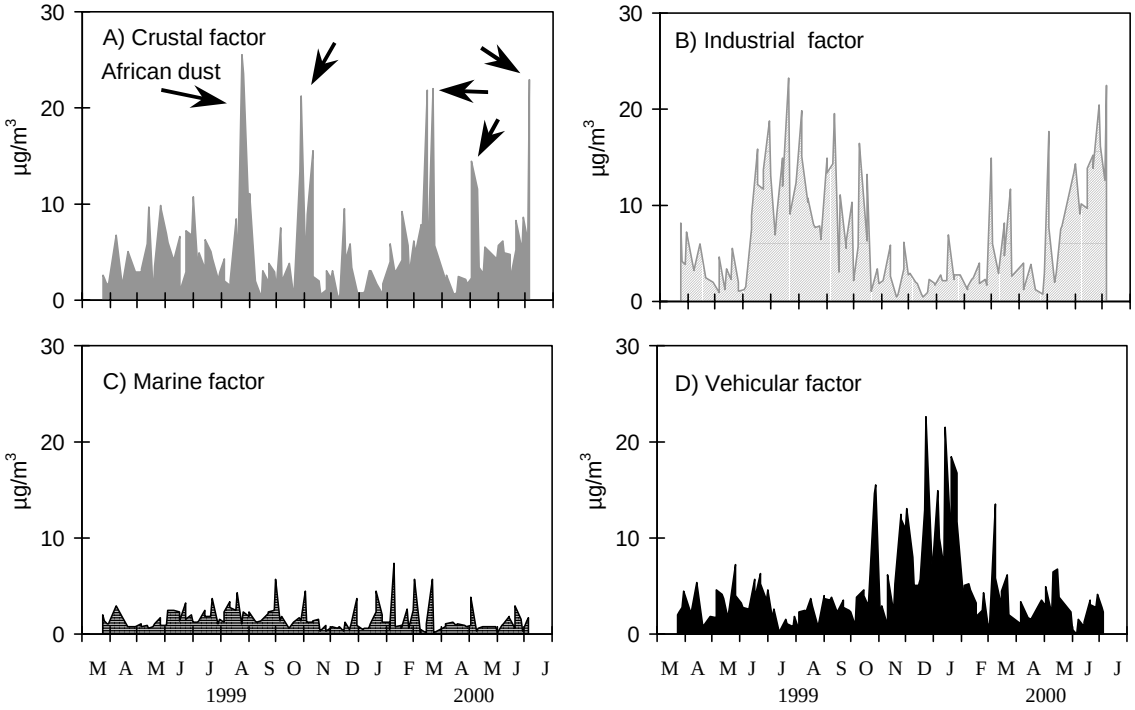

Figure 5-28. Daily mean source contributions to PM10 at the MONAGREGA rural site obtained by MLRA. Arrows in A) indicate the main African dust events.

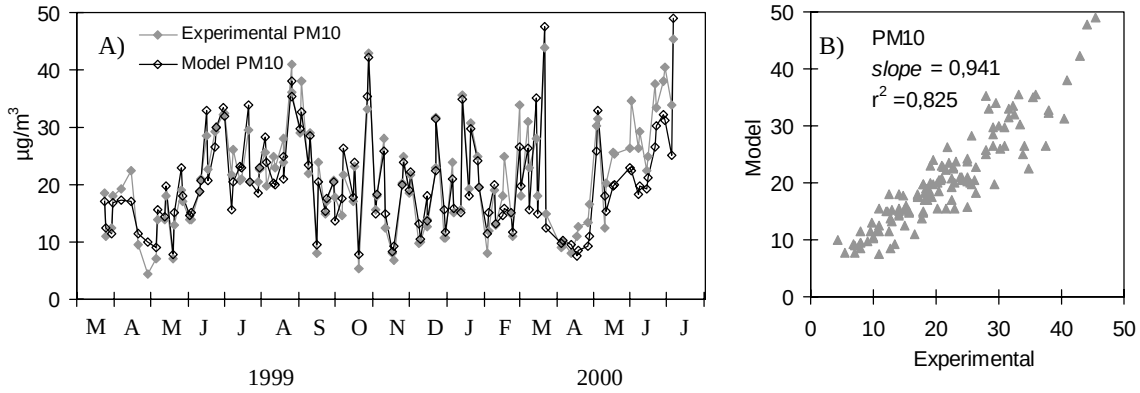

Figure 5-29. Experimental (gravimetric) and modelled (MLRA) daily PM10 concentrations at the MONAGREGA rural site.

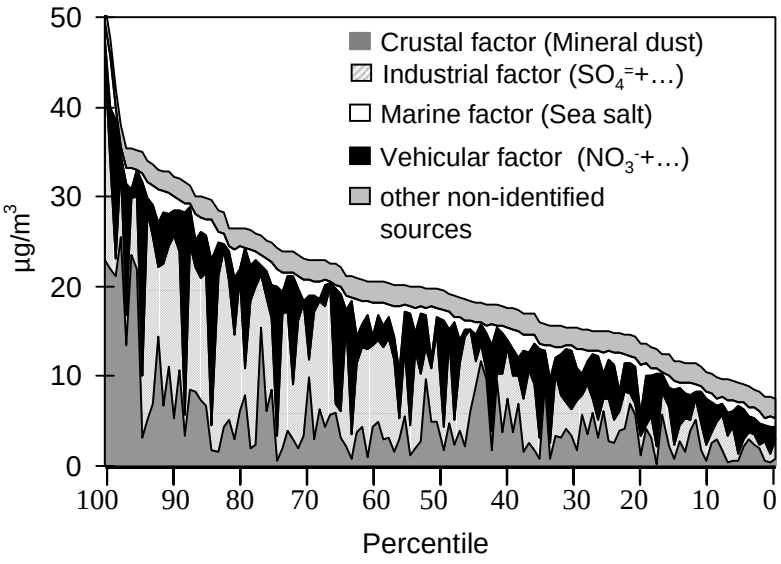

Figure 5-30. Daily PM10 concentrations at the MONAGREGA rural site in the Ebro basin in descending order, showing the contribution of each source obtained by MLRA.

dependent on the thermodynamic properties of nitrate and probably on some organic species. The contribution of other non-identified sources was 2.2µg/m^3 (average contribution from that obtained on a seasonal basis: 2.3µg/m^3 for March - September 1999, 2.2µg/m^3 October 1999 – March 2000 and 2.0µg/m^3 for April-July 2000, respectively).

Levels of PM10 in the model were determined as the sum of each source contribution. Figure 5-29 shows the experimental and modelled daily PM10 concentrations. The model reproduces the experimental data fairly satisfactorily, 6% of underestimation of experimental PM10 concentrations is observed. In summer PM10 levels present a high background (>20µg/m^3), which is caused by the enhanced contribution of the Industrial and Crustal factors. In autumn and winter the Vehicular factor is dominant, and the concentrations of PM10 undergo significant variations (episodically >30µg/m^3 alternating with <10µg/m^3). The highest PM10 concentrations were recorded during outbreaks of African dust, often exceeding 40µgPM10/m^3.

Figure 5-30 shows the daily PM10 concentrations at MONAGREGA in descending order displaying the source contributions. The highest PM10 events are caused by African dust outbreaks which dominate the 100th-95th percentile range. The 50th – 95th percentile range is mainly dominated by the Industrial factor (nss-$SO_4^=$+….), and episodically by the Vehicular factor (source 4: NO_3^- +….). Dust concentrations during intense African dust events fall within the range of 20-25µg/m^3 in PM10 (Figure 5-29 A), which accounts for 40-50% of the EU PM10 daily limit value (50µgPM10/m^3). In the study period (115 days in June 1999-June 2000), on 5 sampling days the mineral dust concentrations exceeded 20µg/m^3 in PM10 during African dust episodes. During these events, the dust load accounted for 50-80% of PM10 at the rural site, respectively.

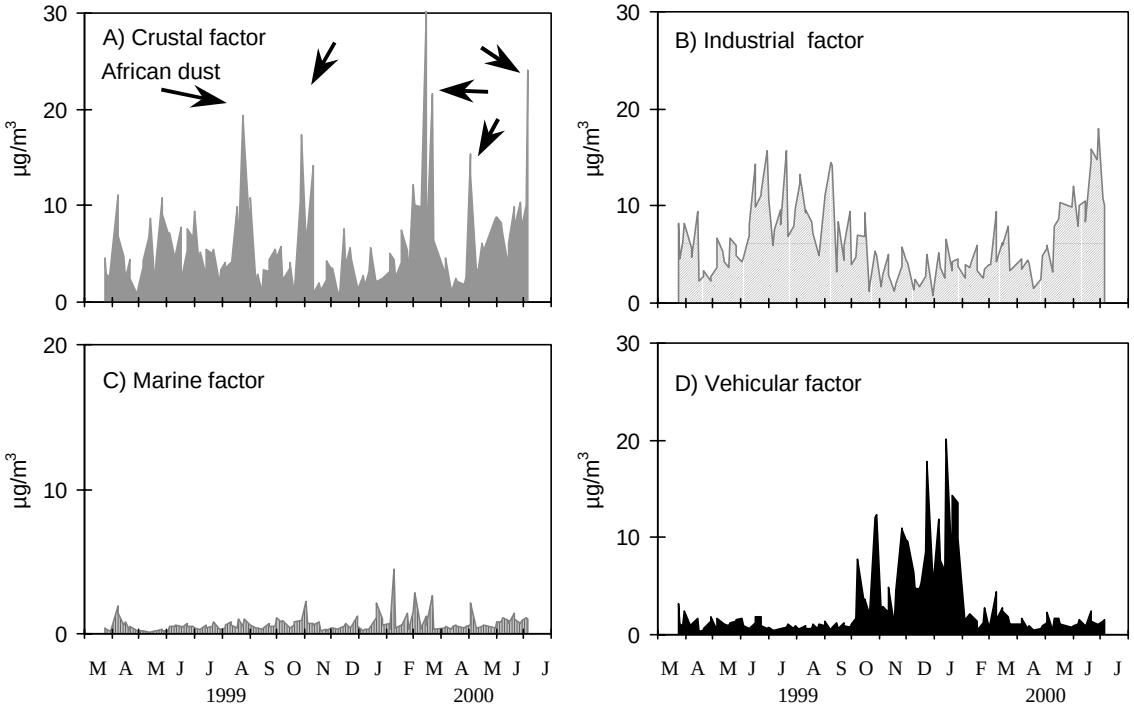

Figure 5-31. Daily mean source contributions to PM10 at the MONAGREGA rural site obtained by MBA. Arrows in A) indicate the main African dust events.

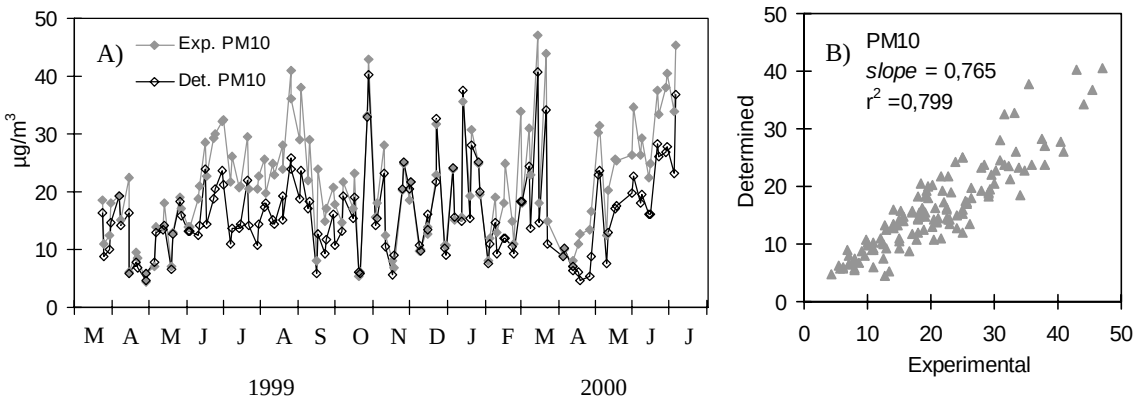

Figure 5-32. Experimental (gravimetric) and modelled (MLRA) daily PM10 concentrations at the MONAGREGA rural site.

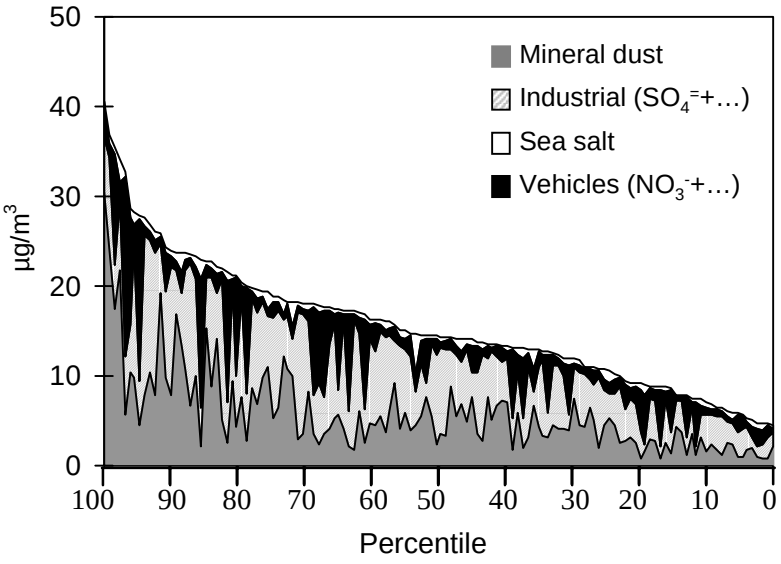

Figure 5-33. Daily PM10 concentrations at the MONAGREGA rural site in the Ebro basin in descending order, showing the contribution of each source obtained by MBA.

5.3.1.2 Mass balance analysis

The source contributions were estimated as the sum of the PM10 components associated with each previously identified source or factor (Table 5-2) following the methodology described in chapter 3. The mass of the PM10 components which presented a significant factor loading in several sources was distributed between these sources in accordance with the results of the mean source apportionment (see details in appendix 6). Moreover, the PM10 components estimated by indirect determinations were included. Thus, the Crustal source included Ca, $CO_3^=$, Al_2O_3, SiO_2, Mg, Mn, Sr, Ti, Fe, 0.7*K and 0.5*V. The marine contribution was calculated as the sum of Na, Cl and ss-$SO_4^=$. The Industrial contribution was estimated as the sum of nss-$SO_4^=$, a fraction of NH_4^+, 0.75*Zn, 0.3*Pb and 0.5*V. The Vehicular contribution was estimated as the sum of NO_3^-, a fraction of NH_4^+, 0.25*Zn, 0.3*K and 0.7*Pb. In the warm season, levels of OC+EC were added to the Industrial source, whereas in the cold season (October – February) they were added to the vehicular source. The fact that ammonium-sulphate occurs during the whole year and ammonium-nitrate only in autumn-winter was taken into account when determining the fractions of NH_4^+ associated with the Industrial and Vehicular sources.

The mean PM10 source contributions were estimated at: 31% Industrial (nss-$SO_4^=$ + others), 28% Crustal (mineral dust), 13% Vehicular (NO_3^- + others) and 3% Marine (sea salt). Figure 5-31 shows the daily contribution of each source. The results of the daily source apportionment are qualitatively similar to those obtained by MLRA. Only quantitative differences are observed, which will be discussed in section 5.3.5.

Figure 5-32 shows the experimental (obtained by the gravimetric method) and determined (sum of the source contributions from MBA) PM10 levels. The determined fraction of the experimental PM10 reached 74%.

Figure 5-33 shows the daily PM10 concentrations at MONAGREGA in descending order displaying the source contributions. The results are qualitatively similar to those obtained from MLRA.

5.3.2 PM10 at the L'HOSPITALET urban site

5.3.2.1 Multi-linear regression analysis

The source (Table 5-3) contribution to PM10 at the L'HOSPITALET urban site was determined using the absolute score factors of PCA applied to the whole PM10 data set (June 1999 – June 2000). Initially, a negative marine contribution was obtained (negative slope of PM10 versus the marine absolute score factors). The negative contribution of the Marine factor was induced by the occurrence of frequent episodes of strongly anti-correlated Na and PM10 variations. This gave rise to an anti-correlation between the Marine absolute score factor and PM10. In order to obtain a better approximation of the source apportionment, the marine contribution was calculated as the sum of Na, Cl and ss-$SO_4^=$. Levels of Cl and ss-$SO_4^=$ were determined from the Cl/Na and ss-$SO_4^=$/Na marine ratio. Thus, the source apportionment was performed for the "non marine – PM10 fraction" (nm-PM10).

The mean PM10 source contributions were estimated at: 43% Vehicular factor (carbon, NO_3^- + others), 29% Industrial factor (nss-$SO_4^=$ + others), 23% Crustal factor (source 1 = mineral dust, Table 5-3) and 5% Marine factor. The contribution of other unidentified sources was not estimated since a negative intersection constant was obtained in the multi-linear regression.

Figure 5-34 shows the daily contribution of each source. The Crustal factor (Figure 5-34 A), which includes both natural and anthropogenic mineral dust, exhibits 5-10µg/m^3 of background contribution. Most of the high crustal PM events were caused by African dust outbreaks, with frequent dust concentrations between 20 and 30µg/m^3. The Industrial factor (Figure 5-34 B) exhibits a high background contribution in the warm season induced by the seasonal evolution of nss-sulphate. The Marine fraction accounts for a low contribution. The contribution of the Vehicular factor (Figure 5-28 D) was higher in the cold season because of the seasonal evolution of nitrate. The contribution of this source is strongly dependent on the thermodynamic properties of nitrate and probably on some organic species.

Levels of PM10 in the model were determined as the sum of each source contribution. Figure 5-35 shows the experimental and modelled daily PM10 concentrations. The model reproduces the experimental data fairly satisfactorily, 2% of underestimation of the experimental PM10 concentrations being observed. In spring-summer the bulk PM10 levels present a low variability, being favoured by the high background contributions of the Industrial and Crustal factors. In autumn and winter the Vehicular factor is dominant, and the concentrations of PM10 undergo significant variations (frequently >75µg/m^3 alternating with <40µg/m^3).

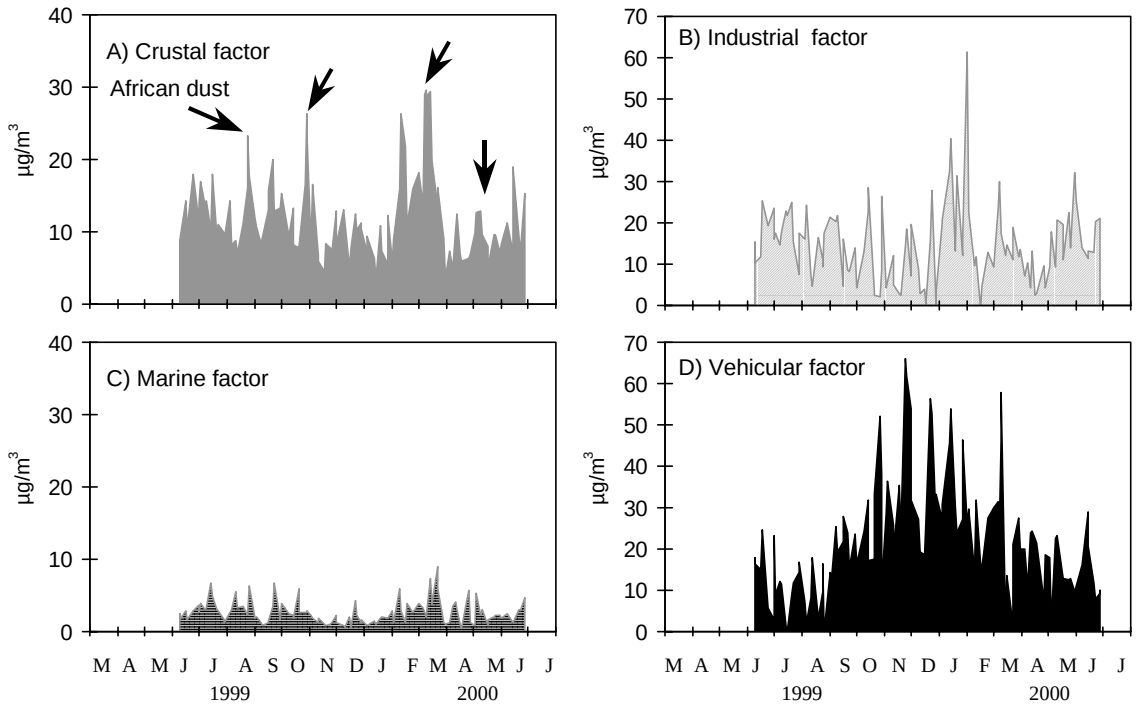

Figure 5-34. Daily mean source contributions to PM10 at the L'HOSPITALET urban site obtained by MLRA. Arrows in A) indicate the main African dust events.

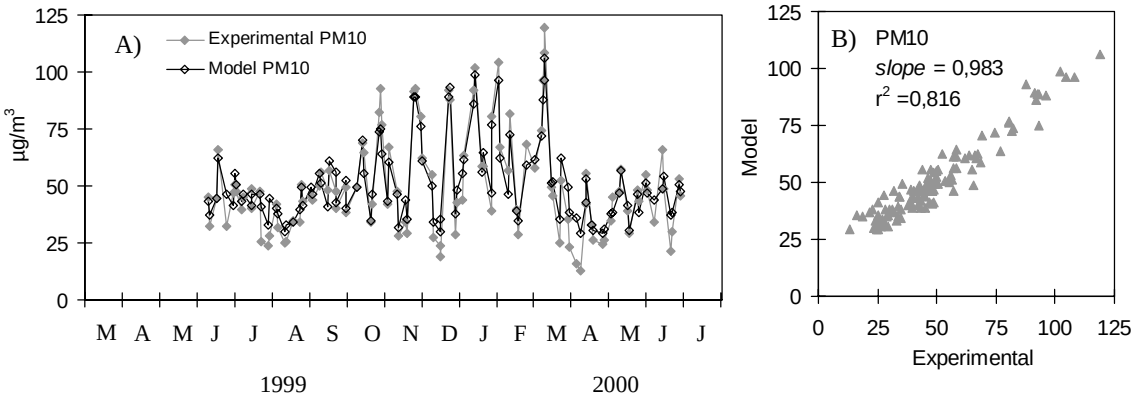

Figure 5-35. Experimental (gravimetric) and modelled (MLRA) daily PM10 concentrations at the L'HOSPITALET urban site.

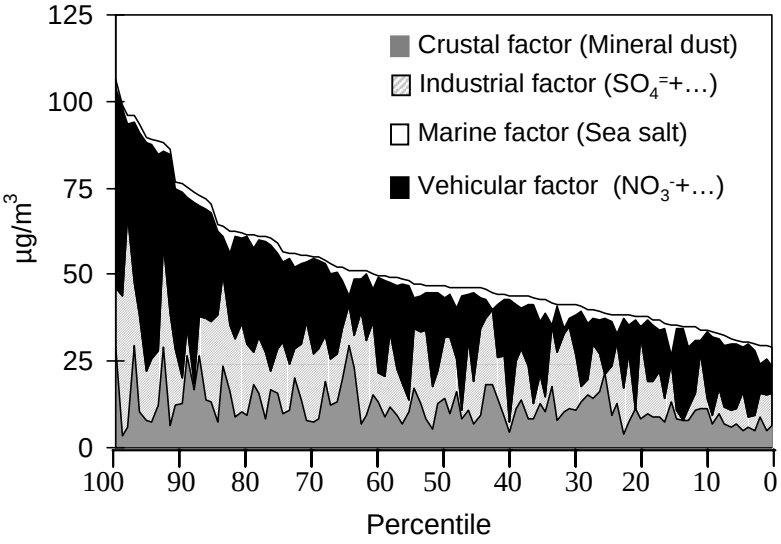

Figure 5-36. Daily PM10 concentrations at the L'HOSPITALET site in the Barcelona Metropolitan Area in descending order, showing the contribution of each source obtained by MLRA.

Figure 5-36 shows the daily PM10 concentrations at L'HOSPITALET in descending order displaying the source contributions. The highest PM10 events are associated with a high contribution of the Vehicular factor, which dominates the 100th-70th percentile range. The Industrial and Crustal factors present sporadic significant contributions in the in the interval 100th-30th percentile range.

5.3.2.2 Mass balance analysis

The source contributions were determined by the sum of the PM10 components associated with each previously identified source or factor (Table 5-3). The mass of the PM10 components, which presented a significant factor loading in several factors, was distributed in accordance with the results of the mean source apportionment of each PM component (appendix 6). The Crustal source included Ca, $CO_3^=$, Al_2O_3, SiO_2, 0.7*Mg, P, 0.6*Mn, Sr, Ti, 0.6*Fe, 0.5*Cr, P and 0.7*K. The Marine contribution was calculated as the sum of Na, marine-Cl (deduced from the Na/Cl ratio), 0.3*Mg and ss-$SO_4^=$. The Industrial contribution included nss-$SO_4^=$, 0.5*NO_3^-, a fraction of NH_4^+, 0.5*Ni and V. The Vehicular contribution was calculated as the sum of OC+EC, 0.5*NO_3^-, a fraction of NH_4^+, 0.4*Fe, 0.3*K, 0.4*Mn, Zn, Cu, 0.5*Cr, 0.5*Ni, Cl-excess (with respect to the marine Cl/Na ratio) and Pb. The fact that ammonium-sulphate occurs during the whole year and ammonium-nitrate only in autumn-winter was taken into account to determine the fractions of NH_4^+ associated with the Industrial and Vehicular sources. As demonstrated above, a fraction of Cl has an anthropogenic origin in the cold season, thus Cl-excess (with respect to the marine Na/Cl) was removed from the Marine contribution and was added to the Vehicular contribution.

The mean PM10 source contributions were estimated at: 33% Vehicular (NO_3^- + others), 25% Crustal (mineral dust), 20% Industrial (nss-$SO_4^=$ + others) and 4% Marine (sea salt).

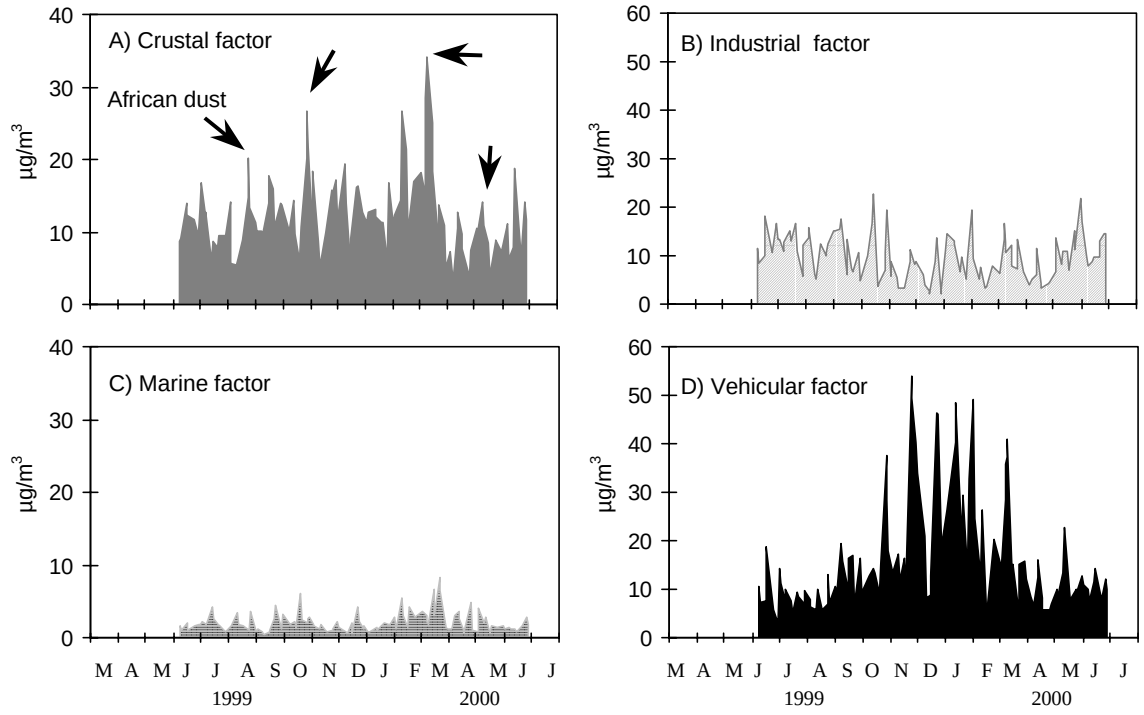

Figure 5-37. Daily mean source contributions to PM10 at the L'HOSPITALET urban site obtained by MBA. Arrows in A) indicate the main African dust events.

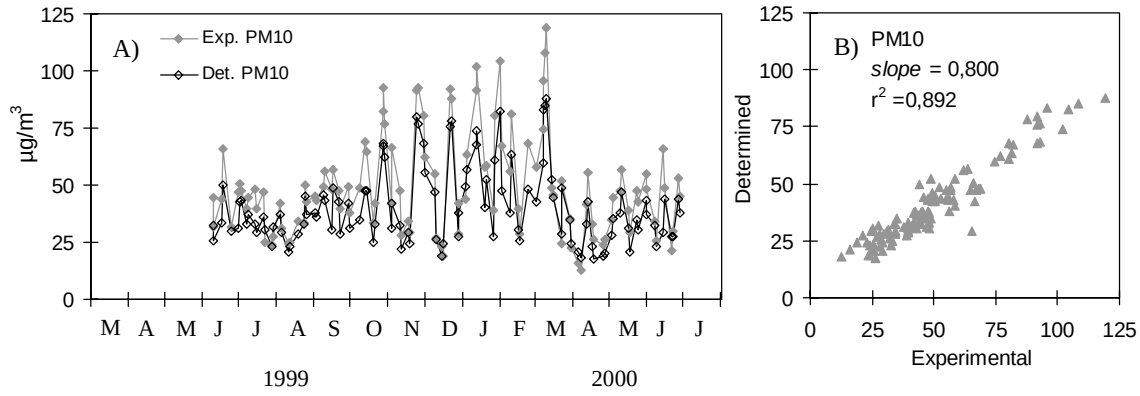

Figure 5-38. Experimental (gravimetric) and determined (MBA) daily PM10 concentrations at the L'HOSPITALET urban site.

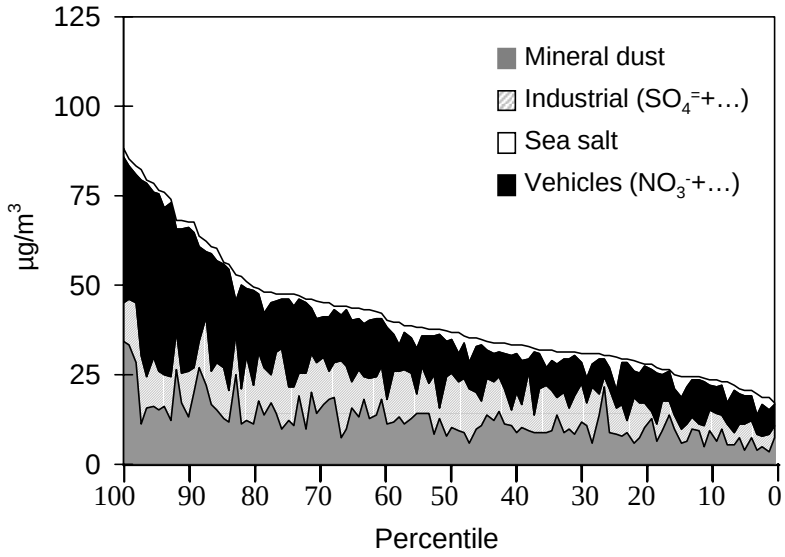

Figure 5-39. Daily PM10 concentrations at the L'HOSPITALET site in the Barcelona Metropolitan Area in descending order, showing the contribution of each source obtained by MBA.

Figure 5-37 shows the daily contribution of each source. The results of the daily source apportionment are qualitatively very close to those obtained by MLRA for most of the PM10 sources. Only quantitative differences are observed, which will be discussed in section 5.3.5.

Figure 5-38 shows the experimental (obtained by the gravimetric method) and determined (sum of the source contributions from MBA) PM10 levels. The determined PM10 fraction reached 80% of experimental PM10 concentrations. When interpreting the origin of the PM10 variations as a function of the different source contributions, similar conclusions to those obtained by the MLRA method are reached. High winter PM10 episodes are caused by high contributions of Vehicle emissions and road dust (Crustal source). In the summer, PM10 levels undergo minor variations, because of the high background Industrial contribution.

Figure 5-39 shows the daily PM10 concentrations at L'HOSPITALET in descending order displaying the source contributions. As in the case of the MLRA method, the Vehicular contribution is the dominant source in the percentiles >80th. However, the MBA method indicates that the highest PM10 levels are recorded when the Crustal factor reaches a maximum contribution (percentile range 100th-95th).

5.3.3 PM2.5 at the L'HOSPITALET urban site

5.3.3.1 Multi-linear regression analysis

The contribution of each previously identified source (Table 5-5) to PM2.5 levels at the L'HOSPITALET urban site was calculated by using the absolute score factors determined by PCA applied to the whole PM2.5 data set (June 1999 – June 2000). In the preliminary stage, a negative contribution from the factor containing Na and P (Table 5-5) was again obtained (as for the marine factor in PM10), due to the occurrence of anti-correlated variations of PM2.5 and Na. Because of

the very low contribution of this factor to PM2.5 levels (228ngNa/m^3 and 25ngP/m^3, less than 1% of mean PM2.5 levels), these components were not considered for the source apportionment (levels of Na and P were subtracted from PM2.5 levels, and Na and P were not considered in the calculations of the absolute score factors or in multi-linear regression analysis).

The mean PM2.5 source contributions were estimated at: 49% Vehicular factor (carbon, NO_3^- + ...), 43% Industrial factor (nss-$SO_4^=$ + others) and 9% Crustal factor. The contribution of other unidentified sources was not calculated since a negative intersection constant was obtained in the Multi-linear regression.

Figure 5-40 shows the daily contribution of each source. The Industrial factor (Figure 5-40 A) exhibits a high background contribution in the warm season induced by the seasonal evolution of nss-sulphate. The contribution of this source is very close to that presented by the Industrial factor in PM10 given that most components included in the Industrial factor occur in PM2.5 (fine fraction of PM). The contribution of the Vehicular factor (Figure 5-40 B) was higher in the cold season because of the seasonal evolution of carbon and nitrate. The contribution of this source is strongly dependent on the thermodynamic properties of nitrate and probably on some organic species. The contribution of this source is also very close to that presented by the Vehicular factor in PM10 given that most components included in the Vehicular factor occur in PM2.5 (fine mode of PM). The Crustal factor (Figure 5-40 C) exhibits a background contribution 2-4µg/m^3. Peak crustal concentrations events in the interval 5-15µg/m^3 were recorded during African dust events. However, the occurrence of non-African crustal peak concentration events provides evidence of urban sources of fine mineral dust. The contribution of the Crustal factor in PM2.5 (9% on average) is very different from that in PM10 (23% on average) owing to the coarse size of most of the mineral dust components (Table 5-4).

Levels of PM.5 in the model were determined as the sum of each source contribution. Figure 5-41 shows the experimental and modelled daily PM10 concentrations. The model reproduces the experimental data fairly satisfactorily, 10% of underestimation of experimental PM2.5 concentrations being observed. In autumn and winter, PM2.5 concentrations undergo wide variations (PM2.5 concentrations frequently >60µg/m^3 alternating with<30µg/m^3), the Vehicular factor being dominant. In spring-summer, PM2.5 levels present a low variability favoured by the high background contribution of the Industrial factor.

Figure 5-42 shows the daily PM2.5 concentrations at L'HOSPITALET in descending order displaying the source contributions. The Vehicular factor shows a dominant contribution in the 95th-70th percentile range, whereas the Industrial factor displays a significant contribution in the percentile ranges 100th-95th and 55th-15th. The contribution of the Crustal factor is relatively low.

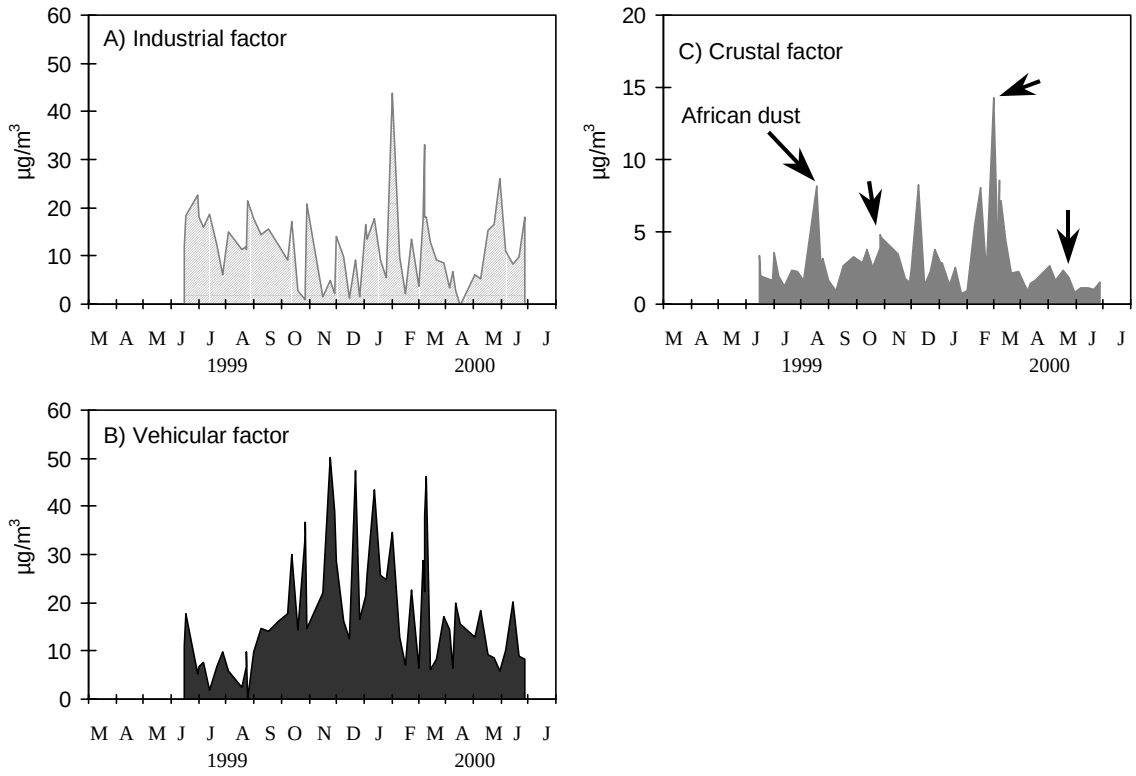

Figure 5-40. Daily mean source contributions to PM2.5 at the L'HOSPITALET urban site obtained by MLRA. Arrows in C) indicate the main African dust events.

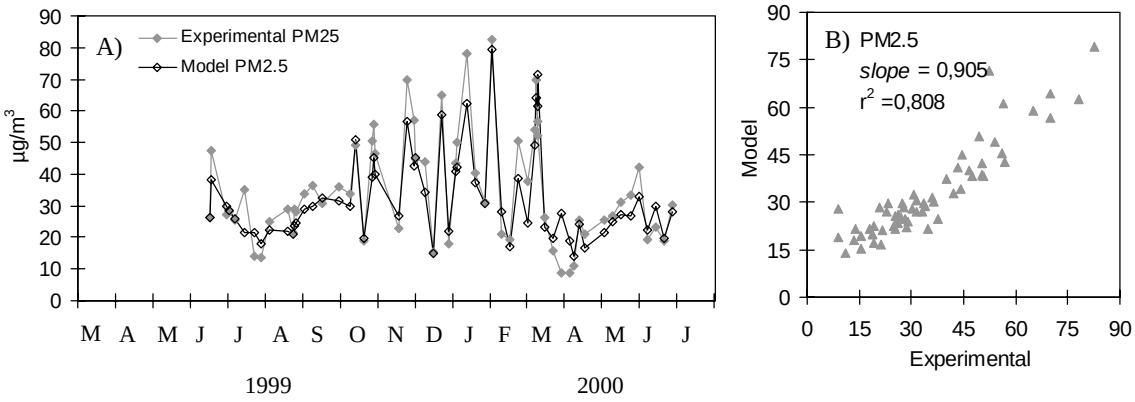

Figure 5-41. Experimental (gravimetric) and modelled (MLRA) daily PM2.5 concentrations at the L'HOSPITALET urban site.

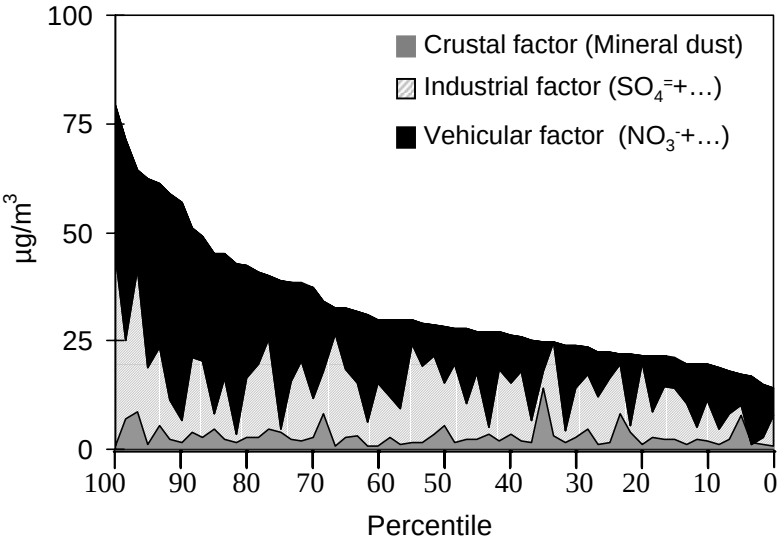

Figure 5-42. Daily PM2.5 concentrations at the L'HOSPITALET site in the Barcelona Metropolitan Area in descending order, showing the contribution of each source obtained by MLRA.

5.3.3.2 Mass balance analysis

The source contributions were calculated by the sum of the PM2.5 components associated with each previously identified source or factor (Table 5-5), following the methodology described in chapter 3. The mass of the PM2.5 components, which presented a significant factor loading in several factors, was distributed between these sources in accordance with the results of the mean source apportionment (appendix 6). The Crustal source included Ca, $CO_3^=$, Al_2O_3, SiO_2, Mg, 0.5*Fe, Ti, Sr, 0.5*K and 0.3*Mn. The Industrial contribution was calculated as the sum of nss-$SO_4^=$, 0.5*NO_3^-, a fraction of NH_4^+, 0.3*Zn, 0.5*Ni and V. The Vehicular contribution included OC+EC, 0.5*NO_3^-, a fraction of NH_4^+, Cl, 0.5*K, 0.7*Mn, 0.5*Fe, 0.5*Ni, Cr, Cu, 0.7*Zn and Pb. The fact that ammonium-sulphate occurs during the whole year and ammonium-nitrate only in autumn-winter was taken into account to determine the fractions of NH_4^+ associated with the Industrial and Vehicular sources. The contribution of the Na and P source of unknown origin was also estimated.

The mean PM2.5 source contributions were estimated at: 40% Vehicular (NO_3^- + others...), 28% Industrial (nss-$SO_4^=$ + others.), 8% Crustal (mineral dust), and 0.7% a Na + P source. The results of the daily source contributions (Figure 5-43) are qualitatively similar to those obtained in by the MLRA method, and only qualitative differences are observed (discussed in section 5.3.5). The contribution of the Na and P unidentified source (non quantified in the MLRA) is <0.5µg/m^3 throughout the study period.

The experimental (determined by gravimetric the method) and determined (sum of the source contributions from MBA) PM2.5 levels are plotted in Figure 5-44. The determined PM10 fraction reached 77% of experimental PM10 concentrations. When interpreting the origin of the PM10 variations as a function of each source contribution, similar conclusions to those obtained with the MLRA method are reached.

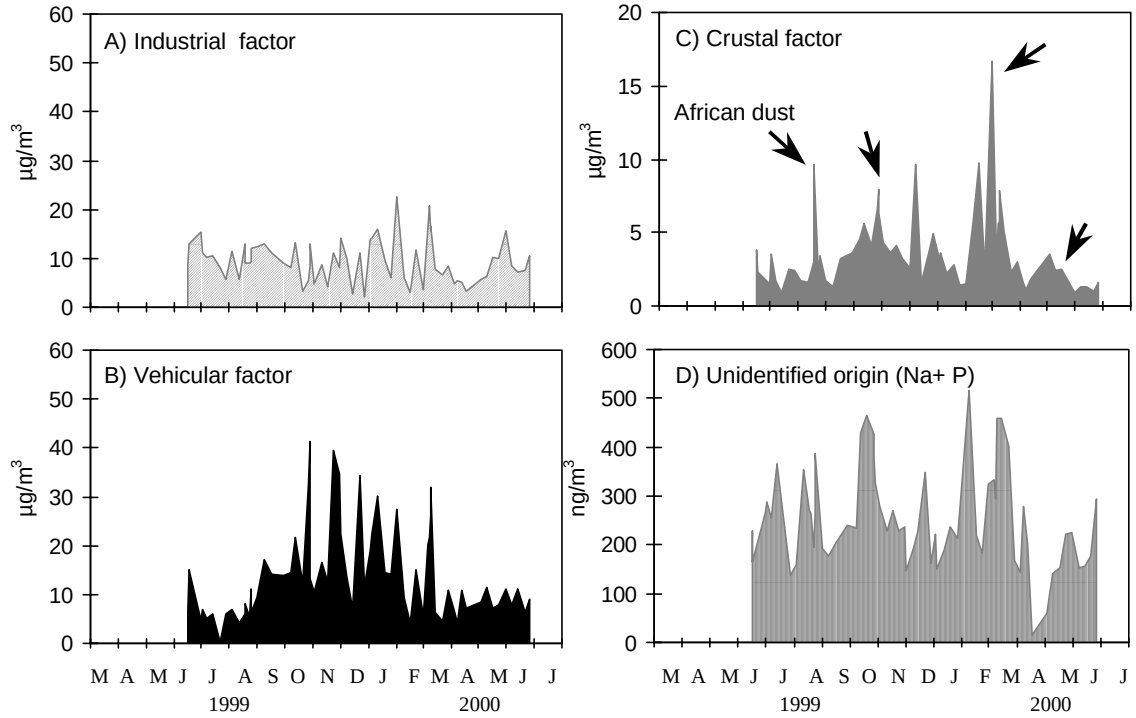

Figure 5-43. Daily mean source contributions to PM2.5 at the L'HOSPITALET urban site obtained by MBA. Arrows in A) indicate the main African dust events.

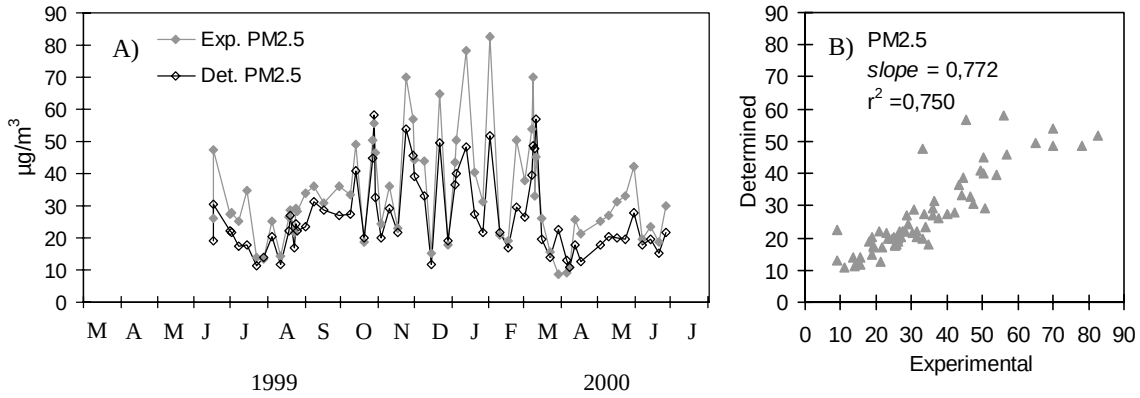

Figure 5-44. Experimental (gravimetric) and determined (MBA) daily PM2.5 concentrations at the L'HOSPITALET urban site.

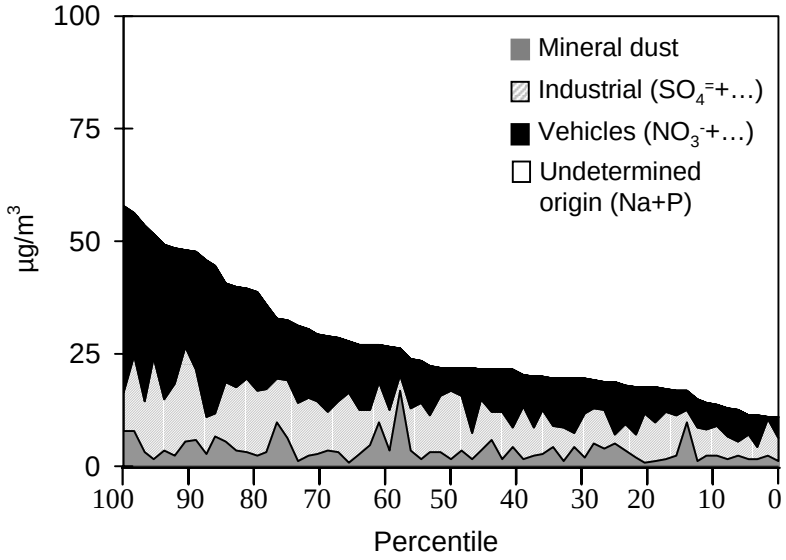

Figure 5-45. Daily PM2.5 concentrations at the L'HOSPITALET site in the Barcelona Metropolitan Area in descending order, showing the contribution of each source obtained by MBA.

Figure 5-45 shows the daily PM2.5 concentrations at L'HOSPITALET in descending order displaying the source contributions. Results are qualitatively very similar to those obtained from the MLRA.

5.3.4 PM10 at the ONDA industrial site

5.3.4.1 Multi-linear regression analysis

The source (Table 5-6) contribution to PM10 at the ONDA industrial site was calculated using the absolute score factors determined by PCA applied to the PM10 data set from mid-June to late September 1999.

The mean PM10 source contributions were estimated at: 29% Industrial-1 factor (source 2 = nss-$SO_4^=$ + others; Table 5-6), 27% Crustal factor (source 1 = mineral dust), 15% bio-mass burning factor (source 5 = carbon and phosphorus), 14% of other non identified sources (determined by the intersection constant of the multi-linear regressions), 8% marine + industrial-2 factor (source 3 = Na + V....) and 5% Industrial-3 factor (Pb+Cu...).

Figure 5-46 shows the daily source contributions. The Industrial-1 factor (Figure 5-46 A) exhibits a high background contribution in July and August, mainly induced by the high levels of nss-sulphate. The Crustal factor (Figure 5-46 B), which includes both natural and anthropogenic mineral dust, exhibits 5-10µg/m^3 background contributions. The highest concentrations of mineral dust were caused by African dust outbreaks in late August and late October 1999, when mineral dust contributions equal to 27 and 23 µg/m^3 were recorded, respectively.

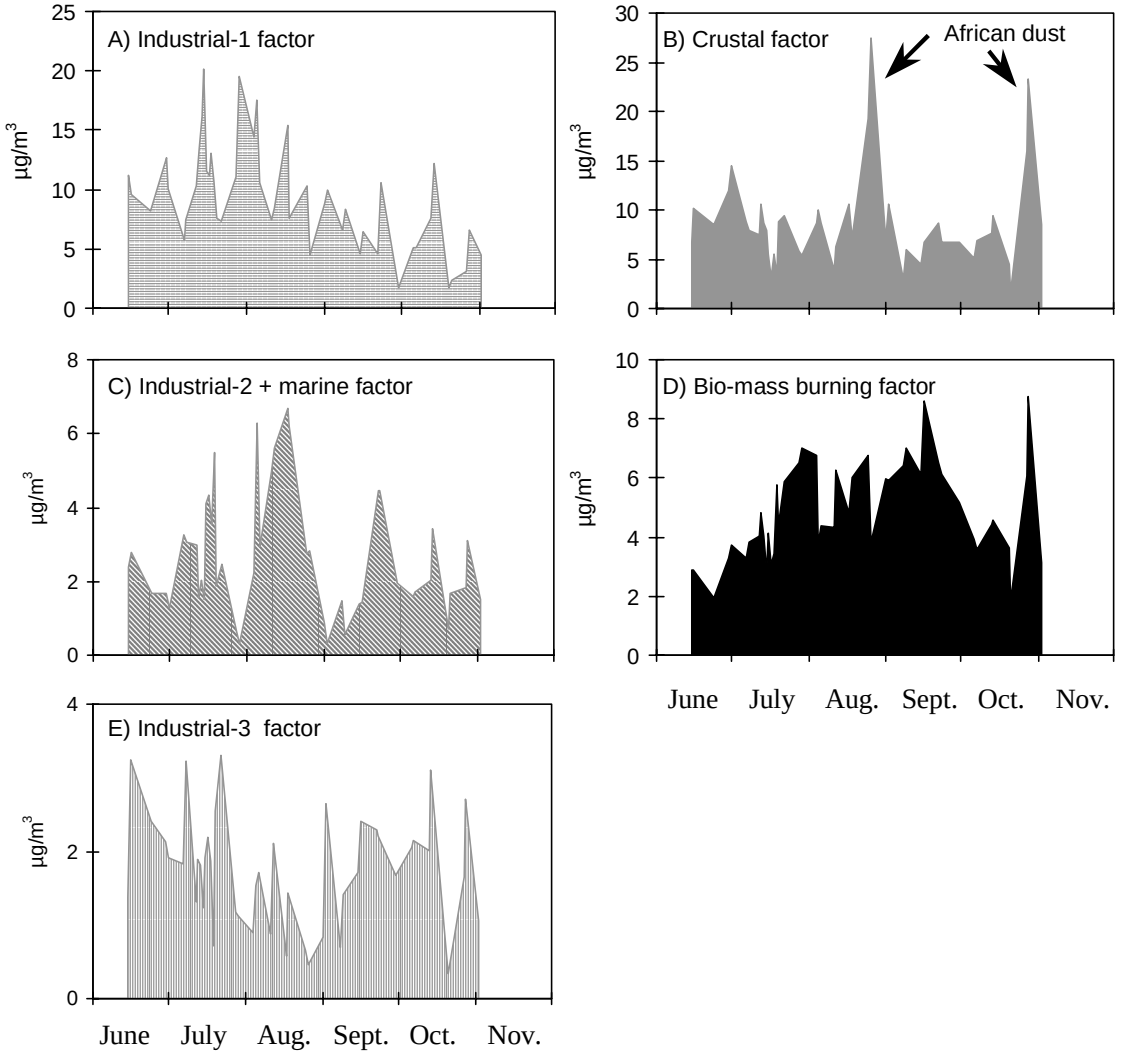

Figure 5-46. Daily mean source contributions to PM10 at the ONDA industrial site obtained by MLRA. Arrows in B) indicate the main African dust events.

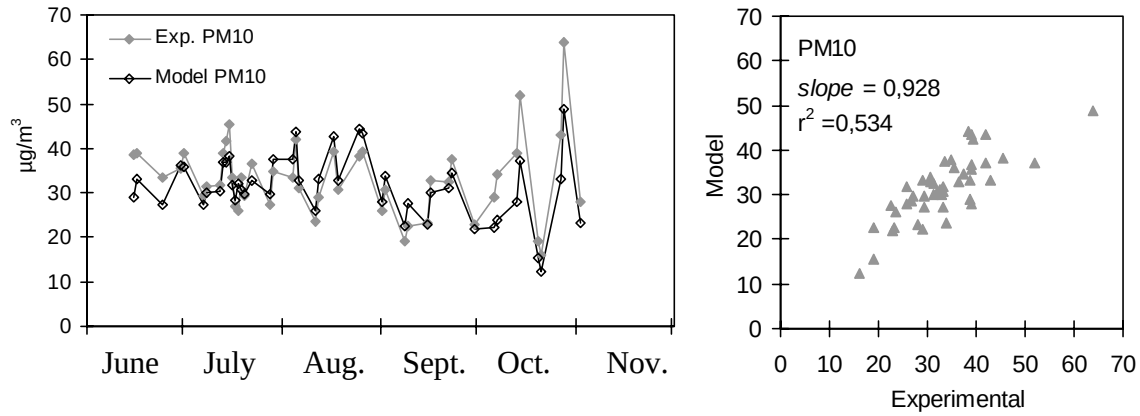

Figure 5-47. Experimental (graviemtric) and modelled (MLRA) daily PM10 concentrations at the ONDA industrial site.

The contributions of the marine+Industrial-2 (Figure 5-46 C) and Industrial-3 (Figure 5-46 E) factors were relatively low since these factors are mainly constituted by trace PM species. Finally, the contribution of the bio-mass burning factor (Figure 5-46 D) is very close to the concentrations of carbon (Figure 5-26) given that this is the main component of this source. The contribution of the other non identified sources was estimated at 4µg/m^3.

Levels of PM10 in the model were determined as the sum of each source contribution. Figure 5-47 shows the experimental and modelled daily PM10 concentrations. The model underestimates the experimental PM10 levels by 8%.

5.3.4.2 Mass balance analysis

The source contributions were calculated by the sum of the PM10 components associated with each previously identified source (or factor, Table 5-6) following the methodology described in chapter 3. The mass of the PM10 components, which presented a significant factor loading in several factors, was distributed between these factors in accordance with the mean source apportionment of each PM10 component (appendix 6). The Crustal contribution was estimated as the sum of Ca, $CO_3^=$, Al_2O_3, SiO_2, Fe, 0.65*Mg, Sr, Ti, 0.45*K, Mn, 0.3*P, 0.3*V and 0.3*Cr levels. The Industrial-1 contribution included nss-$SO_4^=$, NH_4^+, 0.75*Zn, 0.6*V, 0.5*Ni, 0.4*NO_3^-, 0.3*Pb and 0.3*Cr. The marine + Industrial-2 contribution was estimated as the sum of Na, 0.35*Mg, 0.8*Cl, ss-$SO_4^=$, 0.2*K, 0.2*V, 0.4*NO_3^- and 0.5*Ni levels. The Industrial-3 factor included Cu, 0.7*Pb, 0.4*Cr, 0.35*K, 0.2*NO_3^- and 0.25*Zn. Finally, the contribution of the bio-mass burning factor was estimated as the sum of OC+EC and 0.55*P levels.

The mean PM10 source contributions were estimated at: 36% Industrial-1 (nss-$SO_4^=$ + ...), 36% Crustal (mineral dust), 16% bio-mass burning factor (C + P), 8% marine + industrial-2 (Na +....) and 4% Industrial-3 (Pb + Cu...). The daily source contributions from MBA (Figure 5-48) are very close to those obtained by MLRA.

Figure 5-49 shows the experimental (obtained by the gravimetric method) and determined (sum of source contributions from MBA) PM10 levels. The determined fraction reached 77% of the experimental PM10 levels. From June to August, relatively stable PM10 concentrations in the interval 20-45µg/m^3 were recorded. The highest PM10 event (64µgPM10/m^3) was caused by the African dust event recorded in late October 1999, when the mineral dust concentration reached 26µg/m^3 and accounted for 40% of bulk PM10.

The daily PM10 levels from ONDA are not presented in descending order showing the source contributions because of the relatively low number of samples.

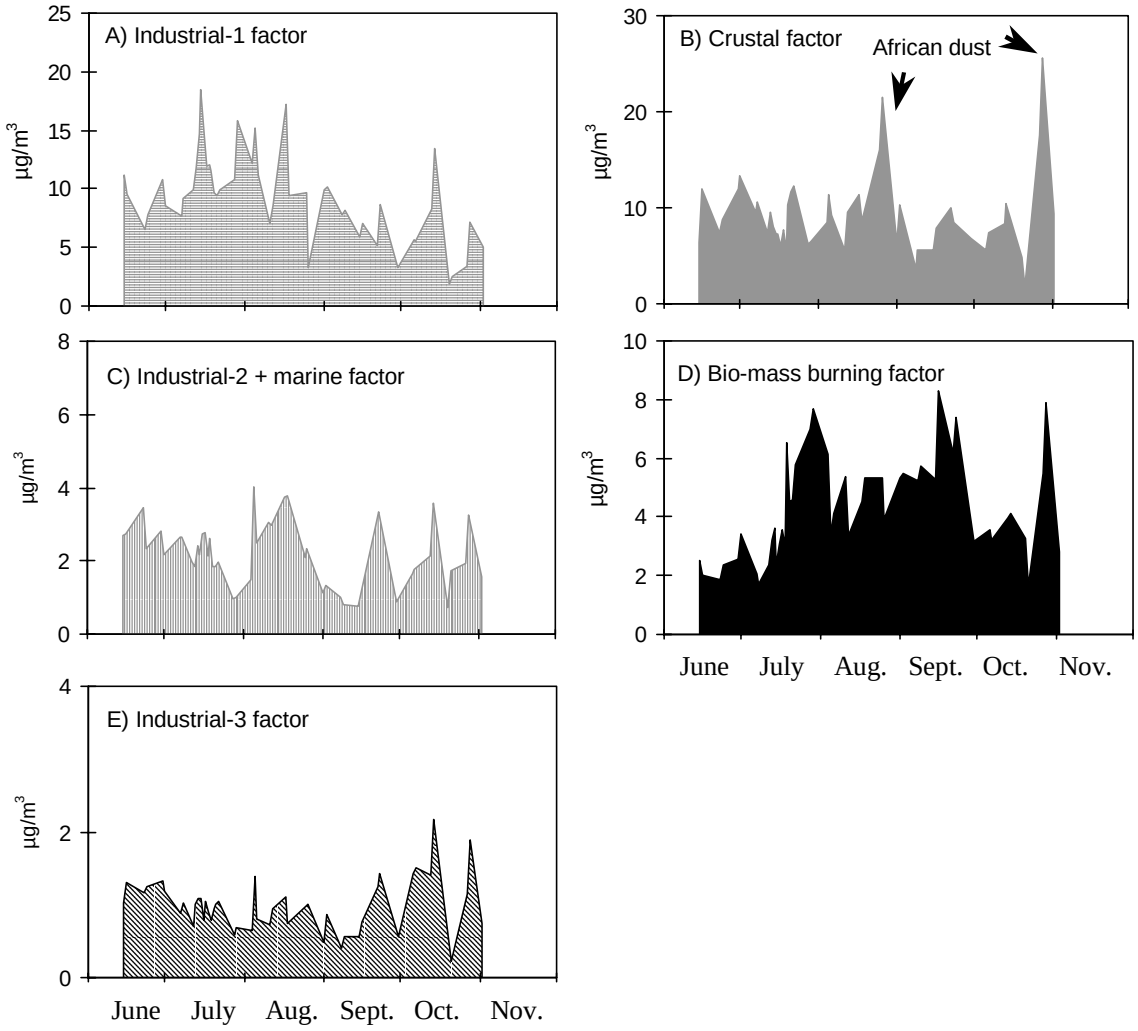

Figure 5-48. Daily mean source contributions to PM10 at the ONDA industrial site obtained by MBA. Arrows in B) indicate the main African dust events.

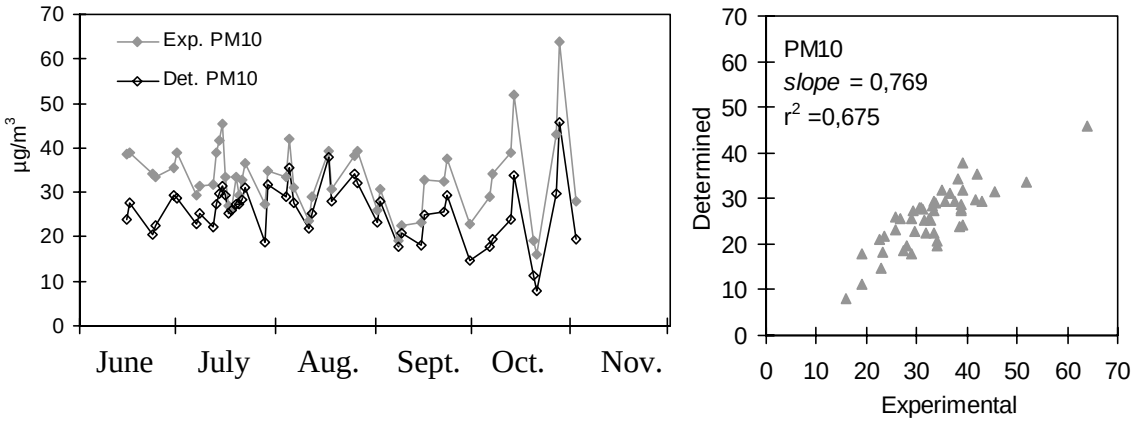

Figure 5-49. Experimental (gravimetric) and determined (MBA) daily PM10 concentrations at the ONDA industrial site.

5.3.5 Comparison of source apportionment methods

The source contributions to PM10 and PM2.5 obtained by MLRA and MBA were compared for result assessment since these methods are based on different procedures. In the MLRA method, the source contribution is calculated on the basis of the degree of correlation between the PM source tracers and PM10 levels. If suitable source tracers are known, the source contributions may be calculated by the analysis of some PM components. However, if any source tracer is anti-correlated with PM10 levels, a negative source contribution will be obtained. This drawback may be avoided if the source contribution is calculated as the sum of the major chemical species associated with each source (identified by PCA), as in the case of MBA. Given that a high percentage of the PM mass was determined (>75% of bulk at each sampling site), the results obtained by the two methods can be compared.

Table 5-7. Mean source contribution (in µg/m^3) to PM10 and PM2.5 obtained by Multi-linear regression analysis (MLRA) and Mass balance analysis (MBA) methods.

		Vehicular	Industry	Crustal	Marine
PM10 - rural	MLRA	4.6	6.9	5.1	1,6
MONAGREGA	MBA	2.9	6.5	5.8	0,7
PM10 – urban	MLRA	22.0	14.7	12.0	--
L'HOSPITALET	MBA	16.2	9.9	12.4	--
PM2.5 – urban	MLRA	17.7	12.1	3.0	--
L'HOSPITALET	MBA	13.9	9.7	3.6	--

As shown in Figures 5-50, 5-51 and 5-52, the daily source contributions obtained by the two methods are qualitatively very similar for most of the PM sources since a high day-to-day correlation is observed. Major discrepancies were only obtained in the marine contribution at the MONAGREGA rural site. Table 5-7 shows the mean source contribution obtained at each site. The Industrial and Vehicular contributions to PM10 and PM2.5 calculated with MLRA are higher than those calculated with MBA at MONAGREGA and at L'HOSPITALET. Moreover, the mean Crustal contribution to PM10 is slightly lower with the MLRA method, although peak concentrations may be higher with the MLRA method at MONAGREGA and L'HOSPITALET. The most important overestimation of the MLRA with respect to MBA is observed in the marine contribution to PM10 at MONAGREGA.

The origin of the differences in the source contributions obtained by means of MLRA and MBA lies in the method. As shown in Table 5-8, the source contributions obtained by the MBA method account for 75-80% of the experimental (gravimetric) PM concentrations. On a daily basis, this undetermined fraction ranges around 10µgPM10/m^3 in summer at MONAGREGA (Figure 5-53 C, D) and 10-20µgPM10/m^3 (Figure 5-54 C, D) and 5-20µgPM2.5/m^3 (Figure 5-55 C, D) at L'HOSPITALET. This undetermined portion of PM is believed to consist mainly of water condensed on the surface of aerosols and water chemically bound to aerosol (e.g. gypsum is present

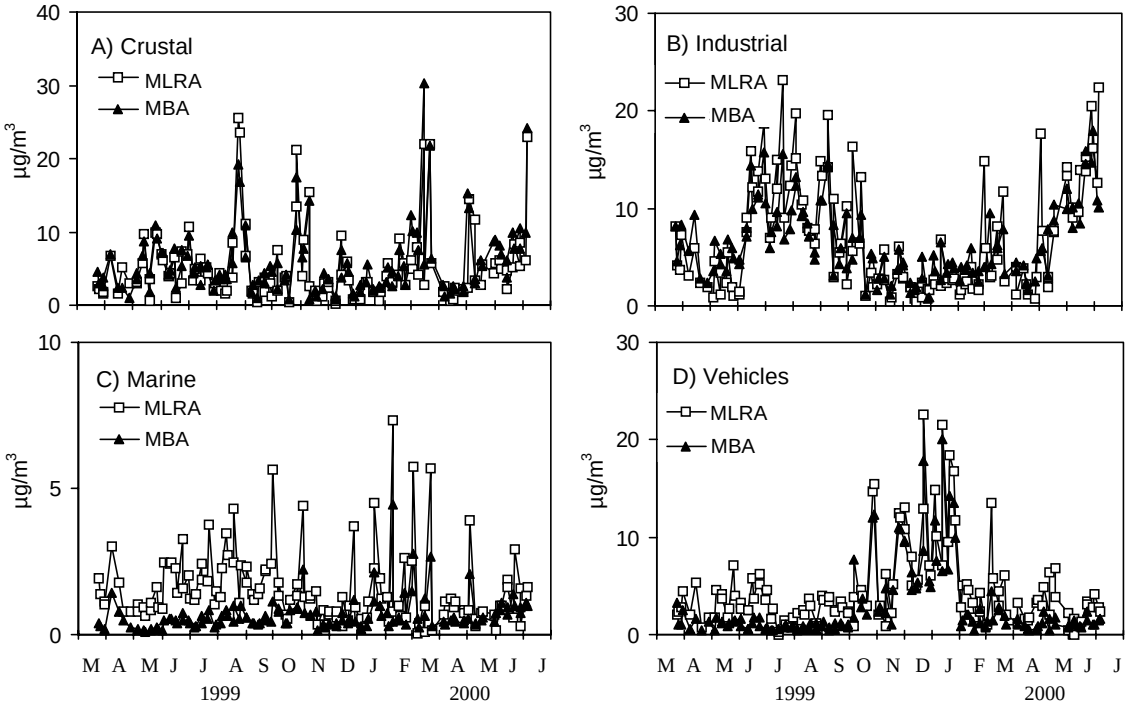

Figure 5-50. Source contributions to PM10 obtained by Multi-linear regression analysis (MLRA) and Mass balance analysis (MBA) at the MONAGREGA rural site.

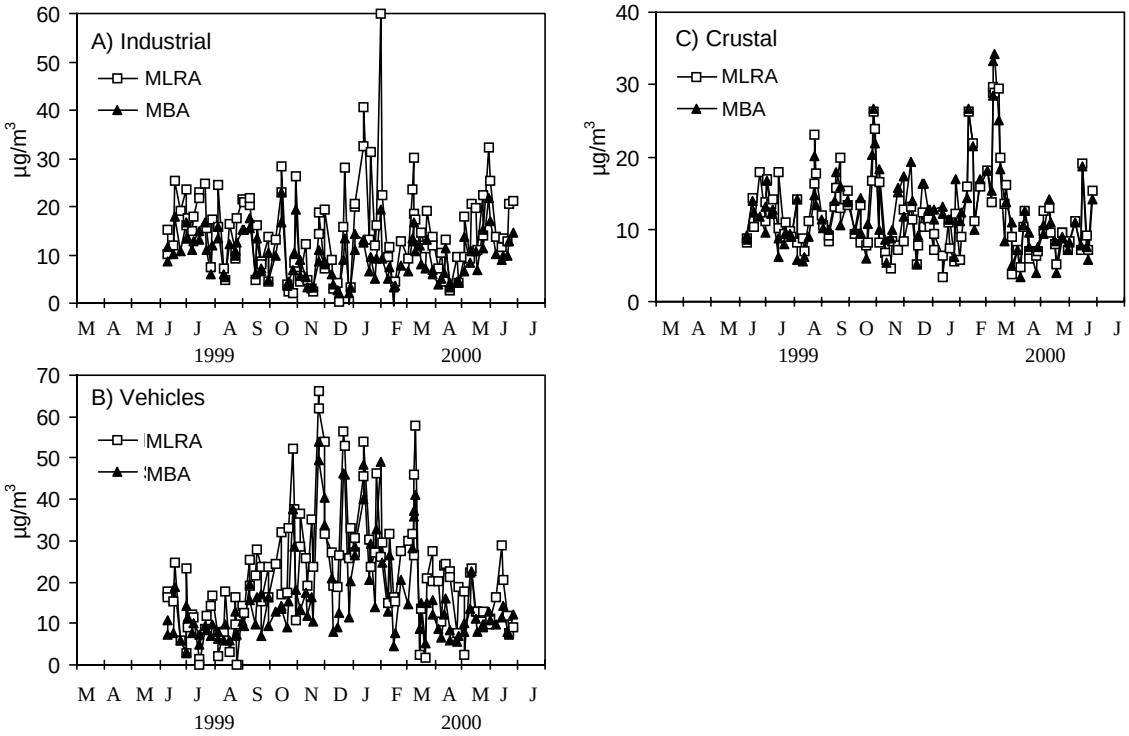

Figure 5-51. Source contributions to PM10 obtained by Multi-linear regression analysis (MLRA) and Mass balance analysis (MBA) at the L'HOSPITALET urban site.

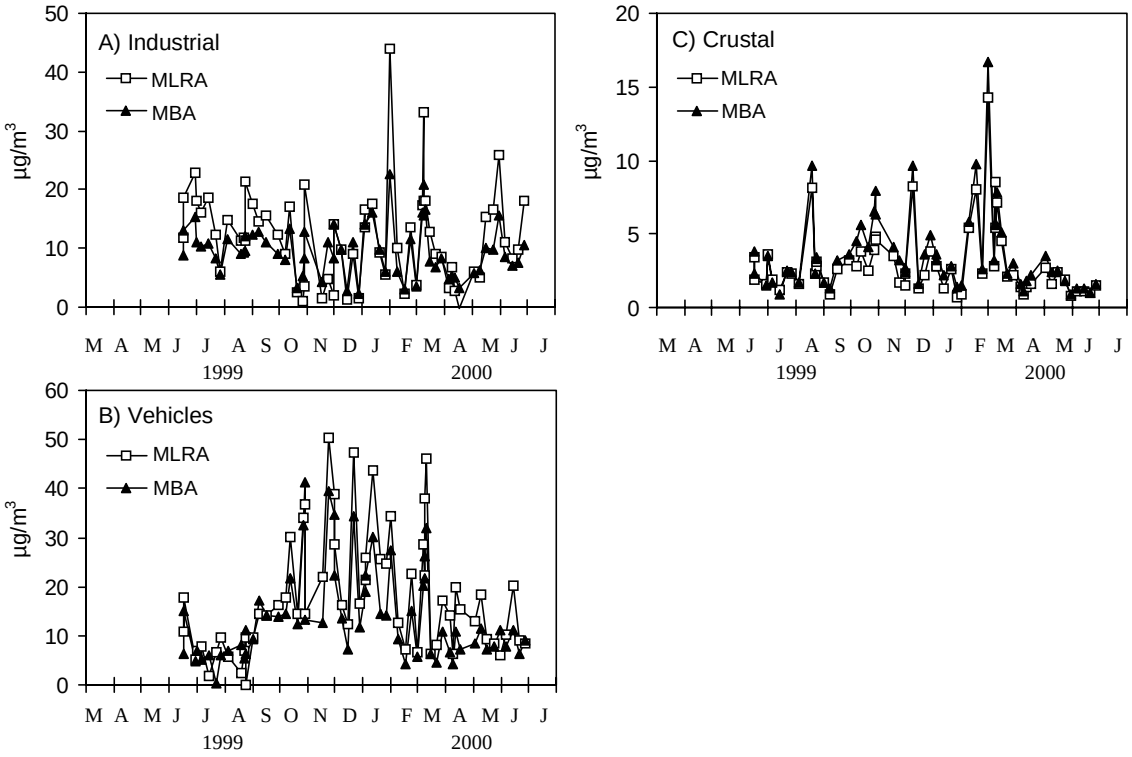

Figure 5-52. Source contributions to PM2.5 obtained by Multi-linear Regression Analysis (MLRA) and Mass Balance Analysis (MBA) at the L´HOSPITALET urban site.

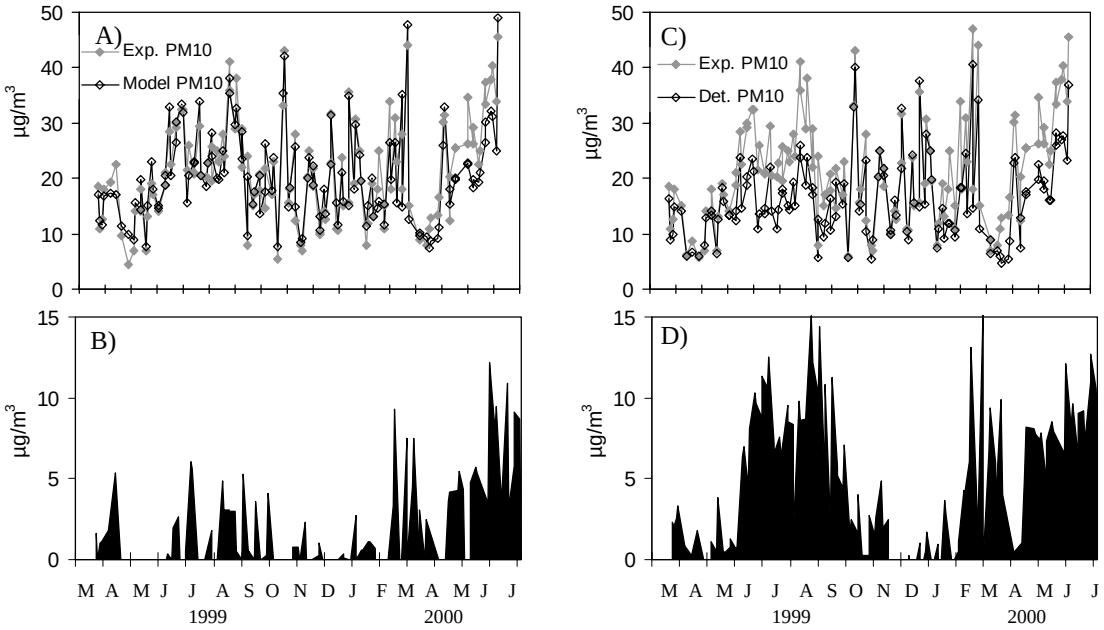

Figure 5-53. A) Experimental (Exp., gravimetric) and modelled (Mod., MLRA) daily PM10 levels at the MONAGREGA rural site. B) Difference between Exp. and Mod. daily PM10 levels: undetermined (by the MLRA) fraction of PM10. C) Experimental (Exp.) and determined (Det.: Mass Balance) daily PM10 levels at MONAGREGA. D) Difference between Exp. and Det. daily PM10: chemically undetermined fraction of PM10.

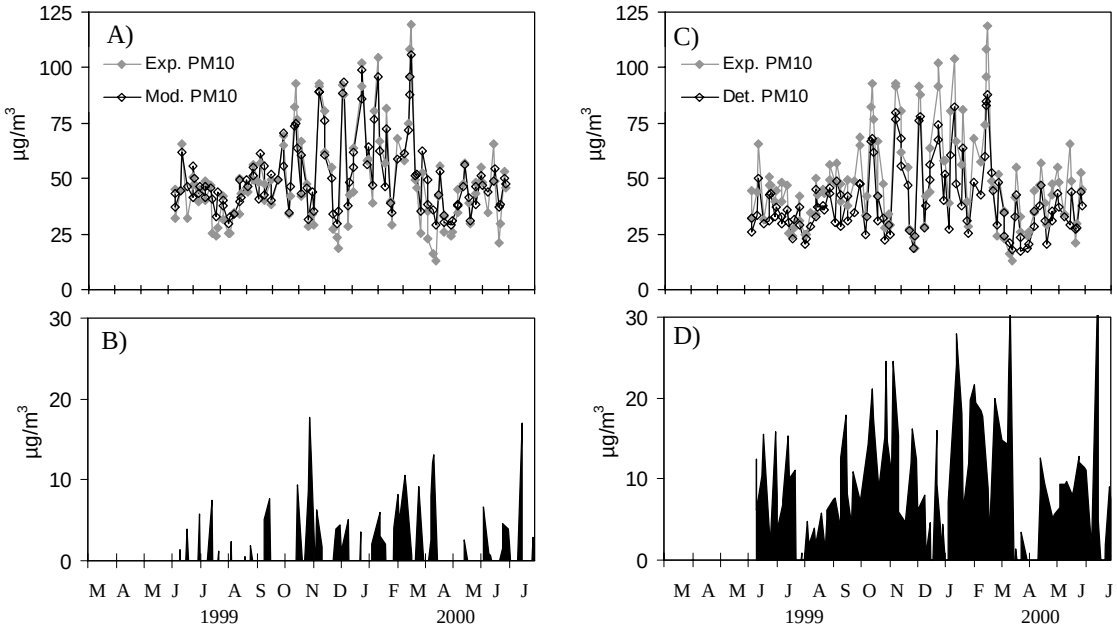

Figure 5-54. A) Experimental (Exp., gravimetric) and modelled (Mod., MLRA) daily PM10 levels at the L'HOSPITALET urban site. B) Difference between Exp. and Mod. daily PM10 levels: undetermined (by the MLRA) fraction of PM10. C) Experimental (Exp.) and determined (Det.: Mass Balance) daily PM10 levels at MONAGREGA. D) Difference between Exp. and Det. daily PM10: chemically undetermined fraction of PM10.

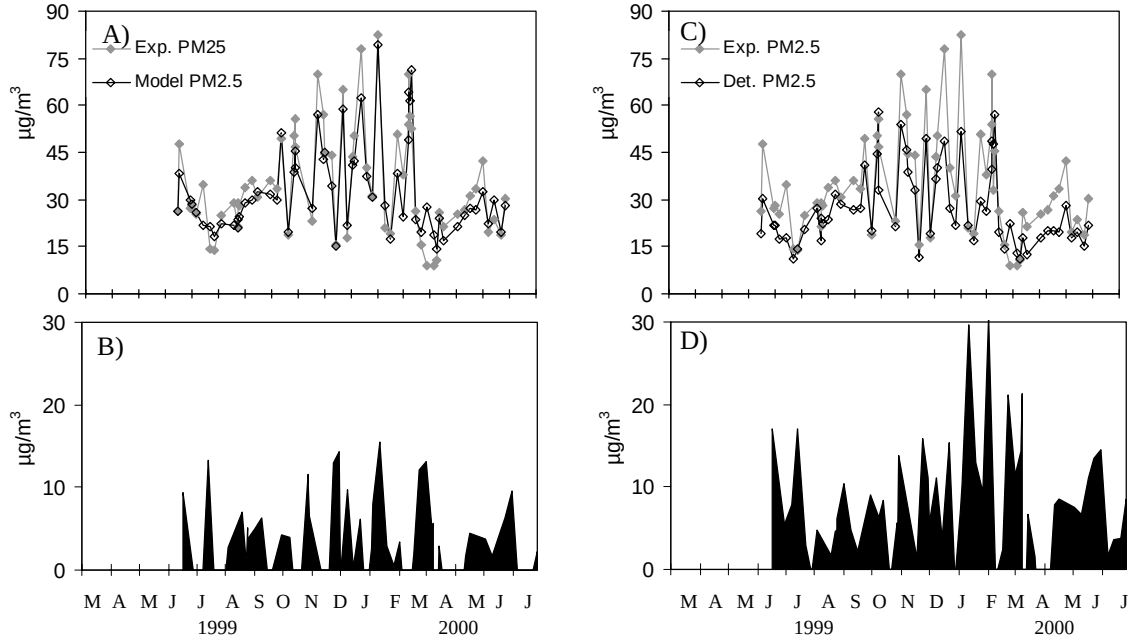

Figure 5-55. A) Experimental (Exp., gravimetric) and modelled (Mod., MLRA) daily PM2.5 levels at the L'HOSPITALET urban site. B) Difference between Exp. and Mod. daily PM2.5 levels: undetermined (by the MLRA) fraction of PM10. C) Experimental (Exp.) and determined (Det.: Mass Balance) daily PM2.5 levels at MONAGREGA. D) Difference between Exp. and Det. daily PM2.5: chemically undetermined fraction of PM2.5.

Table 5-8. Percentage of accounted fraction of experimental PM10 levels obtained by means of Multi-linear regression analysis (MLRA) and Mass balance analysis (MBA). Results shown in Figures 5-29B, 5-32B, 5-35B, 5-38B, 5-41B and 5-44B.

	PM10 MONAGREGA	PM10 L'HOSPITALET	PM2.5 L'HOSPITALET
MLRA	94%	98%	90%
MBA	76%	80%	77%

as $CaSO_4 \cdot 2H_2O$) and to heteroatoms in organic compounds which are not adequately accounted for. In contrast to the results of the MBA method, the source contributions obtained by means of the MLRA method account for 90-98% of the experimental PM concentrations (see also Figures 5-53 A, B , 5-54 A, B, 5-55 A, B). In MLRA, the bulk PM concentrations are distributed among the identified sources as a function of the degree of correlation between the source tracers and the PM mass. Thus, the MLRA method accounts for a larger fraction of PM than the MBA. This is due to the fact that a large proportion of PM which has not been accounted for (mainly water) is distributed among the identified sources. A priori, this could be interpreted as a drawback. However, it should be taken into account that this proportion of water bound to aerosol also contributes to PM10 and PM2.5 levels recorded in the air quality monitoring networks.

Although the results of the PM10 source apportionment at ONDA station have not been discussed in this section because of the short study period, the conclusions reached here are also applicable to the PM10 source apportionment at ONDA.

The difference between the experimental (gravimetric) and chemically determined PM levels and the bulk PM concentrations reached maximum levels simultaneously. This maximum was reached in summer at the MONAGREGA rural site (Figures 5-53C and D) and in autumn-winter at the L'HOSPITALET urban site (Figures 5-54C and D, and Figures 5-55C and D). This is due to the fact that the water associated with the aerosol (condensed on the surface of the aerosols or chemically bound to the aerosols) increases with the PM levels.

5.4 PM10 source contribution in relation to the 2010 annual mean limit value

Table 5-9 shows the annual PM10 and PM2.5 source contributions at the MONAGREGA rural and the L'HOSPITALET urban sites obtained by MLRA and MBA. It also lists the mean source contributions to PM10 at the ONDA industrial site obtained during 5 months of sampling.

As stated above, according to the EU standards for PM10, after January 1 2010 the annual PM10 level should not exceed 20μg/m^3 and the daily PM10 level of 50μg/m^3 should not be exceeded more than 7 days per year (equivalent to the percentile 98).

As deduced from the data of the MONAGREGA rural site, the contribution of the natural mineral dust and of the sea spray to the annual PM10 levels is 5μg/m^3 and 1-2μg/m^3,

Table 5-9. Mean PM source contributions obtained by MLRA (A: upper table) and MBA (B: lower table) at the MONAGREGA rural and the L'HOSPITALET urban sites in one year (June 1999 to June 2000) and mean source contributions at the ONDA industrial site from June to October 1999. PM: PM10 or PM2.5 levels obtained by the gravimetric method. Crustal (mineral dust), Ind.-1(power production: nss-$SO_4^=$+ other), Vehicles (exhaust emissions), Marine(sea spray), Ind.-2(petrochemical: Ni, V and NO_3^-), Ind.-3(tile manufacture: Pb, Cu + others), Ind.-4(Na+P), other: intersection constant in the multi-linear regression. PM levels obtained by MLRA and gravimetric methods are shown. Percentages (%) are expressed with respect to PM10 levels obtained by the gravimetric method.

A) MLRA		Crustal	Ind.-1	Vehicles	Marine	Marine+ Ind.-2	Ind.-3	Ind.-4	Bio-mass burning	PM
Rural PM10	µg/m^3	5	6	5	2					22
MONAGREGA	%	23	27	23	9					
Industrial PM10	µg/m^3	9	9			3	2		5	33
ONDA	%	28	28			9	6		15	
Urban PM10	µg/m^3	12	15	22	3					49
L'HOSPITALET	%	24	31	45	6					
Urban PM2.5	µg/m^3	4	10	14				<1		34
L'HOSPITALET	%	12	29	41				<1		
B) MBA		Crustal	Ind.-1	Vehicles	Marine	Marine+ Ind.-2	Ind.-3	Ind.-4	Bio-mass burning	PM
Rural PM10	µg/m^3	5	6	3	1					22
MONAGREGA	%	23	27	14	5					
Industrial PM10	µg/m^3	9	9			2	1		6	33
ONDA	%	27	27			6	3		18	
Urban PM10	µg/m^3	12	12	17	2					49
L'HOSPITALET	%	24	24	35	4					
Urban PM2.5	µg/m^3	3	12	18						34
L'HOSPITALET	%	9	35	53						

respectively. The natural mineral dust and total natural load (mineral dust + sea spray) accounts for 25% and 30-35% of the 2010 EU annual limit value (20µg/m^3).

At the MONAGREGA rural site, the annual mean PM10 is slightly higher than the 2010 EU annual value, the contribution of the natural mineral dust being as important as the contribution of each anthropogenic source. The 2010 EU limit value for PM10 was exceeded at the urban site because of the high background level of PM10 during the study period.

At ONDA, PM10 was studied only for 5 months so an assessment of the annual mean level and source contributions cannot be performed. During these 5 months, the mean mineral dust concentration was 3µg/m^3 higher than at the MONAGREGA (where was 6µg/m^3) rural site.

At the L'HOSPITALET urban site, annual mineral dust concentration reached 12µg/m^3, which is 7µg/m^3 higher than the natural background (5µg/m^3 at MONAGREGA) due to the contribution of local urban sources. Thus, taking into account the sea spray load, the contribution

of the natural sources to the annual PM10 levels at L'HOSPITALET is estimated at 7-8μg/m^3. This natural load accounts for 35-40% of the 2010 EU PM10 limit value. On the other hand, only the vehicle exhaust emission contribution (17-22μg/m^3) is very close to the 2010 EU PM10 limit value. The local contribution of mineral dust at L'HOSPITALET appears to be very high when compared with that recorded at the ONDA industrial site, which is affected by the emissions from ceramic manufacture. However, it should be noted that L'HOSPITALET is a kerbside whereas ONDA is a background station.

At the L'HOSPITALET urban site, the contribution of the mineral dust to the annual PM2.5 level is much lower than the contribution of the anthropogenic sources.

5.5 PM source apportionment during the different PM episodes

The mean source contributions were calculated for the main types of episodes affecting PM levels at the rural, urban and industrial sites in following the classification described in chapter 4. These results are of especial interest to the managers of the air quality monitoring networks because the main PM events can be identified in the PM time series (in accordance with meteorology, chapter 4) and because these results (Tables 5-9 and 5-10 and Figures 5-56 and 5-57) provide quantitative estimations of the PM origin. The results are shown in Tables 5-10 and 5-11 and Figure 5-56 and 5-57 and will only be summarised.

The highest mineral dust loads in PM10 and PM2.5 were recorded during African dust events at all sites.

During summer Regional episodes, PM10 at the MONAGREGA rural site is mainly constituted by secondary anthropogenic (mainly from industrial emissions for power generation, 43-53% of bulk PM10) and crustal (20%) PM from soil re-suspension. These are also the most important PM10 sources at the L'HOSPITALET urban and the ONDA industrial sites. The difference between the crustal PM levels recorded at ONDA and MONAGREGA and at L'HOSPITALET and MONAGREGA accounts for the local anthropogenic contributions to crustal PM. Significant contributions to PM10 from vehicle exhaust emissions and bio-mass burning at L'HOSPITALET and ONDA, respectively, are also observed. At L'HOSPITALET, the industrial and vehicle exhaust contributions to PM2.5 are close to those in PM10, but the crustal load is significantly reduced.

During the winter Local pollution episodes, vehicle exhaust emissions is the most important source of PM10 and PM2.5. This is also the most important source of PM10 at the MONAGREGA rural site during the eventual winter Regional episodes (40-52% of bulk PM10).

The lowest PM10 and PM2.5 levels were recorded during the Atlantic episodes.

Table 5-10. Mean source contributions to PM10 and PM2.5 levels (in µg/m^3, estimated by MLRA) during the main PM episodes (chapter 4). Ind.-1(power production: nss-$SO_4^=$+ other), Ind.-2(petrochemical: Ni, V and NO_3^-), Ind.-3(tile manufacture: Pb, Cu + others), other: intersection constant in the multi-linear regression. PM levels obtained by MLRA and gravimetric methods are shown.

MONAGREGA Rural	Crustal	Ind.-1	Vehicles	Marine	Other	PM10 MLRA	PM10 grav
African	23	7	5	2	2	40	42
Summer-Regional	7	17	4	1	2	31	32
Winter-Regional	3	3	12	1	2	21	23
Atlantic	2	2	2	1	2	9	9

ONDA Industrial	Crustal	Ind.-1	Ind.-3	Marine + Ind.-2	Bio-mass Burning	Other	PM10 MLRA	PM10 Grav
African	25	6	2	3	6	4	46	52
Summer-Regional	10	8	2	3	5	4	32	36
Atlantic	4	5	1	2	3	4	19	20

L'HOSPITALET Urban	Crustal	Ind.-1	Vehicles	Marine	PM10 MLRA	PM10 grav
African	26	14	17	4	60	67
Summer-Regional	13	15	10	3	41	41
Winter-Regional	8	17	45	2	72	73
Atlantic	7	7	9	3	25	27

L'HOSPITAL Urban	Crustal	Ind.-1	Vehicles	PM2.5 MLRA	PM2.5 grav
African	11	7	15	32	37
Summer-Regional	4	11	7	22	28
Winter-Regional	3	12	27	42	59
Atlantic	2	4	7	13	14

Table 5-11. Mean source contributions to PM10 and PM2.5 levels (in µg/m^3, estimated by MBA) during the main PM episodes (chapter 4). Ind.-1(power production: nss-$SO_4^=$+ other), Ind.-2(petrochemical: Ni, V and NO_3^-), Ind.-3(tile manufacture: Pb, Cu + others), Ind.-4(Na+P), other: intersection constant in the multi-linear regression. PM levels obtained by MBA and gravimetric methods are shown.

MONAGREGA Rural	Crustal	Ind.-1	Vehicles	Marine	PM10 MBA	PM10 grav
African	21	6	4	1	32	42
Summer-Regional	7	14	1	0,5	22	32
Winter-Regional	4	5	9	0,5	18	23
Atlantic	2	3	1	0,4	7	9

ONDA Industrial	Crustal	Ind.-1	Ind.-3	Marine + Ind.-2	Bio-mass Burning	PM10 MBA	PM10 grav
African	24	5	1	3	6	43	52
Summer-Regional	11	8	1	3	5	31	36
Atlantic	4	5	0,5	1	4	20	20

L'HOSPITALET Urban	Crustal	Ind.-1	Vehicles	Marine	PM10 MBA	PM10 grav
African	23	13	17	3	57	67
Summer-Regional	12	12	8	2	34	41
Winter-Regional	13	9	35	2	59	73
Atlantic	8	5	10	3	26	27

L'HOSPITAL Urban	Crustal	Ind.-1	Vehicles	Ind.-4	PM2.5 MBA	PM2.5 grav
African	10	8	8	$5 \cdot 10^{-3}$	27	37
Summer-Regional	3	14	7	$8 \cdot 10^{-3}$	25	28
Winter-Regional	2	11	36	$5 \cdot 10^{-3}$	49	59
Atlantic	2	4	6	$8 \cdot 10^{-3}$	12	14

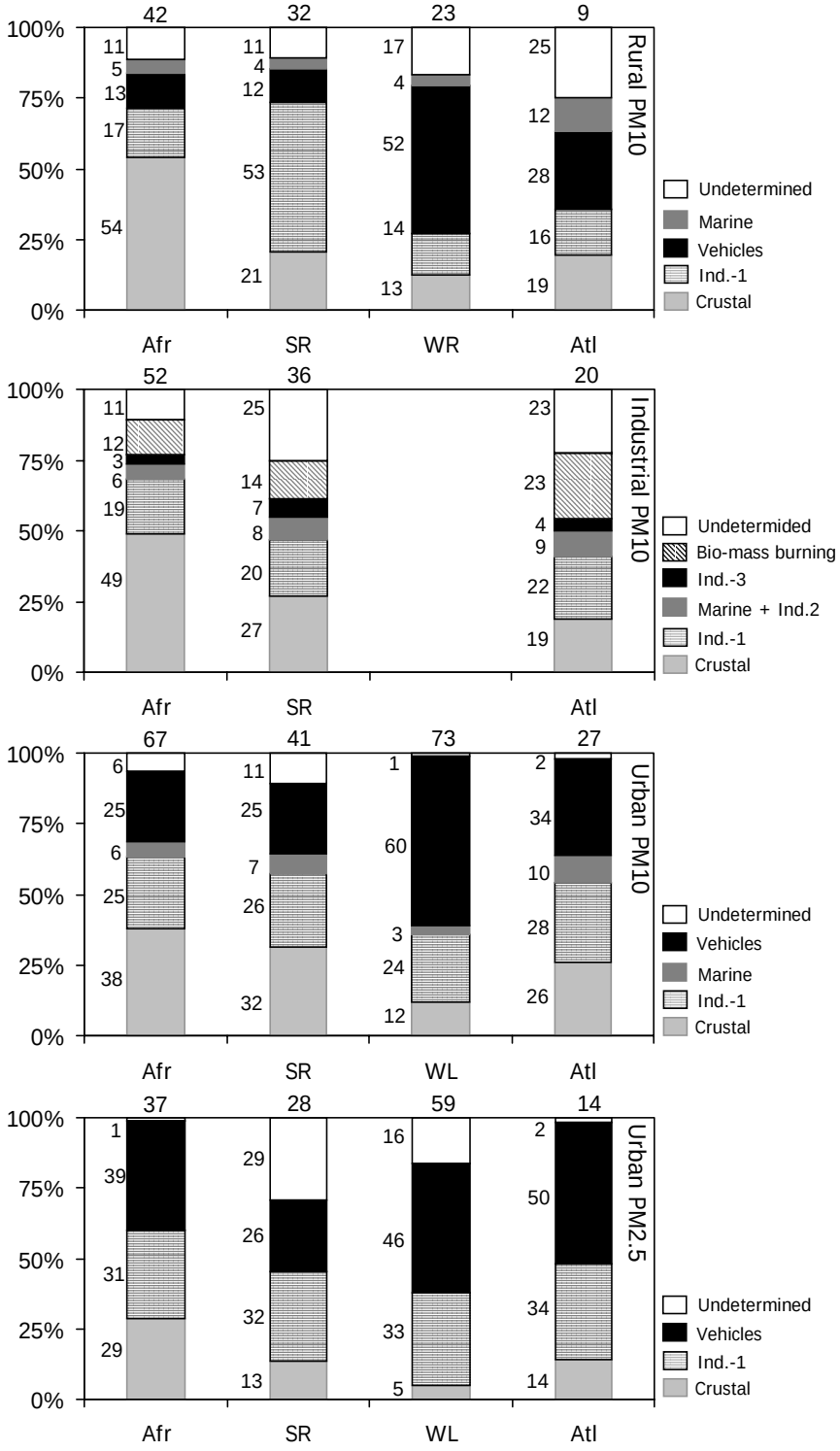

Figure 5-56. Mean PM10 and PM2.5 levels (at the top of each column) and source contributions (in % at the left of each column) calculated by MLRA during African (Afr), Regional Summer (SR), Winter Regional (WR), Winter Local (WL) and Atlantic (Atl) episodes.

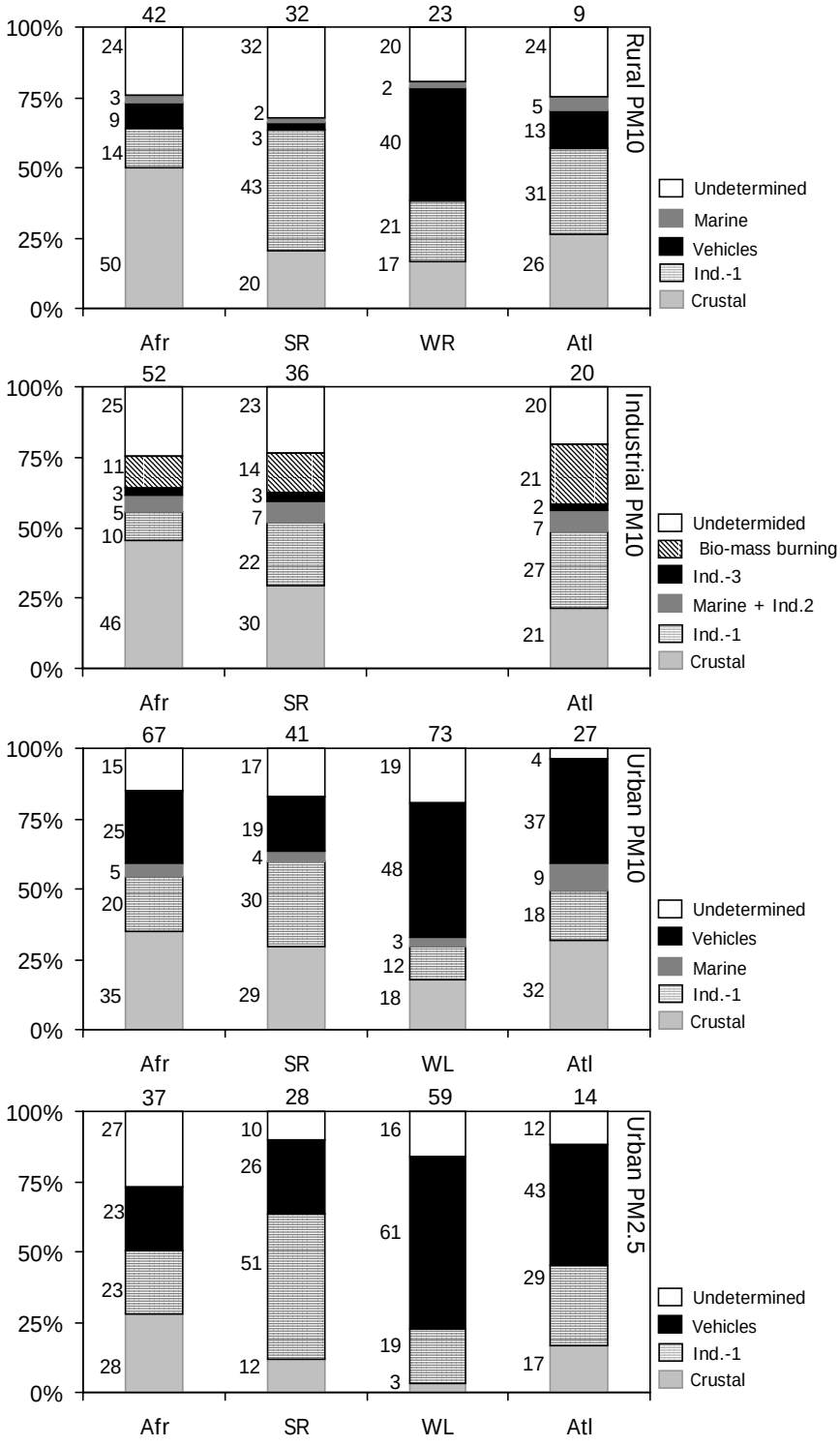

Figure 5-57. Mean PM10 and PM2.5 levels (at the top of each column) and source contributions (in % at the left of each column) calculated by MBA during African (Afr), Regional Summer (SR), Winter Regional (WR), Winter Local (WL) and Atlantic (Atl) episodes.

5.6 Summary and conclusions

The composition of PM10 and PM2.5 was investigated by simultaneous PM10 sampling at a rural, an urban and a ceramic production site and by PM2.5 sampling at an urban site in Eastern Spain. The main objective was to perform a chemical characterisation and a source apportionment of PM in order to evaluate the main natural and anthropogenic contributions. The source contribution was calculated by two methods; the results were compared and the slight differences found were discussed.

The main PM10 components at the urban, rural and industrial sites were mineral dust of natural and/or anthropogenic origin depending on the sampling site, sea spray, vehicle exhaust products (nitrate, carbonaceous PM and other trace elements) and pollutants resulting from power generation (sulphate from SO_2 emissions and other trace elements). With the exception of the sea spray, these components were also identified in PM2.5.

The chemical composition of PM10 and PM2.5 underwent considerable variations along the year. Owing to the thermodynamic properties of nitrogenous species, a maximum nitrate load was attained in winter. In contrast, the load of nss-sulphate was maximum in summer. High mineral dust concentrations were simultaneously recorded at the rural, urban and industrial sites during African dust outbreaks. In these events, the load of mineral dust was in the range 20-30μg/m^3 in PM10 and in the range 10-15μg/m^3 in PM2.5, accounting for 50-80%, 20-45% and 40-55% of bulk PM10 levels at the rural, urban and industrial sites, respectively, and for 10-40% of PM2.5 at the urban site.

At the MONAGREGA rural site the annual mean PM10 level was 22μg/m^3 and the main contributions were 5μg/m^3 of natural mineral dust, 1-2μg/m^3 of sea spray, 6μg/m^3 from industrial emissions and 3-5μg/m^3 of vehicle exhaust products.

At the L'HOSPITALET urban kerbside station, the annual mean PM10 level was 49μg/m^3 and the main contributions were 12μg/m^3 of mineral dust, 2-3μg/m^3 of sea spray, 12-15μg/m^3 from industrial emissions and 17-22μg/m^3 of vehicle exhaust products.

At the L'HOSPITALET urban kerbside station, the annual mean PM2.5 level was 34μg/m^3 and the main contributions were 3-4μg/m^3 of mineral dust, 10-12μg/m^3 from industrial emissions and 14-18μg/m^3 of vehicle exhaust products.

The annual mean natural load in PM10 at the MONAGREGA rural site (5μg/m^3 of mineral dust and 1-2μg/m^3 of sea spray) accounts for 30-35% of the 2010 PM10 EU annual mean limit value (20μg/m^3). The local contribution to mineral dust levels is estimated at 7μg/m^3 in PM10 as the annual mean at the L'HOSPITALET kerbside station and at 4μg/m^3 in PM10 at the ONDA industrial (ceramic manufacture) background station as the summer mean. Only the contribution of vehicle exhaust products to PM10 levels at L'HOSPITALET approaches the 2010 PM10 EU annual mean limit value.

At the rural site the highest PM10 events (>40μgPM10/m^3) are recorded during African dust outbreaks. The other dominant sources (when PM10 levels are in the range 15-40μg/m^3) are of anthropogenic origin related to secondary particles (sulphate, nitrate, ammonium and carbon).

At the urban site, traffic derived pollution is the day-to-day dominant PM10 and PM2.5 source (PM concentrations in the ranges 30-120PM10µg/m^3 and 20-80µgPM2.5/m^3), which is associated with road dust and vehicle exhaust products. The mineral dust fraction is considerably lower in PM2.5 than in PM10.